RAPID MAPPING OF HYDRAULIC CONDUCTIVITY

In a tropical watershed

By

CHRISTIAN THINE OMUTO

B Sc Agric. Eng

Thesis proposal submitted to the Department of Agricultural Engineering of the University of Nairobi in partial fulfillment of the requirements for the degree of

MASTER OF SCIENCE IN AGRICULTURAL ENGINEERING

(SOIL AND WATER ENGINEERING)

UNIVERSITY OF NAIROBI

2003

DECLARATION

I Christian Thine Omuto, hereby declare that, this thesis is my original work and has not been presented for a degree in any other University.

.... 29th/May/2003
Christian Thine Omuto .... Date

This thesis has been submitted for examination with our approval as University supervisors

.... 23rd May 2003
Biamah E.K .... Date

.... 23 May 2003
Shepherd K.D .... Date

DEDICATION

To my beloved father, mother, sisters and brothers

ACKNOWLEDGEMENTS

I wish to acknowledge the constant guidance, encouragement and advice of my supervisors Dr. E. Biamah and Dr. K. Shepherd. I benefited generously from their cogent comments and suggestions and ask for their understanding of those instances when, in my stubbornness, I stuck to my own views. Dr. E. Biamah's encouragement and constant field visits cannot go unnoticed. His concern for my progress was both parental and professional. Similar gratitude goes to Dr. K. Shepherd. I have learnt a lot from him in terms of state-of-the-art approach to problem solution and unshakable confidence he wields in his work. I also thank Professor T. Sharma and Mr. J. Obiero, both from the University of Nairobi, for reading and correcting my thesis. All these encouragements gave me an academic lust for quality research.

Special thanks go to the University of Nairobi and ICRAF for the support they gave me during my study. I honestly thank Dr. B. Swallow of ICRAF for his resolute patience and words of encouragement advanced to me during and after my fieldwork. I cannot forget the professional guidance of Dr. M. Walsh of ICRAF, Kisumu. He greatly assisted me with new techniques for statistical analysis. In addition, he availed to me both his vehicle for fieldwork and his busy schedules, solely to upgrade my progress.

Gratitude is extended to the members of staff of the Department of Agricultural Engineering of the University of Nairobi, who helped me in one-way or the other. I'm particularly grateful to the Chairman Mr. R. Muni for allowing me unlimited access to the departmental materials and equipment for research. I also thank Mr. B. Muliro for sparing his times both at night and during weekends to provide technical assistance in laboratory analysis.

I'm also greatly indebted to all ICRAF members of staff, for their support. I acknowledge the support I received from Mr. C. Otieno during my stay at ICRAF house, Kisumu. I also thank Mr. P. Okoth, Mr. W. Ondiala, Mr. N. Ghai, Mr. N. Shituskane and Mr. S. Mureithi for their co-operation and contribution during the hard moments of my field data collection. I will never forget the valuable support I received from Mr. E. Weullow, Mr. A. Sila and Mr. A. Awiti during data analysis.

For all those who may have given their assistance in one-way or the other and have not been acknowledged, I trust that God's blessing comes your way for the assistance. God bless you all.

Table of contents

List of Tables

List of Figures

List of Appendices

ABSTRACT

Modeling of water and solute dynamics in soils is a major focus in watershed management. In order to model the water flow, soil hydraulic properties have to be known. Spatial information on basic soil data such as particle-size distribution, organic carbon content and bulk density are often available. However, spatial information on soil hydrologic data, which are necessary for soil transport models, is usually not available. Soil hydrologic data are expensive and difficult to obtain on a large area and are often predicted from physical data like particle-size distribution using pedotransfer functions. This study set out to develop a rapid methodology based on relating soil hydraulic conductivity to soil spectral reflectance and using a soil spectral library approach to predict soil hydraulic conductivity in a large area of a watershed.

Soil spectral reflectance was correlated to field saturated hydraulic conductivity and the correlation found to be consistent K_s (index of agreement, d = 0.87, and r^2 =0.63). This consistent relationship provided a foundation for using a spectral calibration model in conjunction with a georeferenced library to predict surface K_s over a large area. The spectral library contained spectral data for the points in the study area for which direct measurement was not made.

In the build up of a map for the whole watershed, spatial variability of surface K_s was studied using classical and geostatistical concepts. Semivariograms were intensively used with actual and kriged estimates to produce an accurate surface interpolation map of surface K_s in the watershed. The map, which shows a general trend of surface K_s with altitude, will be a great asset for the hydrologic modeling of watershed responses.

CHAPTER I

1. INTRODUCTION

1.1 Background

Knowledge of the movement of water in soil is needed in many aspects of agricultural watershed management; management of soil erosion, rainfall water harvesting, and plant water and nutrient management. Movement of water in soil is principally controlled by two factors; resistance of the soil to water flow and the forces acting on each unit of soil-water to cause them to move. Darcy's law, the fundamental equation describing water movement in soil, relates the flow-rate to these two factors. Mathematically, the general statement of Darcy's law for vertical, saturated flow is:

$$Q / At = -K_s \frac{dh}{dz} \tag{1.1}$$

where the flow-rate *Q/At* is the soil flux density, which is the quantity of water *Q* moving past an area *A* perpendicular to the direction of flow in time *t*, $\frac{dh}{dz}$ is hydraulic gradient, the net driving force causing water to move vertically in soil, and K_s is saturated hydraulic conductivity. In terms of water movement, K_s is the inverse of the resistance of the soil matrix to water flow (or the ease with which soil can transmit water). Soils with higher saturated hydraulic conductivity allow water to pass through them faster than those with lower values of saturated hydraulic conductivity.

Resistance to water movement in soils is primarily a function of the arrangement and size distribution of soil pores. Large continuous pores have low resistance to water flow than small or discontinuous pores. Thus, soils with large and continuous pores have higher saturated hydraulic conductivity than soils with small and discontinuous pores. If on the one hand, the large and continuous pores in one soil are severed by soil manipulation so that they collapse and become small, the saturated hydraulic conductivity of the soil will be lowered. On the other hand, if structurally degraded soils are allowed to regenerate and develop large and continuous pores, their saturated hydraulic conductivity will rise. Hence, by measuring saturated hydraulic conductivity of a soil after some changes, information on structural change can be captured. In this regard, K_s can be used qualitatively to describe the effect of natural and anthropogenic activities on soil hydrology.

Saturated hydraulic conductivity, however, is a highly variable soil physical parameter; changing over time and space in a watershed. Due to this fact, accurate measurement and reliable estimation of this parameter has become a critical research problem in the fields of agricultural engineering, soil science and hydrology (Sharma et al., 1983). Many methods for determination of K_s and procedures for approximating it have been proposed. These range from laboratory to field (*in situ*) approximations (Ankeny et al, 1991). In as much as laboratory methods have been used to control variability in determining K_s, field methods have gained ground in representing conditions typical of a watershed. These field methods are known as traditional point-measurement methods (Amoozegar and Warrick, 1986).

The traditional field measurement methods are however limited in their capacity to accurately and consistently measure K_s over a large area. The limitations stem from the fact that they are cumbersome and expensive for area-wide survey. In addition, since not all point-measurements can be made at the same time, these methods suffer from delay in time for acquiring information needed to characterize temporal variability in K_s. There is need therefore to come up with a versatile and practical technique that can rapidly and consistently help in approximating K_s on a larger-area basis.

New opportunities for using Diffuse Reflectance Spectrometry (DRS) and spectral libraries are under development for rapid characterization of soil properties across a watershed (Shepherd and Walsh, 2002). These techniques involve the development of transfer functions based on soil spectral reflectance to estimate soil properties of interest. The approach utilizes non-destructive testing of soils under laboratory conditions, using an artificial light source, to develop robust prediction models based on a selected number of soil samples. Such models can then be used to predict soil properties from the spectral signatures in the spectral library (Shepherd and Walsh, 2002). This is known as spectral library approach, which could allow large number of observations of soil physical properties to be determined cheaply.

This study was thus designed to test the use of DRS and the spectral library approach to spatially characterize saturated hydraulic conductivity in a large tropical watershed. The possibility of developing a robust transfer function between soil hydraulic conductivity and soil spectral reflectance was also explored.

1.2 Relevance of the study

The traditional point-measurement methods used in estimation of field saturated hydraulic conductivity have not been successful in characterizing saturated hydraulic conductivity in a whole watershed. The reasons for this failure have been identified to be the costs involved, the labour intensity required and the prolonged time needed to acquire the necessary data (Sharma et al., 1980).

To reduce these limitations, scientists have resorted to the use of transfer functions, which relate K_s to more easily measured soil properties (Arya et al., 1999). The transfer functions, which include pedotransfer functions (Tietje and Tapkenhinrichs, 1993), and inverse functions (Rawls et al., 1993) combined with scaling theories (Schaap et al., 1998), have offered attractive promise in spatial estimation and characterization of K_s in a whole watershed. However, the use of these functions has been exercised with a lot of caution since they are known to apply well only to the conditions for which they were developed. Furthermore, paucity of the available input data required by the majority of these functions precludes their extensive use.

Nonetheless, the development of a robust and consistent transfer function for prediction of saturated hydraulic conductivity is thus still required and is currently an area for more research. This study attempts to develop such a function. The approach here is involved in development of transfer functions based on soil spectral reflectance signatures to estimate soil saturated hydraulic conductivity. The soil spectral signatures, which are defined by their reflectance or absorbance as a function of wavelength, are unique for a given soil and so can provide reliable prediction of soil attributes over a wide area. These signatures are greatly affected by soil surface roughness – a consequent of soil pore–size distribution and geometry, clay content and mineralogy, and organic matter content, which all are known to influence K_s. Quantification of all these factors in terms of reflectance can also be construed to be quantification of soil K_s. Consequently, this approach may allow consistent prediction of saturated hydraulic conductivity across watersheds.

On the other hand, as much as the soil saturated hydraulic conductivity may be important for watershed surveillance, neither area-wide information on K_s nor a methodology for estimating it exists in tropical watersheds in general and in Lake Victoria basin in particular. There is a need to develop a methodology for obtaining soil hydraulic parameters on area-wide basis to map out the properties across a watershed. Such a method would contribute a very important decision tool in management especially in resolving fallacies of watershed management.

This study has attempted to develop a protocol for predicting soil saturated hydraulic conductivity across a watershed using the spectral library approach

(Shepherd and Walsh, 2002). Soil spectral libraries house spectral data for thousands of soils drawn from a target area. A prediction model, developed on selected direct soil measurements, can be applied to spectral signatures in the spectral library to predict soil hydraulic conductivity for all samples in the library.

1.3 Objectives and scope of the study

1.3.1 Objectives

The overall objectives of this study were to:

1. test to what degree field-measured soil saturated hydraulic conductivity can be related to laboratory-measured soil spectral reflectance
2. develop a methodology for mapping field saturated hydraulic conductivity based on spectral libraries

The specific objectives of this study were to:

1. identify rapid field method for measurement of saturated hydraulic conductivity
2. carry out rapid area-wide, georeferenced survey of saturated hydraulic conductivity in a sub-watershed
3. describe the distribution of soil saturated hydraulic conductivity to laboratory-measured soil spectral reflectance
4. calibrate field-measured saturated hydraulic conductivity to laboratory-measured soil spectral reflectance
5. map out saturated hydraulic conductivity in a tropical watershed using geostatistical techniques

1.3.2 Scope of the study

This study was set to establish a relationship between field saturated hydraulic conductivity and soil spectral reflectance with a view of developing an area-wide map of a tropical watershed. The relationship was therefore developed and tested on a watershed scale in the River Nyando basin in Western Kenya. This basin was chosen because it contains wide variation in soils, land use and physiography.

The study was confined to field saturated hydraulic conductivity and soil spectral reflectance. All terms related to conductivity and reflectances used in this study refer to field saturated hydraulic conductivity and laboratory-measured soil spectral reflectance, respectively.

As a hydrologic study concerned with watershed responses (such as surface runoff and infiltration), the scope of the study was restricted to soil saturated hydraulic conductivity of the top 0 – 20 cm of the soil profile. Thus, all the field measurements, soil sampling and predictions were restricted to this layer only. A cross-section covering about one third of the study area was selected for direct measurements of hydraulic conductivity to establish the relationship. Prediction of hydraulic conductivity for the whole watershed was made possible by the use of spectral library containing the spectral signatures of soil samples previously taken from many locations in the study area. All the direct measurements and library samples were georeferenced to locate the value of hydraulic conductivity accurately in space.

CHAPTER II

2. REVIEW OF LITREATURE

2.1 Definition of hydraulic conductivity

Hydraulic conductivity of a saturated soil is the ease with which the soil allows water to move vertically through it (Suresh, 1997). Mathematically, it is the proportionality factor (K_s) in the Darcy's law for the flow of water in a saturated soil,

$$q = -K_s \frac{dh}{dz} \tag{2.1}$$

where $\frac{dh}{dz}$ is the hydraulic gradient necessitating the flow from higher potential to lower potential (Oswal, 1983) and q is the steady flow rate of water in the porous medium. It represents the reciprocal of the resistance soil offers to water movement through it. Under unsaturated conditions, however, the hydraulic conductivity varies with the soil moisture suction (h) and is normally denoted by K(h) (Kutilek and Nielsen, 1994).

2.2 Importance of hydraulic conductivity

The rate of water movement through soil is of considerable importance in many aspects of agricultural fields and urban grounds. These aspects include, among others, water entry into the soil, water movement to plant roots, solute transport to plant roots and to groundwater, water flow to drains and even evaporation of water from soil surface to the atmosphere. Soil properties that determine this rate of water movement are known as hydraulic properties of the soil. Two fundamental soil hydraulic properties characterizing soil water flow are the field saturated hydraulic conductivity (K_s) and the matric flux potential (ϕ_m) (Reynolds and Elrick, 1990). Besides being the two most important soil parameters controlling steady and ponded infiltration (Philip, 1985; Wooding, 1968; Scotter et al., 1982; Reynolds et al., 1985), they provide a foundation from which several other soil parameters can be derived (Reynolds and Elrick, 1990). These soil parameters include sorptivity, the alpha parameter, the macroscopic capillary length, the characteristic mean pore radius and the wetting-front potential. The relative performance of these parameters is discussed in Reynolds and Elrick (1990).

Apart from being quite necessary in the understanding of water and solute movement under microirrigation, soil hydraulic conductivity is also one of the most important factors affecting spacing between laterals of subsurface drainage systems (Gallichand et al., 1992). In fact, USBR (1978) lists hydraulic conductivity as the item of the subsurface drainage investigation that represents the greatest investment in terms of time, money and manpower.

Soil hydraulic conductivity, which is a measure of the ease of water movement in soil, is highly dependent on arrangement and size distribution of pores. Knowledge of soil pore-size distribution and arrangement can lead to knowledge of soil hydraulic conductivity and vice versa (Cresswell et al., 1992). According to Cresswell et al. (1992), hydraulic conductivity reflects soil structure and soil texture. Thus, the measurement of the effect of management on the structure and texture can be quantified through measurement of soil hydraulic conductivity.

Most of the uncertainties in the assessment of water flow in unsaturated soils at the field scale are attributable to soil spatial variability as caused by soil heterogeneity (Tuli et al., 2001). The progress, thus, in the interpretation of data collected in watershed hydrology studies has mainly been attempted through modeling process to tackle this kind of variability. Numerical models simulating the movement of water and solutes in variably saturated soils have been found invaluable in this respect (Chapman and Dunin, 1975). The models are increasingly being used in a variety of research and engineering projects (Vogel et al., 2001). Such models are approximate solutions of the traditional Richards' equation (eq. 2.2) that describes the unsaturated flow in soils (Vogel et al., 2001).

$$\frac{\partial \theta(h)}{\partial t} = \frac{\partial}{\partial z}\left[K(h)\frac{\partial h}{\partial z} - K(h) \right] \tag{2.2}$$

Where K is unsaturated hydraulic conductivity (which depends heavily on saturated hydraulic conductivity, K_s), θ is volumetric moisture content, t is time, h is the soil capillary pressure head and z is soil depth.

However, the use of eq. (2.2) require accurate description of soil hydraulic properties (Bouma et al., 1971) and the knowledge of the constitutive relationships for the unsaturated hydraulic conductivity, water saturation and soil matric potential (Tuli et al., 2001). According to Ophori and Maharajan (2000), one of the most important properties and most sensitive parameter required by eq. (2.2) and majority of simulation models is the hydraulic conductivity.

Despite the importance of hydraulic conductivity in watershed hydrology, its accurate measurement is generally cumbersome, costly and very time consuming. This arises because of the variation of the parameter in both space and time. These variations may be both systematic and stochastic (Cresswell et al., 1992). The systematic variation is revealed in textural profiles while stochastic variation is considered in the nature of field heterogeneity.

Consequently, many attempts are being made to develop rapid and easier, economical and accurate methods to contend with these variations in the process of estimating hydraulic conductivity.

2.3 Hydraulic conductivity studies in Kenya

In spite of the importance of hydraulic conductivity in agricultural engineering, hydrology, agronomy and related fields, only few hydraulic conductivity studies have been documented in Kenya albeit as a component of a major study. Omulabi (1996), used laboratory methods for determination of hydraulic conductivity on core samples taken from the field in his study on the effects of secondary salinization on hydraulic conductivity. Similarly, Kanake (1982), Asol (1984) and Otieno (1990) did some discrete work on saturated hydraulic conductivity of the Kenyan-salt-affected soils at Kimorigo. Their method of determination of hydraulic conductivity was also basically laboratory oriented. Cheruiyot (1984) and Omulabi et al. (2000a) also used constant head method in the laboratory to determine the hydraulic conductivity of cored samples taken from the field.

The focus of these studies was more or less on determination of a "representative" hydraulic conductivity for the soils in the field. May be lack of time, less concern and perhaps inaccessibility to necessary equipment could have bedeviled any major studies on hydraulic conductivity. This incapacity in mind, some studies with interests on hydraulic conductivity attempted use of predictive methods. Okwach (1994), Obiero (1994) and Onyando and Sharma (1995) used optimization techniques in water balance models to estimate hydraulic conductivity in their studies. The main focus in these studies was to obtain hydraulic conductivity without regard to relevance of the method with respect to other existing methods. It however sufficed to Obiero (1994) during his study that hydraulic conductivity was quite significant parameter in hydrology study. He recommended a study to evaluate the accurate method for determination of hydraulic conductivity, preferably a field method.

Omulabi et al. (2000b), on the other hand, tried to relate hydraulic conductivity with soil measurable properties. They obtained a regression relationship between hydraulic conductivity and soil physical and chemical parameters. They, however, underestimated the fact that saturated hydraulic conductivity has a logarithmic behaviour as had been established by Scheidegger (1960), Vereecken (1988) and Gonclaves (1999).

Gachene (1995) used disc permeameter on the Kabete soils in attempting to quantify effects of soil erosion on soil properties. In this study there was neither concern for evaluation of methods nor with accuracy of the aforesaid method. Sirya (1997) used monographs developed by Rawls and Brakensiek (1983), in estimating hydraulic conductivity on a study of water harvesting in semi arid areas of eastern Kenya. Like Obiero (1994), Sirya (1997) recommended field measurement methods rather than texture based relationships, which do not consider surface sealing and crusting.

In effect, no study however, seems to have attempted to evaluate the methods used for determination of hydraulic conductivity with a view of coming up with a suitable method for large area hydraulic conductivity measurement. In Kenya, like anywhere else, hydraulic conductivity studies would be needed to characterize soils on catchment scale. A study of this nature is one of determining a spatially averaged hydraulic conductivity on the basis of catchment characteristics like land use, land cover, slope etc. that influence infiltration and surface runoff. No attempts have been made so far along lines.

2.4 Hydraulic conductivity studies in general

The preference of field determination of hydraulic conductivity notwithstanding, the method is quite Herculean owing to variability that has to be contended with. The highly spatial variability of hydraulic conductivity in the field has overwhelmed scientists and researchers for a long time. Therefore, there has been a great need to come up with a technique, which is both accurate and capable of accommodating variability it displays. Tuli et al. (2001) used scaling approach to characterize soil hydraulic spatial variability. In their study, the concept of simultaneous scaling of the soil water retention and unsaturated hydraulic conductivity functions was applied to a physically based scaling theory. Working on a total of 143 "undisturbed" soil samples collected from the field, Tuli et al. (2001) described soil spatial variability of hydraulic functions from a single set of scaling factors. They assumed that soils are characterized by a lognormal pore-size distribution, which led to lognormally distributed scaling factors.

Some scientific research attempts have also tried to explore the issue of spatial variability. Gallichand et al. (1992) showed that the density of hydraulic measurements was of primary importance for the design of large-scale subsurface drainage projects. They conducted a study to investigate the effect of sampling density on hydraulic conductivity estimation. Using the results of 3488 hydraulic conductivity tests from 33 500 ha subsurface drainage projects in Nile Delta of Egypt they determined optimal sampling density of hydraulic conductivity for subsurface drainage. Gallichand et al. (1992) also explored kriging techniques to show that the optimal sampling grid spacing for hydraulic conductivity in the Nile Delta was between 400 and 600 m.

From the research findings outlined above, spatial variation of soils, then, would need a large number of surface and subsurface measurements of hydraulic conductivity to characterize a field. This seems massive and practically unachievable. Many methods have, therefore, been developed for rapid and accurate determination of surface and subsurface hydraulic conductivity. In 1990 Reynolds and Elrick (1990) established a method using single rings analysis of steady, ponded infiltration taking into account ring radius, depth of ring insertion and depth of ponding. The test calculations based on shape factors suggested that field saturated hydraulic conductivity could be obtained with accuracy of about ± 20% (Reynolds and Elrick, 1990). This establishment boosted the use of single rings for field determination of hydraulic (Reynolds and Elrick, 1991).

O'Neill et al. (1990) developed Guelph Pressure Infiltrometer for determining in situ measurements of soil hydraulic properties. In their study, they assessed the effects of management on changes in surface hydraulic properties. The temporal changes in hydraulic properties measured with the pressure infiltrometer in two tillage systems were studied (O'Niell et al., 1990).

Talsma and Hallam (1980) in their measurement of hydraulic conductivity of forest catchments reported that simple and rapid measurement methods for hydraulic conductivity were necessary. They described well permeameter (similar to Guelph permeameter) as one of the suited methods for profile characterization. Talsma and Hallam (1980) indicated the usefulness of catchment's hydraulic conductivity data, for inter-catchments comparison, and for explaining storm-hydrograph shapes of individual catchments.

Reynolds and Elrick (1991) developed a procedure for in situ determination of saturated and near-saturated hydraulic conductivity. Using tension infiltrometer, they made a sequence of steady infiltration measurements at several tensions on a single infiltration surface. According to Reynolds and Elrick (1991), the method applies to tension infiltration from either a surface disk or from within a ring inserted a small distance into the soil. Via numerical simulations, the method was found to have an overall accuracy of about ± 7% (Reynolds and Elrick, 1991).

Simunek and van Genuchten (1997) used tension disc infiltrometers for in-situ measurement of the unsaturated soil hydraulic properties. The tension disc infiltrometers were found useful for quantifying the effects of macropores and preferential flow paths on infiltration in the field (Simunek and van Genuchten, 1997). In this case the tension infiltration data was primarily used to evaluate the saturated hydraulic conductivity and a sorptivity parameter. They analyzed the possibility of using an infiltration curve for the purpose of estimating soil hydraulic parameters.

Holland et al. (2000) developed and tested permeameters for estimating subsurface unsaturated hydraulic conductivity. They determined unsaturated hydraulic conductivity by measuring steady flow rates for various values of negative pressures. Apart from being easy to use and have adequate accuracy, permeameters were found to be capable of applying water to soil under tension, which is less likely to be influenced by macropores (Holland et al., 2000).

Similarly, Elsenbeer and Vertessy (2000) worked on a research to quantify saturated hydraulic conductivity on the dominant land cover types on the mountainous watersheds of Montane Mainland, SE Asia. They used a disc permeameter during their field surveys. According to Elsenbeer and Vertessy (2000), the primary activities that lead to fragmentation, timber extraction and swidden agriculture reduce the saturated hydraulic conductivity in the near-surface soil profile. This reduction was thought to be able to increase the likelihood of hortonian overland flow generation and saturated overland flow (Elsenbeer and Vertessy, 2000). They concluded that hydraulic conductivity was the most sensitive and significant soil parameter in generating surface runoff and subsequent soil erosion.

Since accurate measurement of hydraulic conductivity is generally cumbersome, many attempts have been made to develop indirect methods which predict the conductivity function from the easier water retention curve. In 1950 Childs and Collis-George (Brooks and Corey, 1964) first showed that unsaturated hydraulic conductivity could be derived from moisture retention functions. A number of researchers later followed the work of Childs and Collis-George to show the validity of this approach (Jackson, 1972). Jackson (1972) introduced a matching factor to marry Marshall and Millington-Quirk's methods (Millington and Quirk, 1961). He introduced an exponent of 1, to calculate hydraulic conductivities for a field soil from laboratory-determined pressure head - water content relation.

Campbell (1974) established a method of obtaining unsaturated hydraulic conductivity function for a soil from a moisture retention function and a single measurement of hydraulic conductivity at some water content. The method directly calculates hydraulic conductivity with accuracy comparable with experimentally determined conductivities for the five soil samples that were used.

In essence, research in hydraulic conductivity is as old as soil studies. Currently, there is no research method that has offered a lasting solution as to be universally acclaimed. Research is still going on how to resolve the issue of a universally accepted method that can allow rapid, accurate and consistent measurement of K_s in the field.

2.4 Determination of hydraulic conductivity

2.4.1 Factors affecting hydraulic conductivity

Owing to stratification in soils, hydraulic conductivity in one direction is often different from another in the other direction. A soil in which conductivity at any point has preferential directions is called anisotropic (Kessler and Oosterbaan, 1962). If the anisotropy varies from point to point in a given layer, the layer is said to be heterogeneous. However, if the condition of anisotropy is the same from a point to another in the layer, the layer is said to be homogeneous (Kessler and Oosterbaan, 1962). The inherent heterogeneity of soils at catchments scale makes hydraulic conductivity a highly varied soil physical parameter.

Factors which affect soil saturated hydraulic conductivity can be broadly classified as;

1. Surface entry and transmission through the soil
2. Soil characteristics
3. Fluid characteristics

Surface entry and transmission through soil

The soil surface characteristic is strongly influenced by rainfall energy and the presence or absence of protective covers such as vegetation. The raindrops which normally impact on the soil surface destroy the surface structure and form a crust, which reduces the infiltration rate (Arya et al., 1999). According to Arya et al. (1999), the crusts developed on a soil surface is directly proportional to rainfall energy and inversely proportional to soil aggregation and surface cover.

Infiltration on the surface alone, does not explain water movement in the soil. Water cannot infiltrate into the soil faster than it is being transmitted downward through the soil profile. If subsurface transmission rates are low (that is, low K_s), water will rise up the soil profile and reduce the infiltration on the surface.

Soil characteristics affecting K_s

The primary soil factors affecting K_s are: the number and diameter of the pores present in the soil (Arya et al., 1999), aggregate stability, soil texture and soil chemistry (Bresler at al., 1984), bulk density and soil structure (Goncalves et al., 1999), and swelling property of the soil (Lagerwerff, 1969).

Soil factors affecting K_s are also influenced by vegetation. Vegetation promotes higher infiltration rates by protecting the soil surface raindrop impact, by adding organic matter to the soil and by root action, which penetrates the soil and creates macropores when the roots decay (Arya et al., 1999).

Fluid characteristics affecting K_s

Turbid water containing colloids, which can clog the soil pores as it infiltrates have the potential of influencing soil K_s. Similarly, Salts present in water and the water temperature which affect the viscosity of infiltrating water also have the potential of influencing the value of soil K_s (Bresler at al., 1984). In fact, some scientists (Bresler at al., 1984) believe that lower viscosities during the rainy season have a significant effect on the magnitude of floods in the tropical regions (Jaetzold and Schimdt, 1983).

2.4.2 Introduction to the various methods of determination

Hydraulic conductivity can be determined either from soil samples in the laboratory or from soil bodies in situ. According to Kutilek and Nielsen (1994), both these methods impose flow conditions on a soil body from which discharge is measured and the conductivity calculated. The formulae used in the calculation describe the relationship between hydraulic conductivity, the flow conditions and the discharge. When hydraulic conductivity is ascertained by water flux density and potential gradient measurements, the method is known as determination of hydraulic conductivity (Kutilek and Nielsen, 1994). However, depending on the difficulties arising, additional assumptions may be introduced to evaluate these two quantities somewhat less directly. In this case, the methods are known as estimation of hydraulic conductivity (Kutilek and Nielsen, 1994). Many methods for estimation of hydraulic conductivity have been described in numerous literatures (Kessler and Oosterbaan, 1962; Klute and Dirksen, 1986; Amoozegar and Warrick, 1986; Kutilek and Nielsen, 1994; Suresh, 1997). For the choice of any laboratory method, Klute and Dirksen (1986) suggested the following criteria:

1. The available equipment
2. The nature of the soil sampled
3. The kind of samples available
4. The soil water-suction range to be covered
5. The purpose for which the measurements are made
6. The skills and knowledge of the experimenter

The common laboratory methods include constant-head method, falling-head method, triaxial cell method, and transducer response method (Remy, 1973; Kessler and Oosterbaan, 1962; Klute and Dirksen, 1986). Kutilek and Nielsen (1994) established, however, that field experiments are quite important in estimating soil hydraulic functions better than laboratory methods. The following reasons stress the importance of field methods over laboratory methods:

1. Owing to significantly large values of soil water potential, laboratory results tend to be quite different from field measurements.
2. In structured soils, sampling and laboratory measurements are more difficult and time consuming than field investigations (Kutilek and Nielsen, 1994).
3. The overburden pressure which naturally occurs in the field is difficult, if not impossible, to reliably achieve in the laboratory.
4. During sampling for laboratory measurements, the field length continuity of large capillary pores are usually disturbed or destroyed with the standard core rings.

Thus, field methods are preferred in estimation of soils' hydraulic conductivity. There are many field methods for estimation of hydraulic conductivity, whichever is appropriate or accurate is still an area for more research. Furthermore, of the many methods, choice of an appropriate one is still not clear. Ankeny et al. (1991) suggested the following criteria for the choice of required field method:

1. Only steady-state infiltration rates are needed. Knowledge of antecedent moisture content are not necessary,
2. Inserting a ring into soil to obtain one-dimensional flow should not disturb soil structure. This way, larger pores are not truncated or collapsed and infiltration through larger pores is less likely to be underestimated,
3. Measurements should be taken on the soil surface,
4. Calculation of hydraulic conductivity should be straightforward,

In addition to the above,

1. The method should be feasible in terms of water use,
2. The determination of hydraulic conductivity should not take too long. This is necessary especially where fast assessment is required in a large area,

3. The tooling should be portable for outdoor movements,
4. The method should be feasible for stony and sloping areas as well.

The field methods can be differentiated into two categories: shallow water table methods and deep water table methods. The shallow water table methods estimate the saturated hydraulic conductivity of the soil below the groundwater table (Amoozegar and Warrick, 1986). According to Amoozegar and Warrick (1986), the most common methods in this category are the auger-hole method and the piezometer method. Other methods in this category include two-well method, four-well method, well-point method, pit-bailing method, field-monoliths methods and pumping or slug test methods (Bouwer, 1978; Freeze and Chery, 1979, Kessler and Oosterbaan, 1962; Amoozegar and Warrick, 1986). Deep-water-table methods are those which estimate the saturated hydraulic conductivity of unsaturated soils located above the water table. The main difference between these two categories is that the original unsaturated soil in the second category must be artificially saturated to perform the measurements. According to Amoozegar and Warrick (1986), measuring hydraulic conductivity of unsaturated soils located above the water table (or in absence of a water table) by in situ methods is much more difficult than measuring hydraulic conductivity for saturated soils. This fact has prompted most of research and scientific concern to be concentrated on surface and subsurface hydraulic conductivity measurements of unsaturated soils (Holland et al., 2000).

2.5 Field methods for estimation of hydraulic conductivity of unsaturated soils

2.5.1 Disc infiltrometers and minitensiometers

This method was developed by Vandervaere et al. (1997) for the measurement of the crust hydraulic conductivity. It is a field method based on the simultaneous use of disc infiltrometer and minitensiometer (Figure 2.1). The methodology is based on sorptivity measurements performed at different water supply potentials and uses transient flow analysis for the calculation of hydraulic conductivity (Vandervaere et al., 1997). According to Vandervaere et al. (1997) the minitensiometer, placed at the crust – subsoil interface, facilitates the analysis of the infiltration regime.

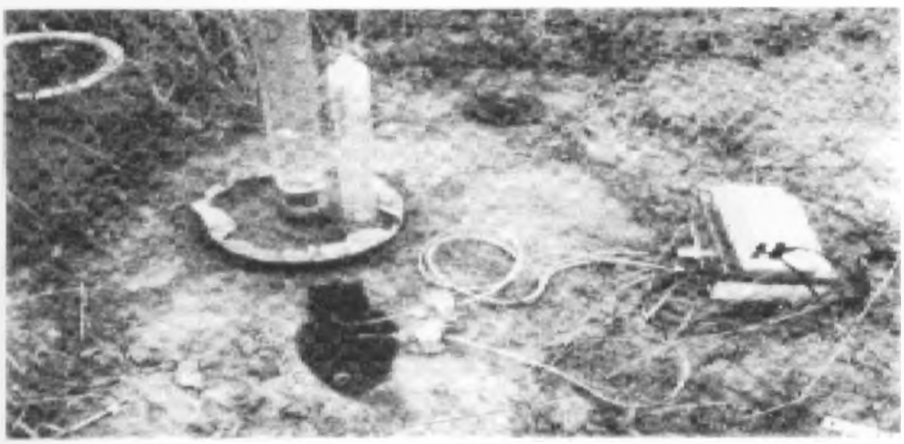

Figure 2.1: Disc infiltrometer fitted with minitensiometer (Vandervaere et al., 1997)

Theory of determination of hydraulic conductivity

In this method, hydraulic conductivity is estimated from sorptivity measurements performed at different supply water potentials (White and Perroux, 1987). According to Vandervaere et al. (1997), sorptivity, initially introduced as the variable driving horizontal absorption, is commonly considered to control the early stages of vertical infiltration, when the effect of gravity is minor. White and

2.5 Field methods for estimation of hydraulic conductivity of unsaturated soils

2.5.1 Disc infiltrometers and minitensiometers

This method was developed by Vandervaere et al. (1997) for the measurement of the crust hydraulic conductivity. It is a field method based on the simultaneous use of disc infiltrometer and minitensiometer (Figure 2.1). The methodology is based on sorptivity measurements performed at different water supply potentials and uses transient flow analysis for the calculation of hydraulic conductivity (Vandervaere et al., 1997). According to Vandervaere et al. (1997) the minitensiometer, placed at the crust – subsoil interface, facilitates the analysis of the infiltration regime.

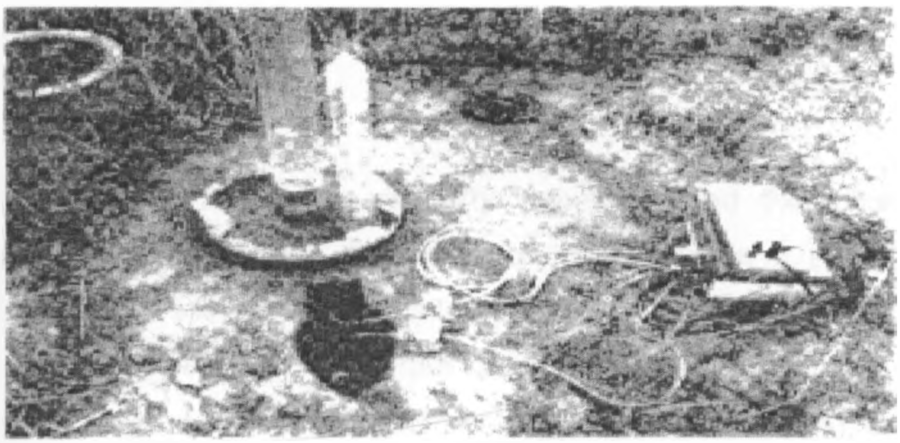

Figure 2.1: Disc infiltrometer fitted with minitensiometer (Vandervaere et al., 1997)

Theory of determination of hydraulic conductivity

In this method, hydraulic conductivity is estimated from sorptivity measurements performed at different supply water potentials (White and Perroux, 1987). According to Vandervaere et al. (1997), sorptivity, initially introduced as the variable driving horizontal absorption, is commonly considered to control the early stages of vertical infiltration, when the effect of gravity is minor. White and

Sully (1987) proposed sorptivity to be related to the matric flux potential (ϕ) through the expression,

$$\phi(h_f) = \frac{bS^2(h_i, h_f)}{(\theta_f - \theta_i)} \tag{2.3}$$

where b is a parameter depending on the shape of diffusivity and having a value range $\frac{1}{2} \leq b \leq \pi/4$, θ is volumetric soil moisture content, i and f are the initial and boundary supply pressure conditions respectively.

Vandervaere et al. (1997) proposed a differential relationship between hydraulic conductivity and matric flux potential of the form,

$$\frac{\partial\phi}{\partial h_f} = K_f - K_i \tag{2.4}$$

where K_f and K_i are the final (or saturated) and the initial soil hydraulic conductivity, respectively. According to Vandervaere et al. (1997) K_i is negligible as compared with K_f in most field situations. Combination of eq. (2.3) and eq. (2.4) enables deduction of K_s from two or more S values. To use, simultaneously, the entire set of (ϕ, h_f) data obtained for each test by eq. (2.4), an analytical form of the $\phi(h_f)$ function would be required. Parlange (1972) and Gardner (1959) suggested the exponential form for ease of integration,

$$\phi(h) = \frac{K_s}{\alpha}\exp(\alpha h) \tag{2.5}$$

Thus, $\log_e \phi$ values when plotted against h_f can be used to determine the parameters K_s and α by fitting the linearized form of eq. (2.5).

Advantages of the method

1. The method estimates hydraulic conductivity of crusts with precision of a factor of 2 (Vandervaere et al., 1997)
2. The method allows the estimation of a functional mean pore size, which is consistent with laboratory measurements
3. The method is also particularly suitable for sandy crusts, for which the decrease in conductivity must be more accentuated
4. Little water is needed for a complete run with the method.

Limitations of the method

1. It is not recommended to use the method where crusts have a high surface roughness because of the need for a thick layer of sand
2. The method is also not recommended for use on crusts thinner than 1cm because of the difficulty of placing the minitensiometer at the crust – subsoil interface
3. The method would be impracticable for large area survey owing to extra carriage needed for tonnage of required sand
4. Measurements on sloppy areas (if crusts may be there) would be cumbersome.

2.5.2 Mini disk infiltrometer

Mini disk infiltrometers have been established to provide quick and convenient measurement of soil hydraulic conductivity (Zhang, 1997). The infiltrometer is constructed of an acrylic tube with a semi-permeable plastic disk, and a rubber stopper (Figure 2.2). A small tube is installed a short distance above the disk to regulate the suction rate (Decagon Inc., 1998). According to Zhang (1997) the infiltrometers are ideal for irrigation scheduling, classroom instruction, and many other applications that rely on accurate measurement of water conductivity.

Figure 2.2: Mini disk infiltrometer (Decagon Inc., 1998)

Theory of determination of hydraulic conductivity

When the disk (full of water) is placed on the soil surface, water infiltrates into the soil owing to the water tension on the disk being broken (Decagon Inc., 1998). During infiltration the volume changes, which are recorded at regular intervals, are used for evaluation of hydraulic conductivity.

The resulting measurements of infiltration vs. time, which are fitted with the function,

$$q = \left(C_1 t + C_2 \sqrt{t}\right) \tag{2.6}$$

are used to evaluate hydraulic conductivity according to,

$$K_s = \frac{C_1}{A} \tag{2.7}$$

where,

$$A = \frac{11.65(n^{0.1} - 1)\exp[2.92(n - 1.9)\alpha h_o]}{(\alpha r_o)^{0.91}} \qquad \forall\ n \geq 1.9 \tag{2.8}$$

or

$$A = \frac{11.65(n^{0.1}-1)\exp[7.5(n-1.9)\alpha h_o]}{(\alpha r_o)^{0.91}} \qquad \forall\ n < 1.9 \qquad (2.9)$$

n and α are the van Genuchten parameters for the soil (van Genuchten, 1980), r_o is the disk radius, h_o is the suction at the disk surface, q is the steady infiltration rate and C_1 and C_2 are constants (Decagon Inc., 1998).

Advantages of the method

1. The standard 2cm infiltrometer is perfect to measure hydraulic conductivity of all soils,
2. The 0.5 cm and 6 cm suction infiltrometers are made available so researchers can glean additional information about the soil by eliminating macropores with an air entry value smaller and larger than the bubble pressure of the infiltrometer,
3. The instrumentation is portable and uses little water.

Limitations of the method

1. As a prerequisite for field measurement, the method requires surface modification to remove things that might prick the membrane of the disk,
2. The method requires a prior knowledge or separate determination of van Genuchten parameters n and α.

2.5.3 Disc permeameter

Disc permeameters (Figure 2.3) were designed to measure hydraulic properties of field soils containing macropores and preferential flow paths (Perroux and White, 1988). According to Perroux and White (1988), there are two designs for disc permeameters: positive and negative water supply potentials. With these designs, both ponded and unsaturated sorptivities can be measured to find the saturated hydraulic conductivity of the soil (Perroux and White, 1988). During infiltration events, the water enters the soil in response to gradients of water potential and gravitational potential. The water potential term is governed by the dryness of the soil and the pore structure of the soil (Wooding, 1968). These two factors combine to form a sorptivity factor, which is made up of the combined influences of capillary action and adhesive forces to soil solid surfaces. This sorptivity of the soil is often expressed as "S" (Philip, 1957). The gravity term being a constant for different soils is due to the influence of the pore size, continuity and distribution on the rate of water flow through soil under the influence of gravity. This term is known as "A" (Philip, 1957). The sorptive forces of the dry soil largely govern the initial water infiltration rate, which is then replaced once the soil wets up, by the gravity term. When too much sand is used during contact surface preparation, sorptivity values become quite high (Philip, 1957).

Theory of determination of hydraulic conductivity

The method for determining soil hydraulic conductivity from disc permeameter in the field is given Perroux and White (1988). This is based on an analysis (Wooding, 1968) of the three-dimensional flow from circular pond or surface. According to Perroux and White (1988) hydraulic conductivity at the surface (K_s) is given by,

$$K_s = \frac{q}{\pi r_o^2} - \frac{2.2 S_o^2}{\pi r_o (\theta_t - \theta_r)} \tag{2.10}$$

Figure 2.3: Disc permeameter (Perroux and White, 1988)

The first term in eq. (2.10) is obtained from the slope of the graph of cumulative infiltration versus time (Perroux and White, 1988).

Advantages of disc permeameter

1. They are very easy to set up, operate and transport
2. Obtaining data from these permeameters is a lot easier than the double ring infiltrometer (Perroux and White, 1988)
3. The method is quite accurate (Vandervaere et al, 1997)

Limitations of the method

1. The measurement of air entry pressure is not well elaborated in the method though very important for the estimation of K (Holland et al, 2000)
2. When using the disc permeameter, a good intimate contact between the disc and the soil surface needs to be established (Holland et al, 2000). This is often achieved by using contact material such fine sand. The drawback of using such a material is that it will interfere with the

measurements especially in the early stages of infiltration, giving inaccurate sorptivity values

3. Where there is a large proportion of macropores in a site, inaccurate results are inevitable with ponded version (positive head) of disc permeameter. This is due to the water tower being not able to supply water quickly enough (White et al, 1992).

2.5.4 Tension infiltrometer

This is an instrument which can determine in situ unsaturated hydraulic conductivity made at several tensions (30 – 150 mm of water potential) on the same infiltration surface (Ankeny et al., 1991). According to Ankeny (1992) the method utilizes unconfined infiltration measurements to determine unsaturated hydraulic conductivity (Figure 2.4). The unconfined measurements provide a less destructive method of measuring infiltration properties than methods requiring the establishment of one-dimensional flow (Ankeny et al., 1991).

Figure 2.4: Tension infiltrometer (Ankeny et al., 1991)

Theory of determination of hydraulic conductivity

Reynolds and Elrick (1991) used Wooding's solution for infiltration from shallow pond (Wooding, 1968) to describe and derive steady tension hydraulic conductivity. Using shape factor G_d (~0.25) Reynolds and Elrick (1991) showed a straight line equation for steady infiltration rate with the supply tension given by,

$$\ln q = \alpha\varphi_o + \ln\left[\left(\frac{a}{G_d\alpha} + \pi a^2\right)K_s\right] \tag{2.11}$$

where a is the diameter of the surface disc. Saturated hydraulic conductivity and α parameter can thus be estimated from the *lnq* intercept and slope measurement.

Advantages of the method

1. It has two pressure transducers which eliminates bubbling noise in a Marriott system, and increases measurement precision (Ankeny, 1992)
2. Possible automation reduces labour required for data collection and analysis
3. Water reservoirs of various diameters can be interchanged to match soil infiltration properties to reservoir size
4. The method requires neither measurement of the change in volumetric water content on the infiltration surface, nor estimation of sorptivity from the early square-root-of-time infiltration behaviour (Smetten and Clothier, 1989)
5. The approach in the method requires only one setup and only one infiltration surface. This eliminates possible errors resulting from use of different infiltrometer radii on soils that are spatially heterogeneous (Reynolds and Elrick, 1991).

Limitations of the method

1. According to Reynolds and Elrick (1991), the main theoretical limitation is the requirement that initial infiltration rates be very small compared to final infiltration rates. This technically limits the analysis to low tension applied to relative dry soil
2. A small $\Delta\varphi_l$ (~ 0.01m) may be required to maintain a high level of accuracy (~ ±7%) (Reynolds and Elrick, 1991). This can significantly increase the number of data pairs needed to cover the wet-end range of φ_o
3. Sand requirements hinder its extensive use for large area diagnosis.

2.5.5 Subsurface tension permeameter

This method works nearly on the same principles as the disc permeameter. The instrument was developed by Holland et al. (2000), during their study for measurement of subsurface unsaturated hydraulic conductivity. The permeameter includes a probe (Figure 2.5) that is placed in contact with the soil and connected to a monitored supply of water at negative pressure (Holland et al., 2000). In the field, fine sand is packed between the cup and the soil to provide the conduction pathway (Holland et al., 2000).

Theory of determination of hydraulic conductivity

Using Philip's approximate solution (Philip, 1985) for flow from spherical cavities with gravity and Gardner's exponential model, Holland et al. (2000) derived a log-linear relationship of steady water flow rate and matric potential.

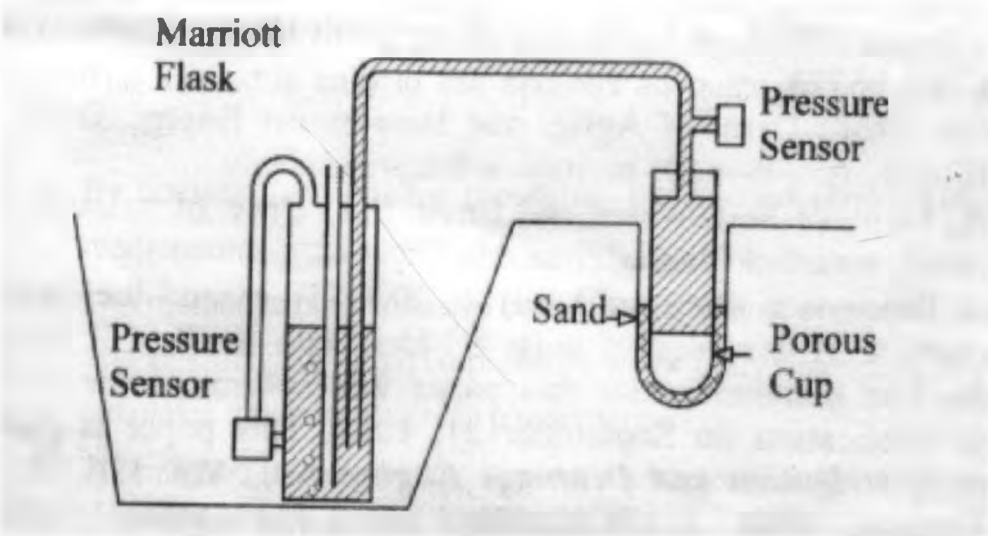

Figure 2.5: Schematic diagram of subsurface tension disc permeameter (Holland et al., 2000)

For a dry soil the relationship is given by (Holland et al., 2000),

$$\ln q = \ln\left(\frac{4\pi r_o K_s}{\alpha(1-0.5\alpha r_o)}\right) + \alpha h_o \tag{2.13}$$

where r_o is the probe radius, which is given by (Holland et al., 2000),

$$r_o = \left[\frac{3d^2 s}{16} + \frac{d^3}{16}\right]^{1/3} \tag{2.14}$$

and d is the cup diameter while s is the length of the cylindrical part not including the hemispherical end. When steady-state flow-rate is plotted against matric potential on log-linear graph, the slope and intercept of expression (2.13) leads to α and K_s (Holland et al., 2000).

Advantages of the method

1. The method is easy to use and has adequate accuracy (Holland et al., 2000)
2. By operating at negative pressures, the method eliminates influence of macropores
3. The method is not expensive both in terms of time and equipment.
4. The utilization of negative-pressure water entry procedure in the method simulates the natural rainfall phenomenon.
5. The method is versatile and appropriate for rapid field measurements.
6. Low water volume and depth-necessity requirements make the method ideal.

Limitations of the method

1. The calculation of hydraulic conductivity by this method requires graph drawing. It thus becomes cumbersome for numerous data collected from the field.
2. The depth requirements for the negative water entry pressure may not be feasible in shallow soils and stony areas.
3. The need for fine sand may preclude its application for large area survey.
4. The line between the measured matric potential and suspected wetting front suction is quite tenuous

2.5.6 Double tube infiltrometer

Bouwer developed this method in 1959 (Bouwer, 1961). It consists of two tubes, which are filled with water during infiltration tests (Figure 2.6). The principle involves initial monitoring of infiltration in both tubes followed with monitoring of the infiltration in the inner tube when the outer tube is kept at a constant head. To counteract the rate of infiltration in the inner tube, head difference with the outer tube is increased (Bouwer, 1961).

Theory of determination of hydraulic conductivity

According to Bouwer (1961), the hydraulic conductivity is computed from the following relationship:

$$K = (r_p)^2 / \left[(r_i)^c \Delta h \int_0^t h_c(t)dt \right] \tag{2.15}$$

where r_p is the radius of inner tube standpipe (mm), $\Delta h = h_e(t) - h_c(t)$ (mm), $h_e(t)$ is the drop of water level in inner tube under equal level condition in time t minutes, $h_c(t)$ is the drop of water level in inner tube under constant outer level condition in a time interval of *t* minutes, and *c* is geometry factor

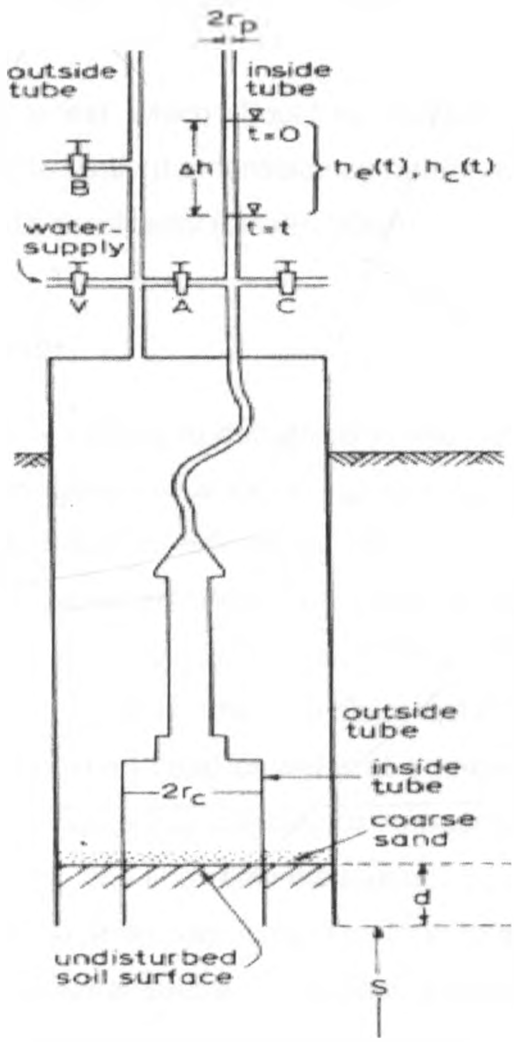

Figure 2.6: Schematic diagram of Double Tube Infiltrometer (Kessler and Oosterbaan, 1962)

Advantages of the method

1. According to Bouwer (1966), this method is good as it takes into account sorptivity losses in infiltration.
2. It is possible with the method to sustain a steady flux of water into the soil

Limitations of the method

1. The heavy apparatus together with the precautions that must be taken makes the method fairly involving and cumbersome.
2. Linsen (1969) suggested after experimentation that the method could not be recommended as a quick and efficient technique, since the application of equation (2.15) above is valid if the infiltration rates remain fairly constant during the test.
3. The constant outer level test, which should be carried out as quickly as possible, and the need to verify the consistency before and after the test, all preclude the method's practicality (Linsen, 1969).

2.5.7 Borehole permeameter

The borehole permeameter is a method to determine in situ saturated hydraulic conductivity of unfissured, homogeneous, isotropic soil and rock above the water table (Stephens, 1992). The method has been variously referred as well permeameter, constant-head borehole infiltration test, reverse auger-hole method, and well pump-in test (Reynolds et al., 1983; Stephens, 1992). According to Reynolds et al. (1983), the principle behind the borehole permeameter is to provide a constant head of water at a known depth down a hole. The equipment (shown in Figure 2.7) consists of four-constant-head tubes, a four-litre water reservoir, a one-litre flow-measuring cylinder, a water-dissipating unit, and a base with a three-way valve. The four constant head tubes can provide up to -200 cm of water pressure. In each constant-head-tube is another tube referred to as the bubble or air tube, which allows the potential to be varied. The principles of operation are contained in Stephens (1992).

Theory of determination of hydraulic conductivity

According to Stephens (1992), by measuring infiltration over time, saturated hydraulic conductivity can be calculated once steady state flow has been reached.

Stephens (1992) developed a solution for the saturated hydraulic conductivity given by,

$$K_s = C\frac{q}{2\pi H^2} \tag{2.16}$$

where C is given by,

$$C = \sinh^{-1}(H/r) - \left[(r/H)^2 + 1\right]^{1/2} + r/H \tag{2.17}$$

and r is the auger hole radius, H is the constant depth of water in the hole and q is the stead-state flow rate.

Advantages of the method

1. It is very easy to transport and set up in the field
2. With the four-constant-head tubes, it is possible to maintain a constant head of water up to two meters below the soil surface and therefore measure the hydraulic conductivity anywhere from the soil surface to a depth of two meters.

Limitations of the method

1. A drawback when using this device is that during auguring, smearing of the hole may occur and consequently interfere with infiltration. Applying araldite and then peeling it off can overcome smearing at the bottom of the auger hole to create an undisturbed surface (Erick and Reynolds, 1992)
2. The method is cumbersome in stony areas

3. Air entrapment and temperature influence infiltration data obtained by this method. Thus, accuracy is a lot more compromised (Stephens, 1992).

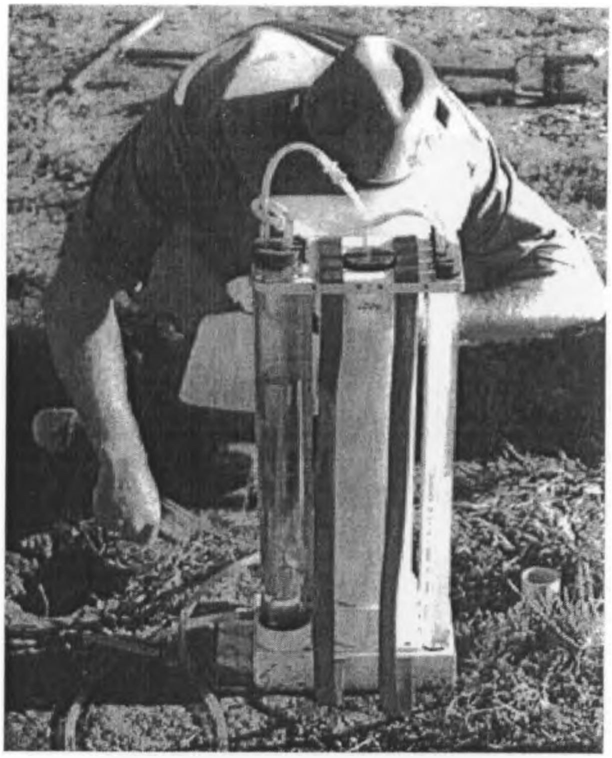

Figure 2.7: Borehole permeameter (Stephens, 1992)

2.5.8 Guelph permeameter

The Guelph permeameter consists essentially of a Marriott bottle that is lowered into a well or a borehole augured into unsaturated soil or other porous media (Talsma and Hallam, 1980). The Marriott serves as a water supply reservoir (Figure 2.8), as a means for maintaining a steady depth of water in the well and as a means for measuring the rate of water flow out of the well and the surrounding unsaturated soil.

Theory of determination of hydraulic conductivity

Talsma and Hallam (1980) derived formulation for hydraulic conductivity based on solution of steady infiltration rates into holes given by Zangar (1953). For steady infiltration rate *q* into a hole of radius *r* and wetted depth *H*, Talsma and Hallam (1980) derived expression for hydraulic conductivity,

$$K = q\{\sinh^{-1}(H/r) - 1\}/2\pi H^2 \qquad (2.17)$$

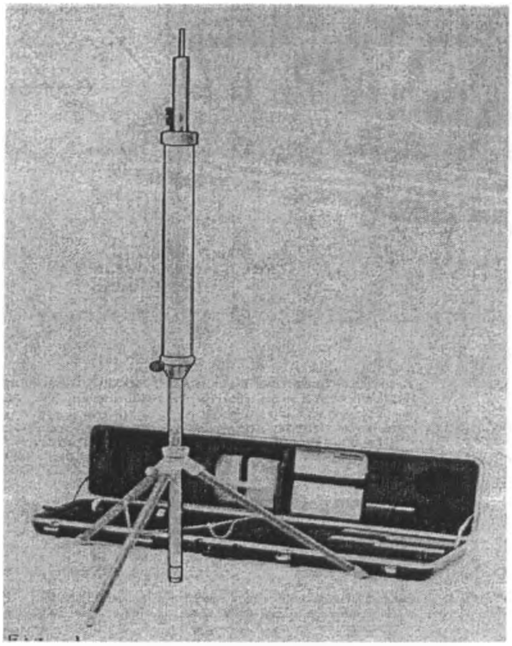

Figure 2.8: Guelph permeameter (Talsma and Hallam, 1980)

Beginning from eq. (2.17), Soilmoisture Inc. (1991) developed an expression (eq. 2.18) taking into account variations on well radius and head of water in the well. They introduced shape factors to contain these variations as follows,

$$K_s = G_2 q_2 - G_1 q_1 \qquad (2.18)$$

where,

$$G_2 = \frac{H_1 C_2}{\pi\left[2H_1 H_2 (H_2 - H_1) + a^2 (H_1 C_2 - H_2 C_1)\right]} \qquad (2.19)$$

and

$$G_1 = G_2 \frac{H_2 C_1}{H_1 C_2} \tag{2.20}$$

Advantages of the method

1. The equipment is portable and convenient for field measurements.
2. The method has been found fairly accurate regardless of soil type (Elrick and Reynolds, 1992).
3. The method is quite versatile in profile characterization.

Limitations of the method

1. The calculation procedure may result with negative hydraulic conductivity, which has no physical meaning
2. Smearing, remolding, and/or compaction of the well surfaces during auguring may affect the accuracy of the method
3. The method utilizes positive headwater entry method, which is not necessarily the replication of the natural phenomenon.

2.5.9 Cylinder infiltrometers

These consist of metal ring(s) driven into the ground surface such that the inner part of the ring can be filled with water. The rate at which this water infiltrates into the ground is measured using a float gauge secured in float-guide. There are two types of cylinder infiltrometers: double ring (Figure 2.9) and single ring cylinder infiltrometers (Rogers, 1970). According to Rogers (1970), the early infiltrometers consisted of a single ring. However, the theoretical objection voiced regarding single ring infiltrometer concept were the alleged lateral movement of water in the soil under the ring. This was thought to cause too high infiltration reading (Rogers, 1970). Owing to this objection, double ring infiltrometers were developed. With the double ring method, the outer ring would supply water to migrate laterally at the same time saturating the soil next to the inner ring (Vijay, 1992). Despite this development, Swartzendruber and Olson (1961) and

Reynolds and Elrick (1990) established that radial flow is not significant in the determination of saturated hydraulic conductivity especially when the ring diameter is incorporated in the analysis. The critical issue is the diameter and not the number of rings used (Swartzendruber and Olson, 1961; Reynolds and Elrick, 1990).

Figure 2.9: Double ring infiltrometer for measuring soil moisture regimes (Amoozegar and Warrick, 1986)

Theory of determination of hydraulic conductivity

The concept of Horton (1933) is utilized in ring infiltrometers to determine the saturated hydraulic conductivity. In this concept, infiltration capacity is perceived to approach a constant minimum, often considered to be the saturated hydraulic conductivity of the soil (Scotter et al., 1982). Scotter et al. (1982) developed an expression for saturated hydraulic conductivity from double ring, based on Wooding 's solution (Wooding, 1968) given by,

$$K_s = \frac{(q_1 r_1 - q_2 r_2)}{(r_1 - r_2)} \tag{2.21}$$

where r is the ring radius and the subscripts 1 and 2 represent outer and inner cylinders respectively.

By including depth of insertion and shape factor, Reynolds and Elrick, (1990) developed an expression for determination of saturated hydraulic conductivity given by,

$$K_s = (\alpha G q)/T \tag{2.22}$$

where shape factor *G*, is given by,

$$G = 0.316\frac{d}{a} + 0.184 \tag{2.23}$$

and T,

$$T = \lfloor a(\alpha H + 1) + G\alpha\pi a^2 \rfloor \tag{2.24}$$

where *d* is the depth of ring insertion, *a* is the ring diameter, *α* is the soil alpha parameter, *H* is the ponding depth, and *q* is the steady infiltration volume.

Advantages of the method

1. The one-H-level calculations have the advantage of speed and simplicity over other procedures, by virtue of the fact that only one level must be ponded and one q value measured
2. The derivation of hydraulic conductivity in this method is not complex.
3. The use of single rings is quite versatile for rapid large area assessment
4. Since the method measures surface hydraulic conductivity, it is ideal for studies on surface runoff generation and watershed response analyses
5. With carefulness, less surface destruction can be registered with the method (Scotter et al., 1982)
6. Field water consumption can be made modest with minimum recommended diameter, (Swartzendruber and Olson, 1961)
7. The tooling is simple and easy to administer.

Limitations of the method

1. When water moves into the soil, reducing the height of ponded water to below that of the bubble tube, more water is fed rapidly into the ring. This might cause disturbance of the surface loose soil, which may later seal the surface.
2. One of the drawbacks of the double ring is that it is time consuming, requiring trial and error when adjusting the bubble tubes to get the equal water levels in each ring.
3. Since the method takes rather too long, inaccuracy in conductivity estimation is compounded by the fact that evaporation is not accounted for.
4. For the double rings, the practicality of the instrument is reduced by the fact that the rings are extremely heavy to move.
5. The method does not duplicate rainfall conditions and must have a substantial depth of water in the ring in order to provide sufficient depth for measurements (Ward, 1989).

2.6 Empirical predictions of hydraulic conductivity

Direct hydraulic conductivity measurements for evaluation of hydraulic functions have been shown to be difficult owing to one or more of the following reasons (Mualem, 1986):

1. The measurements are costly and time consuming
2. The soil variability is such that the amount of data required to represent the hydraulic properties accurately is enormous
3. The hydraulic functions of soils are of a hysterical nature
4. The values of hydraulic conductivity of some soils may vary by several orders of magnitude within the water content range of interest. Most measurement systems cannot efficiently cover such a wide range.

Thus, many predictive formulae have been proposed for some more easily measured soil parameters. These include pedotransfer functions, monographs and empirical formulae.

2.6.1 Pedotransfer functions

Models have been developed to predict field saturated hydraulic conductivity from easily measured and more available soil properties, like particle-size distribution, organic matter content, dry bulk density, soil texture and soil structure. Often, but not exclusively, these models are developed through regression equations (Vereecken et al., 1989). These models are referred to as PedoTransfer Functions (PTFs) (Bouma, 1989).

There are three main groups of PTFs. Group 1 estimates the hydraulic conductivity at a certain matric potential using multiple linear regression (Gupta and Larson, 1979; Rawls and Brakensiek, 1982) or artificial neural networks (Schaap et al., 1998). Group 2 PTFs predict hydraulic conductivity from a closed-form equation (Brooks and Corey, 1964; Rawls and Brakensiek, 1985; van Genuchten, 1980). The procedure also involves artificial neural networks or multiple linear regressions. Group 3 PTFs are based on a physical-conceptual approach of the water retention phenomenon (Ahuja et al., 1985) and uses fractal mathematics and scaled similarities (Tyler and Wheatcraft, 1989; Comegna et al., 1989).

The assumption when developing and using the PTFs is that soils with similar textures have similar structures and pore architectures, and so may have comparable field saturated hydraulic conductivities. However, this assumption holds only within a restricted pedotop. The implication is that such functions remain entirely locally applicable.

2.6.2 Estimation of hydraulic conductivity using monograph

The argument voiced in this technique is that if physical soil parameters have to be useful in hydrologic operations, procedures must be developed to estimate them (Rawls and Brakensiek, 1983). Rawls and Brakensiek (1983) developed a procedure with necessary tables and graphs (Figure 2.10) for estimating soil hydraulic conductivity.

The procedure for estimating soil saturated hydraulic conductivity (as one of the Green and Ampt parameters) based on Rawls and Brakensiek (1983) model is given in figure 2.10 below.

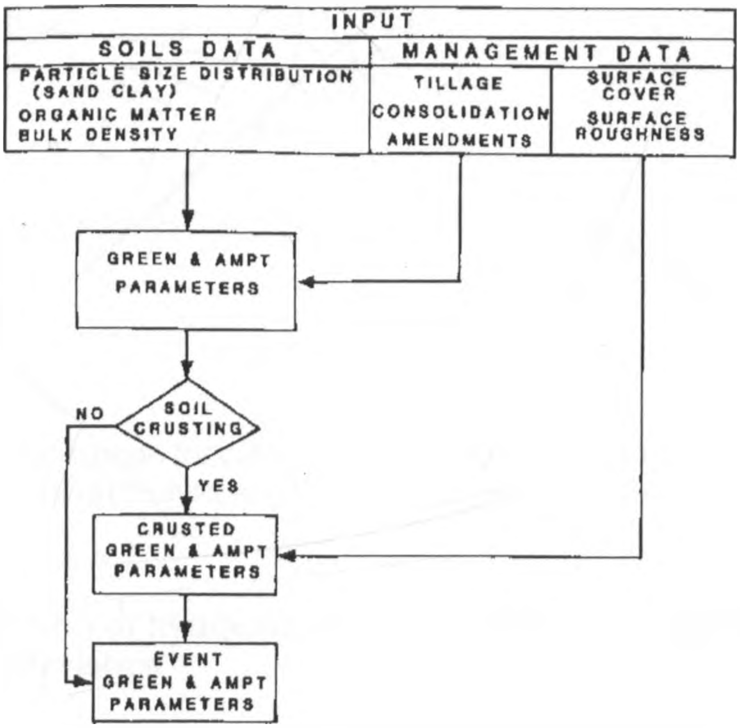

Figure 2.10: Procedure for estimating saturated hydraulic conductivity from monograph (Rawls and Brakensiek, 1983).

While using the flowchart in figure 2.10 above, the soil texture centroid values of sand and clay are used as the base values to determine saturated hydraulic conductivity using figure 2.11 below. If the value of saturated hydraulic conductivity falls between two graphs in the chart, a linear interpolation is used (Rawls and Brakensiek, 1983).

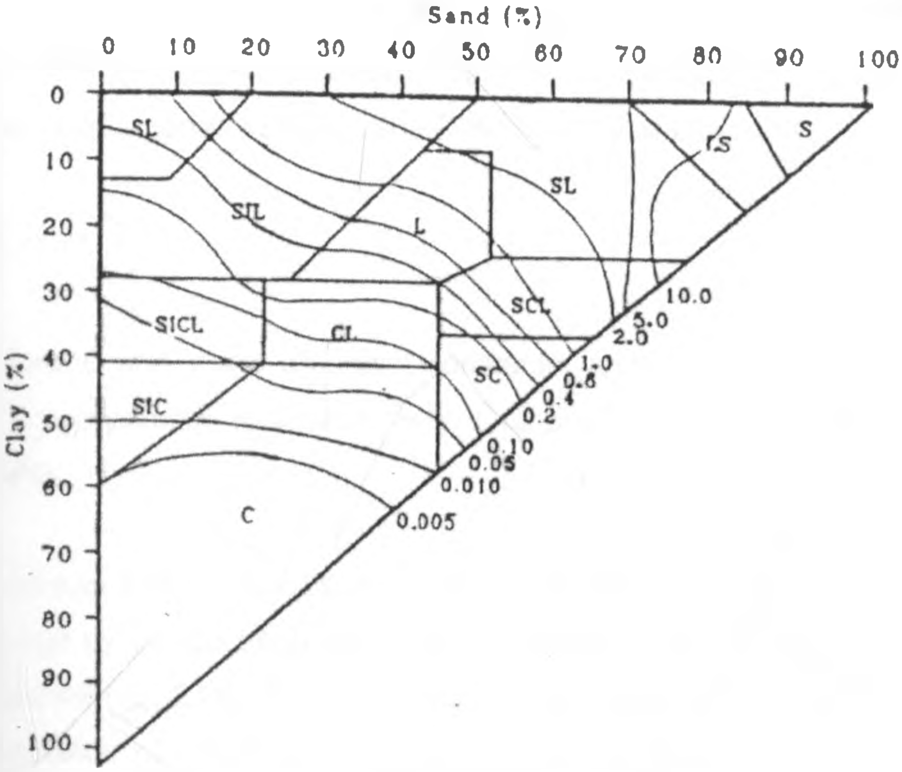

Figure 2.11: Monograph for calculating soil saturated hydraulic conductivity (cm/hr) (Rawls and Brakensiek, 1983)

2.6.3 Estimation of hydraulic conductivity from moisture retention characteristics

One of the factors affecting the flow of water in a saturated soil is size and distribution of macropores in the soil. In developing functions that can relate soil K_s to other soil factors, inclusion of soil macropore terms would be a great asset (Messing, 1989). According to Messing (1989), the possibility of using water retention characteristics in estimating saturated hydraulic conductivity has been of general interest since the retention data is fundamental in describing soil macropore characteristics.

Saturated hydraulic conductivity can be estimated from soil moisture characteristics while utilizing an empirical power equation on the effective porosity of the soil (Ahuja et al., 1984). Ahuja et al. (1984) developed a relationship between saturated hydraulic conductivity (K_s) and effective porosity based on a generalized Kozeny-Carman equation given by:

$$K_s = B * (f_e)^x \tag{2.25}$$

where B and x are empirical constants, and f_e is the effective porosity. The effective porosity was taken to be total porosity less field capacity (Ahuja et al., 1984).

Suleiman and Ritchie (2001) modified the Ahuja et al. (1984) equation (eq. 2.25 above) by introducing a term '*Relative effective porosity*' which incorporates field capacity (eq. 2.26). They viewed the field capacity to be an important factor in estimation of saturated hydraulic conductivity since it is a resistance factor in saturated flow analysis (Suleiman and Ritchie, 2001).

$$K_s = 75 * (f_{er})^2 \tag{2.26}$$

where f_{er} is defined as effective porosity divide by field capacity.

2.7 Soil spectral reflectance and soil properties

In describing soil properties, soils scientists have long used soil colour to help in classifying soils and to infer soil characteristics (Ben-Dor and Benin, 1990). According to Ben-Dor (1999), certain qualitative relationships have since been established between colour and soil properties on the basis of the collective observations and conceptual understanding of the interaction of visible light with soil material. The interaction of light and soil material often can be studied in reflectance pattern (or spectrum) which allow distinctive characteristics to be screened out. Recent advances in the use of visible-near-infrared reflectance for rapid characterization of soil properties provide new opportunities for development of pedotransfer functions that relate soil hydrological properties directly to soil refelctance, which is a rapaid and non-destructive measurement (Shepherd & Walsh, 2002).

2.7.1 The concept of soil spectral reflectance signatures

The technique of soil spectral reflectance to unveil soil properties utilizes the principle of light interaction with matter to reveal certain properties of the matter as displayed in the reflected light radiations. Light as an electromagnetic radiation, is a dynamic form of energy that is capable of passing through a vacuum and yet becomes apparent when it interacts with matter such as soil (Suits, 1983). Often, the characteristics of reflected light after interaction with matter give some distinctive properties of the reflected light which correlates uniquely with the properties of the matter (Suits, 1983). The success of screening informative characteristics of that matter from reflected radiations lies in the sensitivity of the reflectance detecting device. Modern spectrometers and radiometers have been used to allow observation of reflected radiations more precisely and objectively (Suits, 1983).

During reflectance and absorbance of light by matter, the energy changes cause electronic transition of atoms and vibrational stretching and bending of structural groups of atoms that form molecules and crystals of the matter. The transition and vibrations of atoms at higher levels of energy give reflectance with fundamental features, which may spread over a span of wavebands (Figure 2.11). The relationship between reflectance or absorbance and wavelength of light has been termed a 'spectrum' (Ben-Dor and Benin, 1990).

Spectral reflectance refers to the amount of light at each wavelength reflected from an object as compared to a pure reflection (e.g., from a pure white object that reflects 100% at all wavelengths). Spectral transmittance refers to the amount of light at each wavelength that is transmitted through an object as compared to the amount transmitted through a clear medium such as air. The scientific concept of using spectral reflectance to describe object features has often been referred to as reflectance spectroscopy (Cudahy and Ramanaidou, 1997).

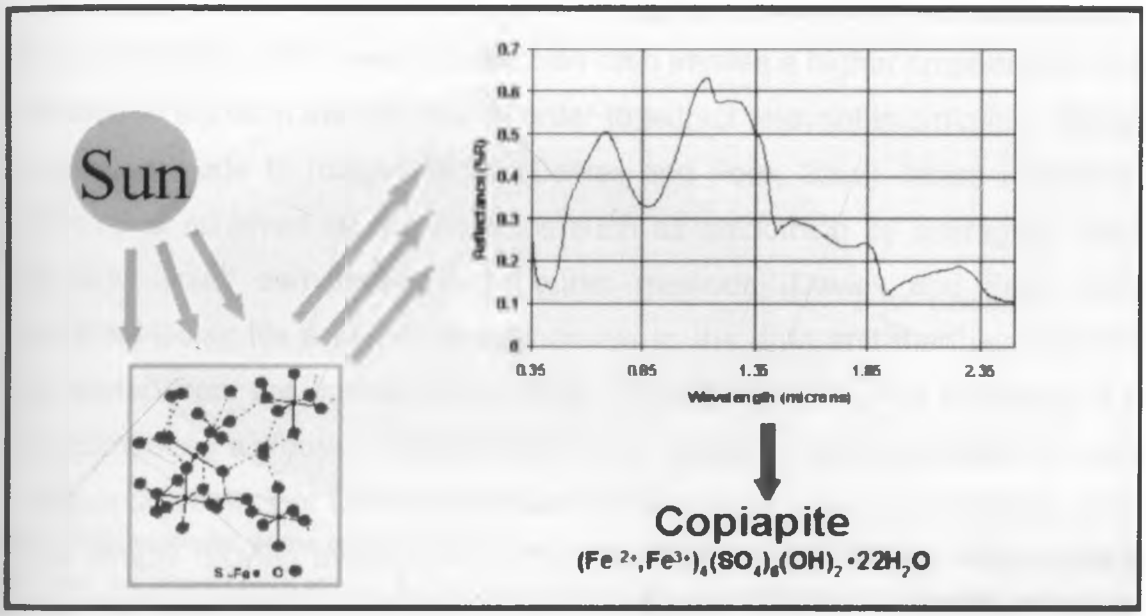

Figure 2.11: Spectral reflectance of light (Cudahy and Ramanaidou, 1997)

In soils, spectral reflectance and transmittance features occur in the visible range (V, 400nm – 700nm), near infrared range (NIR, 700nm – 1000nm) and the short wave infrared (SWIR, 1000nm – 2500) ranges. Certain qualitative relationships between these spectra and soil properties have been well recognized by scientists (Ben-Dor et al., 1999). In soil science, reflectance spectroscopy has proven invaluable in characterizing the surface of soils of the earth for purposes as varied as mineral exploration (Cudahy and Ramanaidou, 1997) or soil property determination (Ben-Dor et al., 1999).

2.7.2 Characterization of reflectance spectra

Most spectral reflectance emitted from illuminated bodies has background absorption, which mask meaningful identification of the features of the spectra. The mask that drapes spectrum reflected from illuminated bodies is known as a continuum. Continuum removal enables isolation of particular absorption features for analysis and identification (Clark and Roush, 1984) as shown in Figure 2.12. Even with removal of continuum, spectra still contains information about analyte of interest alongside information about other properties and noise from the instrument and the environment. This background noise is characterized by the signal-to-noise ratio: low signal-to-noise ratio implies a higher proportion of noise relative to signal in the spectra. In order to extract relevant information, attempts are often made to remove noise (Davies and Fern, 2002). Noise reduction in spectra is achieved by the methods such as smoothing by averaging, use of Savitzky-Golay derivatives, and Fourier methods (Davies and Fern, 2002). Savitzky-Golay fits a series of polynomials to the data and then uses the data computed from the curves (Fern, 2002). Fourier removes high frequency noise by computing a Fourier transformation and setting a large proportion of higher frequency coefficient to zero and then transforming (Cowe and McNicol, 1985). The simple moving average is by far the most popular. Other noise reduction methods also often used through pre-processing include: derivatives, multiple scatter correction (MSC), standard normal variate (SNV), optimized scaling (OS) and orthogonal signal correction (OSC) (Naes et al., 2002).

Soil spectral reflectance can be acquired in the laboratory or directly from the field. Soil reflectance data acquired from the field involve additional difficulties such as low signal-to-noise ratio and atmospheric attenuation where solar radiation is used as a light source. In addition, problems with artificial-light source in the field include variable moisture content, soil surface structure and small area (point-measured) of soil scanned. These problems greatly hinder meaningful use of in situ spectral scanning in the field. Thus laboratory oriented spectral scanning has gained popularity over the decades as spectral data acquired from the laboratories are often done under controlled conditions, which rather minimizes spectral variation (Ben-Dor et al., 1999).

To describe objectively soil spectral reflectance signatures with a view of identifying principal absorption areas, characterization of features is normally done (Tsai and Philpot, 1998). Characterization of spectral features (Figure 2.13) involves determination of:

1. centre of absorption, which is the wavelength of the most intensely absorbed radiation feature
2. depth of absorption feature or spectral contrast, which is the difference between lowest and highest point of feature in the units of reflectance
3. full width at half maximum, and
4. symmetry of absorption , which is the ratio of the left side to the right side of feature at full-width-at-half-maximum.

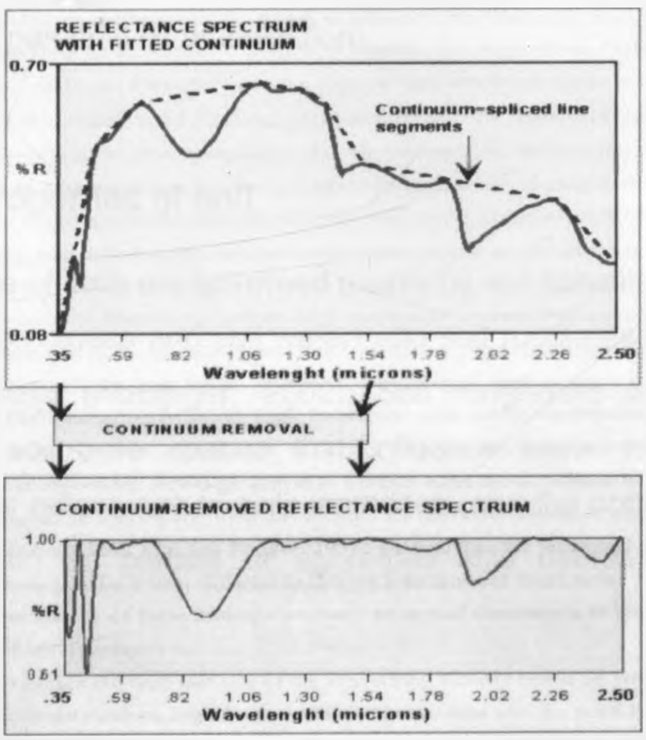

Figure 2.12: Process of continuum removal (Montero et al., 2001)

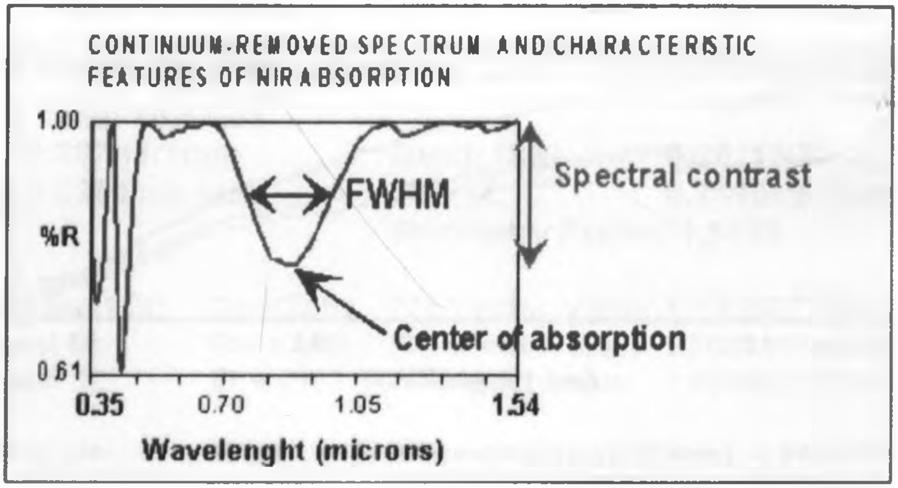

Figure 2.13: Features of absorption (Montero et al., 2001)

Soils, however, are extremely complex medium and the spectra are of many overlapping absorption features due to overtones. Thus it is difficult to interpret individual absorption features in soils and emphasis is placed on relating soil properties of interest to subtle variations in the shape of the spectra (Shepherd and Walsh, 2002, personal communication).

2.7.3 Optical properties of soil

Spectral properties of soils are governed mainly by soil constituents (such as soil organic matter, iron oxides and soil water) and soil roughness (such as particle and aggregate size) (Atzberger, 2002). Soil roughness is quite critical in determining the soil pore spaces that influence water movement in soil. Generally, spectral reflectance of soils increases (and the contrast of absorption features decreases) as particle or aggregate size decreases (Figure 2.14) (Atzberger, 2002).

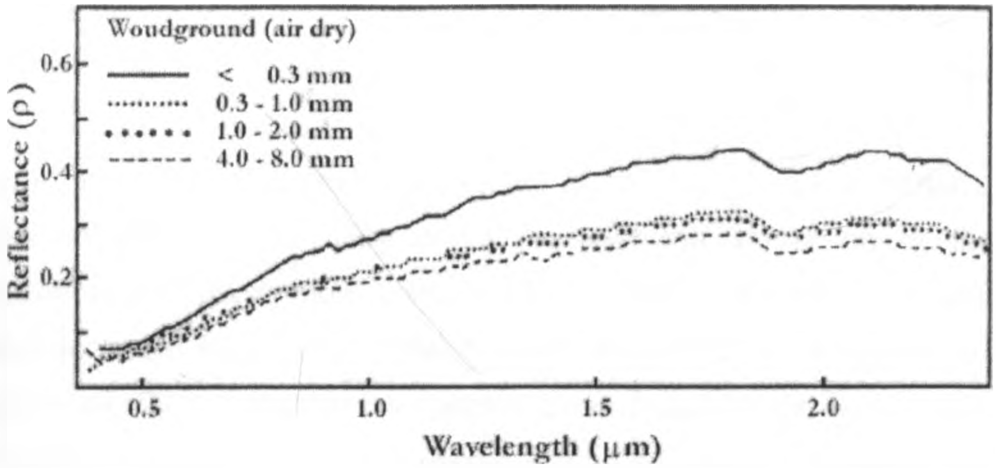

Figure 2.14: Variation of spectral reflectance with soil particle size (Atzberger, 2002)

From the fact that a given wavelength of a material of a given refractive index reflects light with an intensity that varies with the particle diameter (Montgomery and Baumgardner, 1974), the importance of surface roughness is thus evident. Studies of Montgomery and Baumgardner (1974) found that silt content is the most significant parameter explaining the spectral variations in their soils. They, thus, suggested the dependency of spectral reflectance on soil-pore distribution. Since silt content also affects the pore-size distribution and geometry, it affects water flow properties in general and saturated hydraulic conductivity in particular (Gerberman and Neher, 1979).

Empirical research has also established relationships between soil properties and the characteristics of scattered radiation focused predominantly on the spectral distribution (Cooper and Smith, 1985). For example, Ben-Dor and Benin (1990) demonstrated a correlation between reflectance spectra and carbonate concentration in soil. They used a calibration set of soil spectra and soil chemical data to find three wavelengths that best predicted the calcite content in arid soil samples. Ben-Dor and Benin (1990) concluded that the strong and sharp absorption features of the C-O bonds (carbon-oxygen bonds) provided an ideal tool for studying the carbonate content in soils purely from reflectance spectra.

Leger et al., (1979) also studied the effect of soil water, organic matter and iron oxides on soil spectra. They concluded that the interaction of the three components was much more important for understanding the soil spectra than considering them individually. Similarly, Da Costa (1979), working on sandy soils, observed significant changes on spectral curve shapes upon wetting of the soil. He suggested that this kind of change could be attributed to the spectral activity of water in the soils. Still further, Condit (1970) obtained a good correlation between particle distribution, water holding capacity and soil spectral reflectance.

Even though no study has been done so far in relating soil K_s and soil spectral reflectance, the studies above give an encouraging promise to institute a study of relating soil K_s and soil spectral reflectance.

2.7.4 Soil spectral studies in Kenya

Spectral reflectance studies have been going on in many parts of the world with an application significantly shifting from chemometrics to soil science (Ben-Dor et al., 1999). Despite the relevance and the opportunity that spectral reflectance technique offers to soil science, little progress has been shown in its practical application.

In Kenyan soils, Kariuki et al. (2001) used spectroscopy to determine soil activity in the Kenyan soils. In their model development, they found out that although soil is a complex material (and in that case soil spectra), a remarkable amount of information whose physical basis is well understood was hidden in the reflected and absorbed photons (and under controlled conditions). They established from the models that the water representative absorption features are central to estimation of soil activity. They defined soil activity as the term generally applied to the ability of a soil to take in and dispose water under changing moisture conditions. They, thus, demonstrated that soil spectral reflectance could be used to rapidly characterize soil activity.

Shepherd and Walsh (2002) used DRS to predict a number of chemical properties and physical properties of wide range of African topsoils, including many samples from Kenya. They not only developed robust prediction models (which were well calibrated and validated) using new analytical techniques but also built a generalized spectral library approach. Their results demonstrated the feasibility of using reflectance spectrometry for broad diagnosis of soil physical and chemical properties and have opened ways of mapping soil functional attributes across a watershed.

2.8 Spatial structure and mapping of hydraulic properties

2.8.1 Spatial structure of soil hydraulic properties

Soil properties usually vary appreciably within a soil type (Nielsen et al., 1973; Sharma et al., 1980; Webster and Burgress, 1980). The magnitude of variability usually increases with increasing volume (or area) sampled. As the hydrology of an area is strongly influenced by the extent and nature of variability in soil hydraulic parameters, the determination of sizes and numbers of measurements required to define watershed characteristics is important. The sizes and the numbers of measurements required to characterize a given land area depends not only on the variability of the hydrologic parameter but also on its spatial distribution (McBratney and Webster, 1983). The nature and extent of this spatial distribution has to be evaluated to ascertain the systematic and stochastic components.

Many scientists have applied statistical approach to quantify the spatial correlation and structure of soil hydraulic properties (Russo and Bresler, 1981). Both the conventional statistics and geostatistics have been used. As the conventional statistical approach neglects the spatial structured arrangements of the natural porous medium, a more complete approach to treat field variability of soil hydraulic properties must use statistical descriptions that incorporate the spatial structure of the properties.

Since the soil system is always regarded as a continuum, its properties are then continuous functions of space co-ordinate. The hydraulic properties continuum is represented as a realization of a spatial (three-dimensional) stochastic process that is governed by probability laws (Yevjevich, 1972). Conceptually, each such stochastic process can be considered as an ensemble of realizations that have the same statistical properties. The spatial variations of a given hydraulic property in one realization of the ensemble have been found to represent all the possible variations of the property in all realizations of the ensemble (Yevjevich, 1972). This revelation enables scientists to replace ensemble averages by space averages. Consequently, description of spatial structure has been achieved with this concept through the use of spatial correlations expressed in form of semivariograms and cross-semivariograms (Kachanosky et al., 1985).

2.8.2 Spatial correlation and mapping of hydraulic properties

An implicit assumption in the spatial analysis of hydraulic properties is that the observations of a given property are independent of one another, regardless of their location in the field. With this assumption and by using the central limit theorem, scientists have drawn some consequences about the sampling scheme that can help in area-wide mapping of the property. (Cassel and Bauer, 1975; Warrick and Nielsen, 1980). More recently, an emphasis has been placed on the fact that variations of a soil property are not always completely disordered over a field and that spatial structure must be taken into account in the mapping of the soil property (Russo and Bresler, 1981). This has lead to discovery of spatial correlation between measurements of a property that can be chained together in a network of interrelationships to form a map.

In order to establish these interrelationships, a large number of samples that are spatially distributed need to be taken. However, in many practical situations one variable presenting spatial structure may not have been sampled sufficiently (due to experimental difficulties) to provide estimations of acceptable accuracy. In order to overcome this limitation, precision of mapping can be improved by considering the spatial correlation between measurements that can allow spatial estimation at points not visited. This procedure is known as kriging (Journel and Huijbregts, 1978). Thus, mapping of soil functional attributes has been based on spatial correlation between point-measurements of the property investigated (Webster and Burgress, 1980). Geostatistical kriging technique has been found invaluable in this respect (Vauclin et al., 1983).

CHAPTER III

3. MATERIALS AND METHODS

3.1 The study area

The study was conducted in Awach watershed of the Lake Victoria Basin (Figure 3.1). The watershed lies between the latitudes 0^{o} 15' S and 0^{o} 24' S and the longitudes 34^{o} 59' E and 35^{o} 06' E, covering an area of approximately four hundred square kilometers. The watershed was selected on the basis of various reasons. The watershed is very heterogeneous in terms of soils and climatic conditions, resulting into diverse land use and land cover types. This is a true representation of a tropical watershed. Secondly, the watershed is one of the prime contributors of sediment plume, which is generally viewed as a major cause of the lake eutrophication (Hecky, 1993; Mugidde, 1993; Hecky, 2000). Lastly, Awach watershed is one of the densely populated watersheds in the Lake Victoria basin where poverty lurks on humanity (Hoekstra and Corbett, 1995). Scientific interventions are being sought to increase understanding of the watershed responses (such as infiltration and runoff) that can culminate into improved agricultural watershed management. Area-wide mapping of hydraulic conductivity is one such positive step towards achieving this objective.

Awach watershed experiences two climatic regimes: humid subtropical climate in the upland areas and warm tropical climate in the lowland areas (Appendix B). Besides these climatic variations, there is also diversity in precipitation between seasons (alternating dry and wet seasons) in the extreme parts of the watershed. Heavy showers of 6 mm/min and daily totals of 600 mm do occur in the upland areas while lowland areas experiences fairly lower than that (Jaetzold and Schimdt, 1983). Unlike rain in the upland areas, rainwater in the lowland areas is warm (Jaetzold and Schimdt, 1983), a very important fact in the viscosity of infiltrating water.

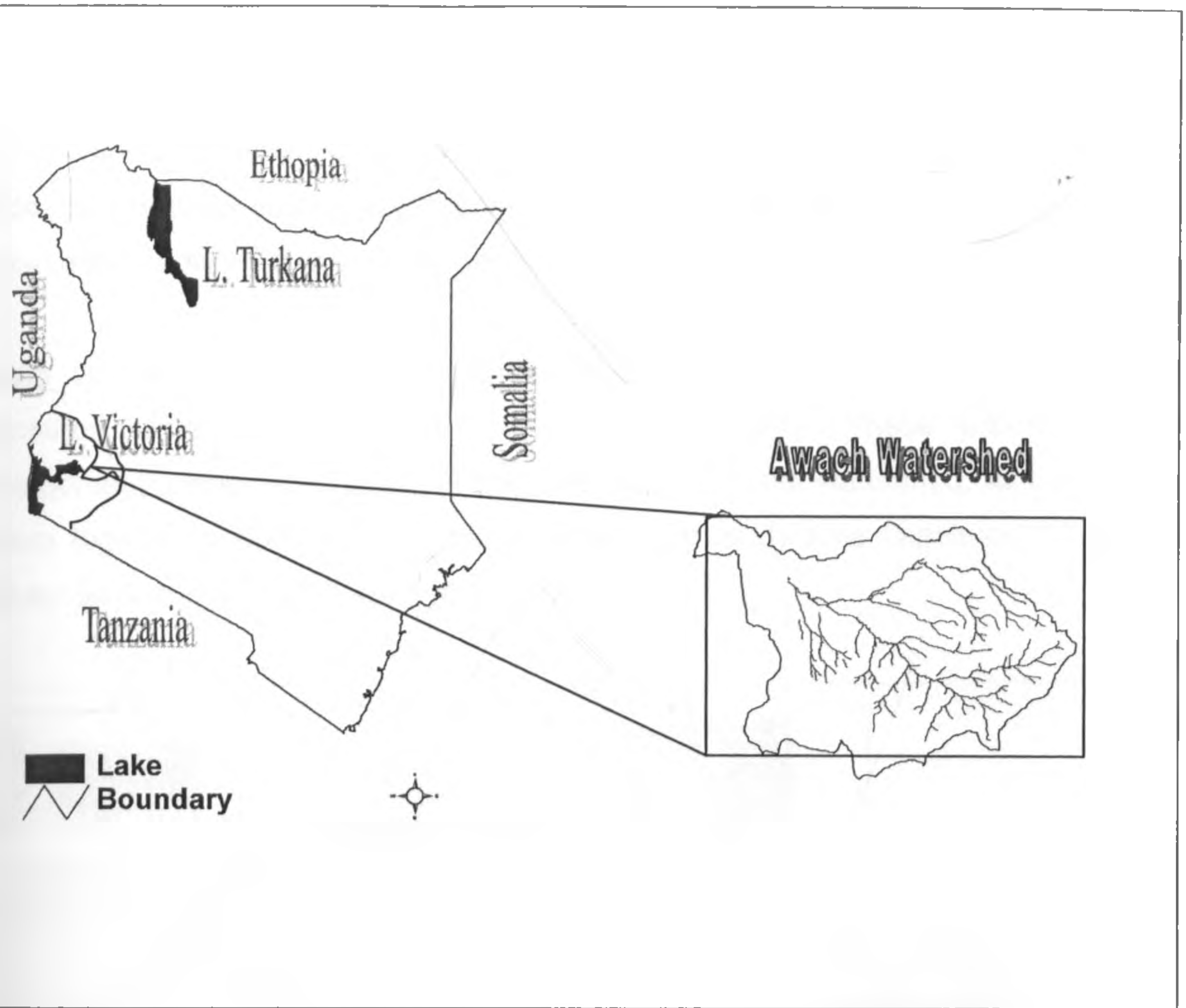

Figure 3.1: Location of Awach watershed in Kenya.

The natural vegetation of the watershed is one of diversified type. The upland and midland Woodland consist of multifarious species of plants while the lowlands consist of a few sparse grasses. For soil formation, these differences are quite important especially in the view of organic matter content. Production of organic matter thus varies from very little in the lowlands to good quantity in the upland and midland areas. Organic matter governs many soil properties, and soil hydraulic properties in particular (Marshall and Holmes, 1979).

Soils in the watershed are differentiated in terms of slope zones: lowland soils, midland soils and upland soils. Lowland soils are by majority imperfectly drained verto-eutric planosols, which are sodic and/or cracking clay or clay loams. The midland soils of the watershed have gleyic/orthic luvisols that are partly over petrophlinthite (Jaetzold and Schimdt, 1983). These soils are well drained to moderately drained sandy clay loams. The upland soils are well drained deep dark-reddish-brown humic Nitisols (Jaetzold and Schimdt, 1983).

Owing to the variations in the atmospheric climate and pedoclimate, the watershed experiences a lot of management problems. These watershed management problems (Figure 3.2) are stratified across the watershed. All these factors together make the watershed an important study-area candidate for a pioneer work in mapping of soil hydraulic properties.

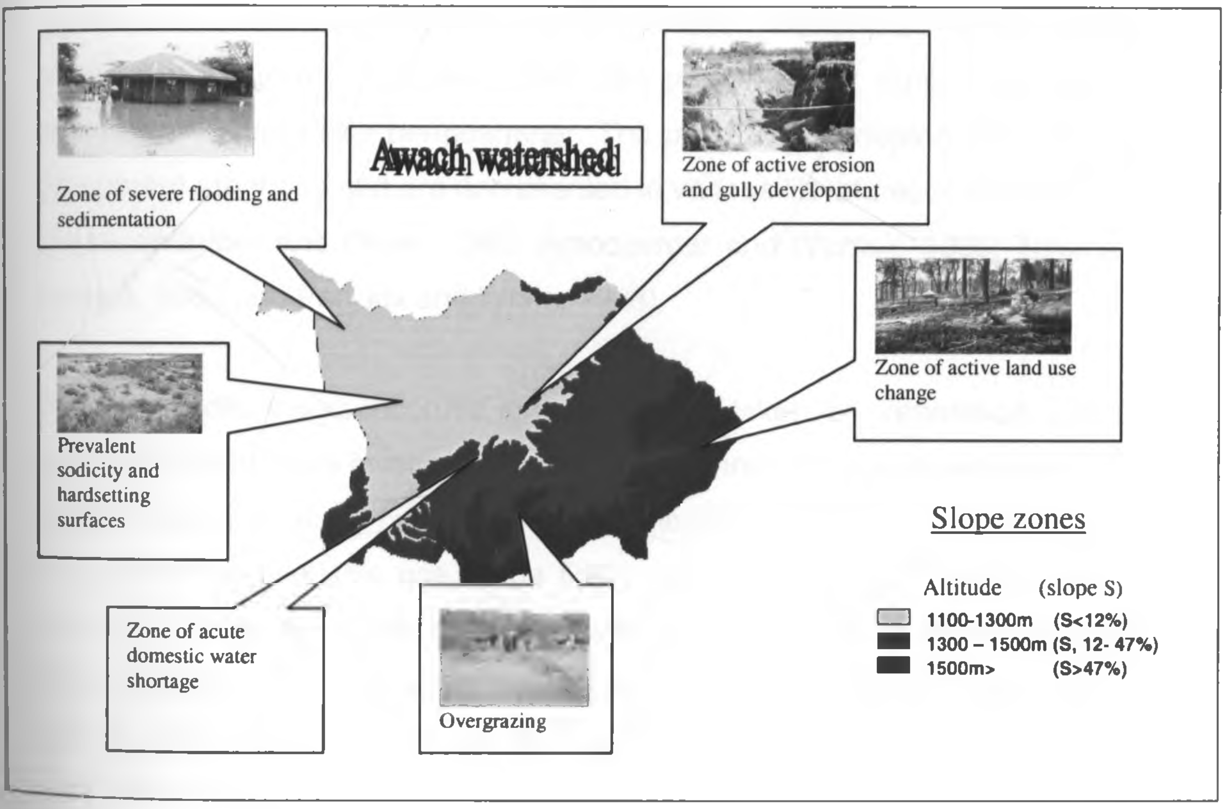

Figure 3.2: Distribution of management problems in Awach watershed (Photos by Shepherd, in 2000)

3.2 Identification of rapid field measurement method

Much as direct field measurements have been applauded for representing true hydrologic status of a field, the methods still suffer from a number of limitations: expensive, cumbersome, time consuming and lack of consistency. It is against this background that a methodology was adopted for identification of a suitable method for rapid field survey.

In order to identify suitable method for rapid survey of K_s, field saturated hydraulic conductivity was repeatedly measured at different spots in a homogeneous field. Six available equipment were each used in a field of approximately 0.8 ha at Upper Kabete Campus of the University of Nairobi. The equipment tested were: double-ring infiltrometer, kamphorst rainfall simulator, single-ring infiltrometer, positive-head disc permeameter, guelph permeameter, and negative-head disc permeameter. The procedures adopted for use of each equipment are those that are documented in various literatures (Constantz, 1983; Swartzendruber and Olsen, 1961; Amoozergar and Warrick, 1986; Talsma and Hallam, 1980 and Perroux and White, 1988).

Time expenditure was recorded in terms of time taken for preparation, execution and calculation; costs involved in terms of personnel, associated accessories and amount of water used; complexity of the method in terms of robustness of the equipment for extensive use in the field; and repeatability of measurements in terms of variability in the measured values. A grading system was adopted (Bouma, 1983) for the methods according to the above criteria. The method that cumulatively ranked highest was then adopted as the suitable method for area-wide field survey.

3.3 Field data collection

3.3.1 Sampling plan

In order to sample as wide variation in hydraulic conductivity as possible in the watershed, one hundred and fifty 30 metre–squared plots were randomly selected over 5100 hectare site in the study area (Figure 3.3). Since saturated K_s has been shown to vary with slope as well as land use type (Bouma, 1983), the sampling was stratified (Appendix C) in terms of slope zones based on the recommendations in the Agriculture act cap 318 of the Kenyan laws (Thomas, 1997); the lowland areas (slopes < 12%), midland areas (12% ≤ slope ≤ 47%), and upland areas (slope > 47%). Nested within each slope zone, different land use types were randomly sampled for K_s. The dominant land use types considered were sparse/bare land (with vegetative cover < 5%); cropland land (all the freshly tilled and those that had crops on them), grazing land (with woody cover < 25%) and Woodland (open woodland with woody cover >50%). The land use types were sampled as extensively as possible within each slope zone, giving rise to unequal number of replications of land use treatments in each slope zone.

The plots, which were georeferenced at the centre with differentially corrected global positioning system (GPS), were laid such that six replicates were made for surface K_s and three replicates for the topsoil (5-20 cm) K_s (Appendix C).

3.3.2 Measurement of hydraulic conductivity and soil sampling

Surface K_s was measured using six single-ring cylinders, 16 cm inner diameter each. The rings were driven into a pre-wetted soil surface according to procedure outlined by Eijkelkamp Agrisearch Equipment Inc. (1983). After two to two and a half hours of ponding water in the rings, steady infiltration (Q_s, in cm^3 per hour) and steady ponding depth (*W*, in cm) the depth of ring insertion (*d* in cm) were recoded for each ring.

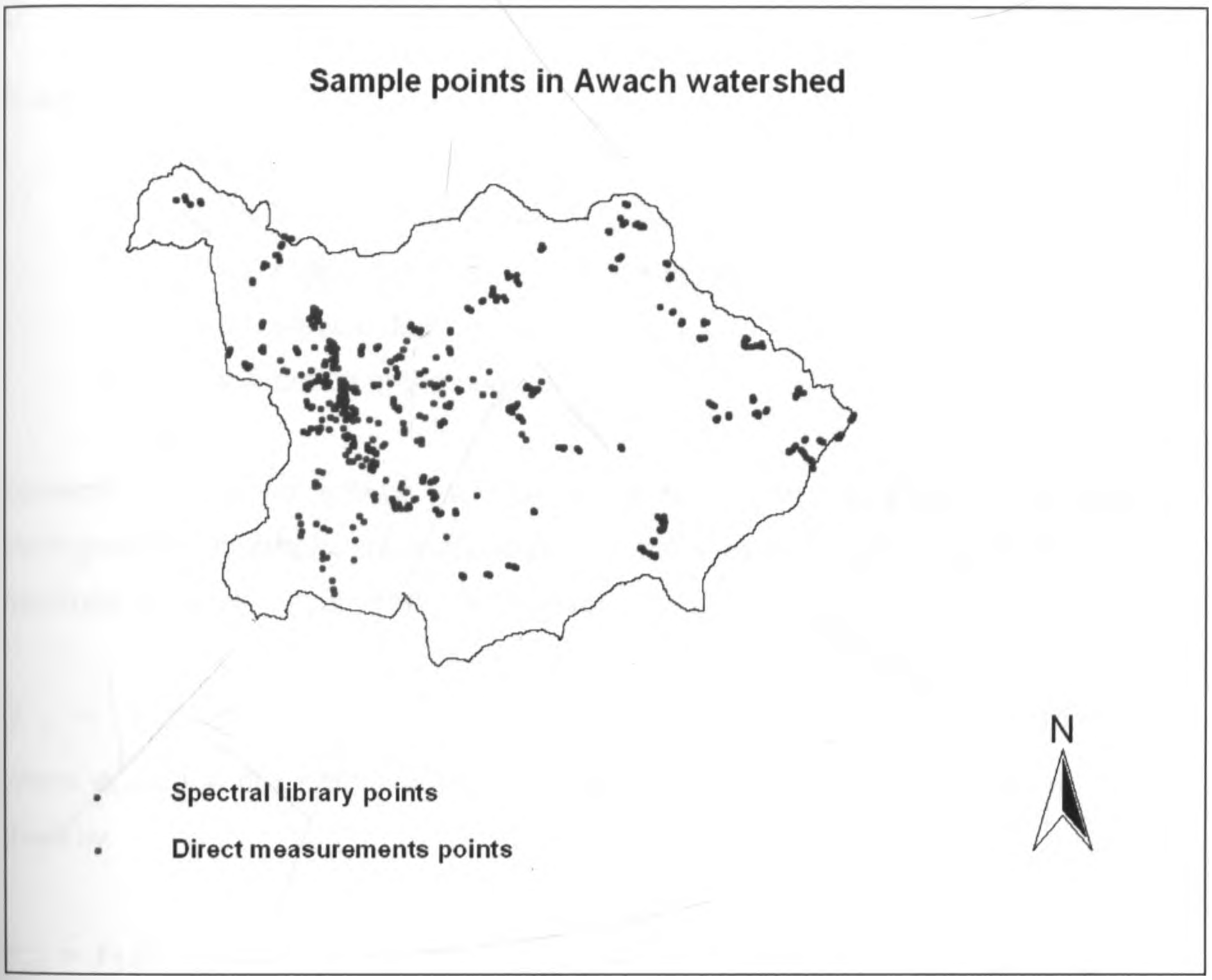

Figure 3.3: Sample plots in the study area

The determination of field K_S was based on mass balance equation of flow into soil. According to this criterion, the steady infiltration from a single ring (Q_s) can be approximated by

$$Q_t = Q_p + Q_g \qquad (3.1)$$

where Q_p and Q_g are the steady water out flows from the ring due to hydrostatic and capillary pressure, and due to gravity, respectively.

$$Q_g = \pi a^2 K_s \tag{3.2}$$

$$Q_p = 2\pi \int_0^a \left. \frac{\partial \phi}{\partial z} \right|_{z=0} r dr \tag{3.3}$$

In equation (3.2) and (3.3):

ϕ	is the water flux potential
K_s	is the soil saturated hydraulic conductivity
r	is the radius space co-ordinate of infiltrating surface
z	is the vertical depth of soil
a	is the radius of the ring cylinder

Considering a point source of steady pressure and capillarity in a rigid, homogeneous, isotropic, semi-infinite porous medium, outflow from a ring can be assumed (Reynolds et al., 1985) to be given by

$$Q_p = 2\pi a \phi_{a,0} \tag{3.4}$$

where $\phi_{a,0}$ is the flux potential at cylindrical co-ordinates $(a,0)$ (figure 3.4) and is given by

$$\phi_{a,0} = f(K(h))$$

Expanding $\phi_{a,0}$ numerically produces

$$\phi_{a,0} = \int_{\varphi_i}^{\varphi_{a,0}} K(h)dh = \int_0^{\varphi_{a,0}} K(h)dh + \int_{\varphi_i}^{0} K(h)dh \tag{3.5}$$

$$= K_s h_{a,0} + \phi_m \tag{3.6}$$

where $h_{a,0}$ is the hydrostatic pressure head (m) at ($a,0$), which is taken to be equal to the steady ponding depth (W),

ϕ_m is the matric flux potential

$K(h)$ is the unsaturated hydraulic conductivity which is a function of the capillary pressure head, h

Substituting equation (3.6) into equation (3.4) and combining with equation (3.2) and (3.1) gives

$$Q_s = 2\pi a(K_s W + \phi_m) + \pi a^2 K_s \tag{3.7}$$

Since $K_s \equiv \alpha\phi_m$ (Gardner, 1959), where α is the soil alpha parameter, equation (3.7) can be rewritten as

$$K_s = \frac{\alpha}{\pi\left(2a[\alpha W + 1] + \alpha a^2\right)} Q_s \text{ m/s} \tag{3.8}$$

However, equation (3.8) does not include gravity-capillary interaction. To incorporate this interaction effect, Reynolds et al. (1985) introduced a dimensionless shape factor G so that equation (3.8) becomes

$$K_s = \frac{G\alpha Q_s}{[a(\alpha W + 1)] + G\alpha\pi a^2} \tag{3.9}$$

G can be interpolated from tables or approximated from (Reynolds and Elrick, 1990)

$$G = 0.316\frac{d}{a} + 0.184$$

where d is the depth of ring insertion into the soil. With measurements of steady infiltration rate Q_s, the ring radius a cm and steady ponding depth W, and determination of α from water retention characteristics, equation (3.9) was used in the study to calculate K_s from single ring cylinders. On the one hand, the steady infiltration rate Q_s was measured as the final steady drop rate of ponded water in the ring (Appendix, C). The steady rates of drop in water level were measured with transparent rule slid at one side of the ring (Figure 3.4). On the other hand, determination of α was done in the laboratory (see section 3.4).

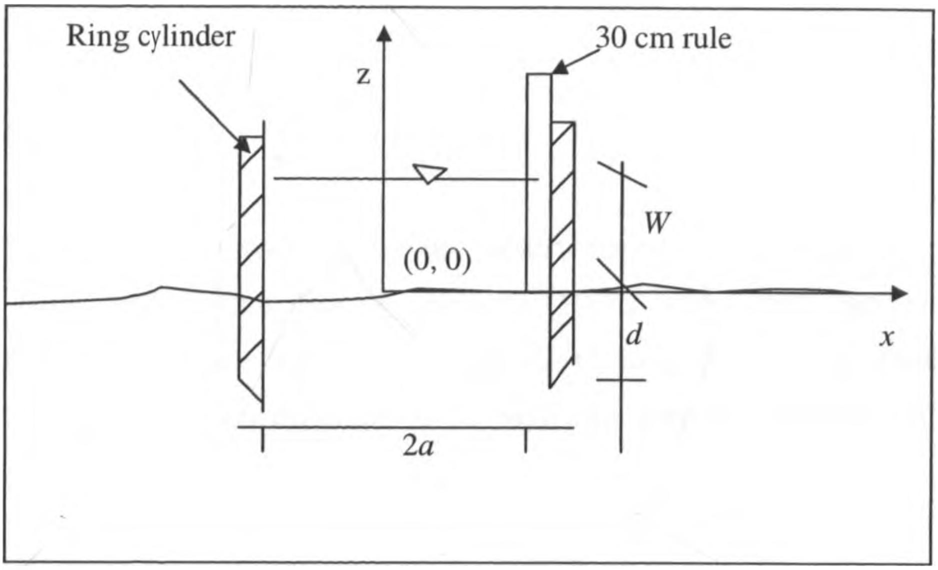

Figure 3.4: Measurement of saturated hydraulic conductivity with ring cylinder

On the other hand, measurements of topsoil K_s were made using guelph permeameter. The procedure involved drilling a hole (or well), of internal radius *a* cm, and flooding it with water. The rates of water out flow at known ponding depths were measured according to methods given in Soilmoisture Equipment Inc. (1991) (AppendixC.4).

The steady water out flow from an auger-hole due to hydrostatic and capillary pressures depends primarily on the ratio of ponding depth to well radius (*W/a*) (Reynolds and Elrick, 1991). Thus from equation (3.1)

$$Q_s = Q_g + Q_p$$

$$= \pi a^2 K_s + \frac{W}{G_p}(K_s W + \phi_m) \quad (3.10)$$

G_p which is a function of ponding depth, well radius and soil texture (Gp = f(W,a, soil texture)) is evaluated from monographs using the well documented procedures in Soilmoisture Equipment Inc. (1991).

From equation (3.10), if ϕ_m is replaced with K_s/α, it becomes

$$K_s = \frac{1}{\pi a^2 + \frac{W}{G_p}\left(W + \frac{1}{\alpha}\right)} Q_s \tag{3.11}$$

$$= GQ_s \tag{3.12}$$

Equation (3.12) contains two unknowns, which cannot be solved with one equation. Thus Soilmoisture Equipment Inc. (1991) suggested use of two ponding depths (W_1 and W_2) to evaluate K_s more precisely. Soilmoisture Equipment Inc. (1991) used equation (3.13) with two steady infiltration rates to solve for K_s

$$K_s = G_2 Q_2 - G_1 Q_1 \tag{3.13}$$

where

$$G_2 = \frac{W_1 C_2}{\pi\left[2W_1 W_2 (W_2 - W_2) + a^2 (W_1 C_2 - W_2 C_1)\right]}$$

and

$$G_1 = G_2 \frac{W_2 C_1}{W_1 C_2}$$

C_1 and C_2 are obtained from monographs following the steps reported in Soilmoisture Equipment Inc. (1991). In this study, equation (3.13) was used in calculating K_s of topsoil.

During the K_s survey, disturbed and undisturbed soil samples, for spectral analysis and pF analysis respectively, were also collected at every point of saturated hydraulic conductivity measurements at depths between 0 – 20 cm deep. There were three replicates of these soil samples in each plot visited

(Appendix C.2). Disturbed soil samples were collected using a soil auger and packed in polyethene bags for laboratory analysis. Undisturbed soil samples were collected using cylindrical core rings (52 mm high and 51 mm wide) according to procedures documented in Reginato and van Bevel (1962).

3.4 Laboratory methods

3.4.1 Determination of soil alpha parameter

The determination of soil alpha parameter required establishment of soil water retention characteristic curve. Thus, on each sample, water retention at pressure heads of 0.0, 0.1, 0.5, 1, 3, 5, 7, 10, and 15 bars was measured using pressure membrane (Reginato and van Bevel, 1962) (Figure 3.5). The van Genuchten (1980) model for soil water retention characteristics was used in deriving soil alpha parameter.

The van Genuchten's water retention model is given by

$$\frac{\theta-\theta_r}{\theta_s-\theta_r}=\left[\frac{1}{1+(\alpha h)^{1/1-m}}\right]^m \qquad (3.14)$$

where α is the soil alpha parameter, m is van Genuchten's curve shape factor, θ is volumetric soil moisture content, h is soil capillary pressure head and the subscripts r and s denote the residual and saturated soil moisture conditions, respectively (van Genuchten, 1980).

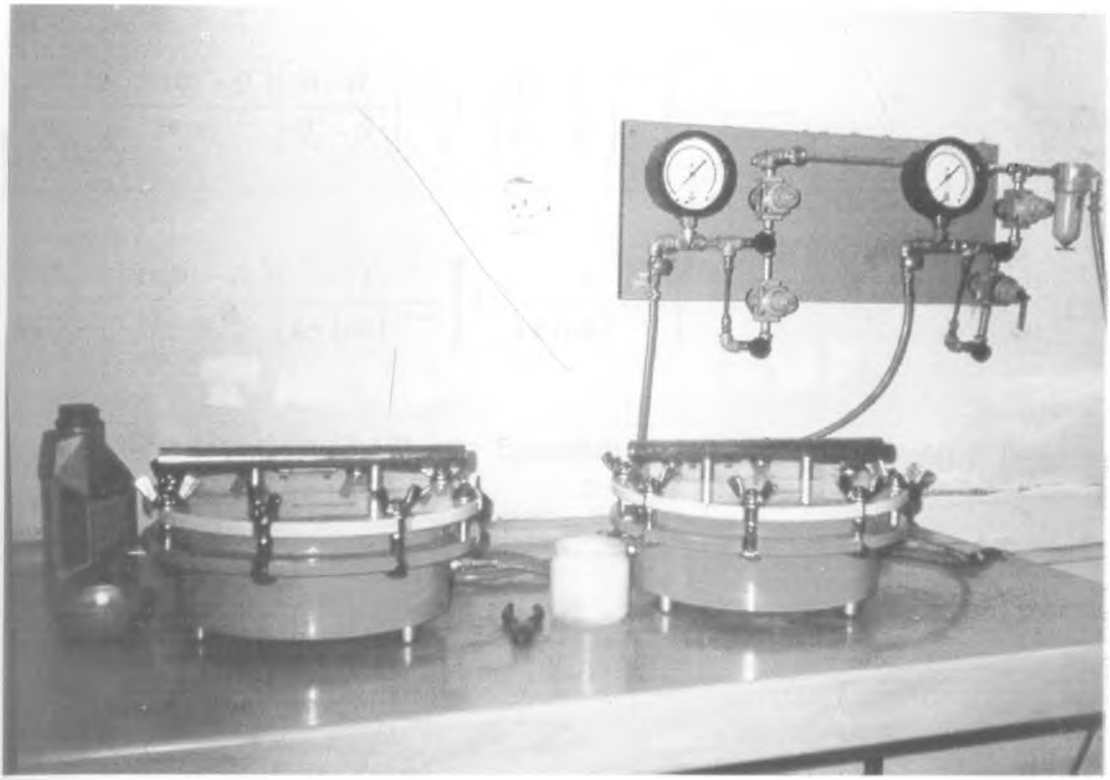

Figure 3.5: Pressure membrane for pF determination

Equation (3.14) can be rewritten as

$$\theta = \theta_r + \frac{\theta_s - \theta_r}{\left[1 + (\alpha h)^{1/1-m}\right]^m} \qquad (3.15)$$

In terms of the alpha parameter

$$\alpha = \frac{1}{h}\left[\left(\frac{\theta - \theta_r}{\theta - \theta_s}\right)^{-1/m} - 1\right]^{1-m} \qquad (3.16)$$

In order to determine α from equation (3.16), the value of m must be known from the soil water retention curve. Knowledge of m from the soil water retention curve requires numerical treatment of equation (3.15). Thus, differentiating equation (3.15) with respect to capillary pressure head gives

$$\frac{d\theta}{dh}=\frac{-\alpha m(\theta_s-\theta_r)}{1-m}\left[\frac{\theta-\theta_r}{\theta_s-\theta_r}\right]^{1/m}\left(1-\left[\frac{\theta-\theta_r}{\theta_s-\theta_r}\right]^{1/m}\right)^{1/m} \tag{3.17}$$

$$\frac{d\theta}{dh}=\frac{-\alpha m(\theta_s-\theta_r)}{1-m}\left[\frac{1}{1+(\alpha h)^{1/1-m}}\right]\left[1-\frac{1}{1+(\alpha h)^{1/1-m}}\right]^{m} \tag{3.18}$$

Substituting equation (3.16) into Equation (3.17) and expressing h in terms of $(\theta-\theta_r)/(\theta_s-\theta_r)$ yields

$$h\frac{d\theta}{dh}=\frac{-m(\theta_s-\theta_r)}{1-m}\left[\frac{\theta-\theta_r}{\theta_s-\theta_r}\right]\left\{1-\left(\frac{\theta-\theta_r}{\theta_s-\theta_r}\right)^{1/m}\right\} \tag{3.19}$$

In this study equation (3.19) was used to solve for the value *m*. The determination of *m* was simplified by considering $\frac{d\theta}{dh}$ as the slope of the soil water retention at the midpoint (van Genuchten, 1980) (Appendix A.1). The alpha parameter,α of eq. (3.16) was used in eq. (3.9) to determine the soil surface K_s with single ring method.

3.4.2 Determination of soil spectral reflectance signatures

Determination of soil spectral reflectance signatures was achieved by scanning the soils with FieldSpec™ FR spectroradiometer (Analytical Spectral Devices Inc. (1997) (Figure 3.6) under laboratory conditions. FieldSpec™ FR spectroradiometer measures intensity of reflected light in the range from 350 nm to 2500 nm (spanning Ultraviolet, Visible and Near-infrared light) with a spectral resolution less than 0.03 μm (Analytical Spectral Devices Inc., 1997). The intensity of reflected light, which was plotted as a function of wavelength gave distinctive patterns known as spectral reflectance signatures.

In this study, soil spectral reflectance signatures were obtained on air-dried soil samples collected from the field. The choice of air-dried samples was basically for handling convenience as well as to minimize variation due to soil moisture (Ben-Dor et al., 1999). The air-dried samples were first ground gently with wooden pestle and mortar and then passed through a 2 mm sieve (Hunt and Salisbury, 1970). The samples were then illuminated with quartz-halogen lamp housed in a mug-probe (Figure 3.5). The procedure adopted for use of the equipment in scanning are those reported in Shepherd and Walsh (2002).

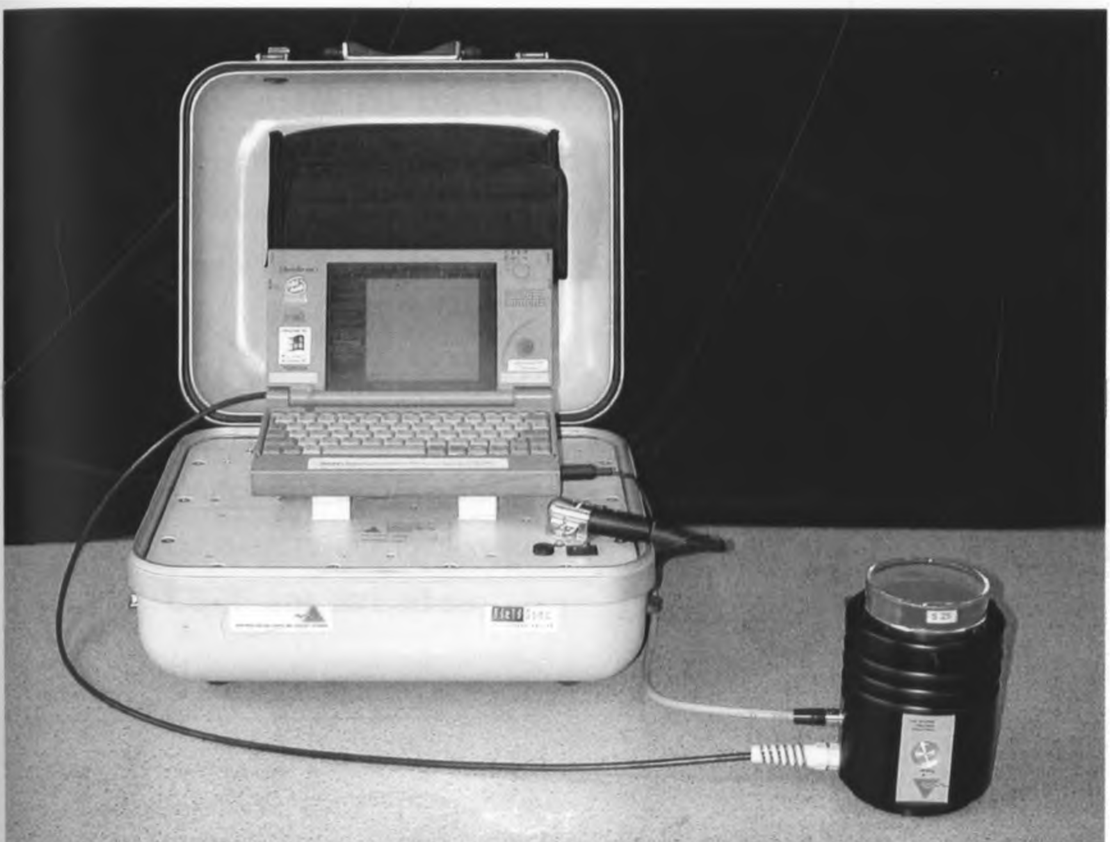

Figure 3.6: FieldSpec^{TM} FR spectroradiometer (Photo by Shepherd)

3.5 Statistical analysis

3.5.1 Analysis of effects of land use type and slope zone effect

Assessment of the variability of measured soil K_s

Before analysis of effects of land use type and slope zone on variability of measured K_s, test for normality of measured K_s was performed. The test was carried out in two stages: (1) check for normality and (2) determination of Probability Density Function (PDF). In checking for normality, the measured values were fitted to the normal distribution function model:

$$f(x) = \frac{1}{\sqrt{2\pi\sigma}} \exp\left(-\frac{1}{2}\left(\frac{K_s - \mu}{\sigma}\right)^2\right) \tag{3.20}$$

where σ and μ are the standard deviation and mean of the measured K_s, respectively. The expected values from equation (3.20) and the measured K_s values were then plotted on a probability graph. The criterion for the normality was based on a near straight-line fit of the graph.

Since many literatures (see chapter 2 of this thesis) have been cited in support of lognormal distribution of field measured soil K_s, the determination of lognormal PDF was performed with Kolmogorov – Smirnov test.. The test was based on empirical cumulative distribution function (ECDF) of N ordered data points K_1, K_2.., K_N, . ECDF was defined as;

$$E_N = \frac{n(i)}{N} \tag{3.21}$$

where $n(i)$ is the number of the points less than K_i, and K_i are ordered K_s values from the smallest to the largest (Miller and Freud, 1985). This step function was increased by $1/N$ at the value of each ordered data point. The criterion for judging the lognormal PDF was based on the hypothesis given as;

H_o: The data follow lognormal PDF

H_a: The data do not follow lognormal PDF

The test statistic for the above hypothesis was pegged at:

$$D = \max\left| g(K_i) - \frac{i}{N} \right| \text{ for all } 1 \le i \le N$$

where

$$g(\ln K_s) = \frac{1}{\sqrt{2\pi\sigma_l}} \exp\left(\frac{\ln K_s - \mu_l}{\sigma_l} \right)$$

and σ_l and μ_l are the standard deviation and mean of the log transformed K_s values.

Null hypothesis regarding the lognormal PDF was accepted as long as the test statistic D was less than 0.05 at 5% level of significance.

Analysis of measured K_s

The structure of measured soil K_s was explored based on the median values of the measured values at plot level. The median values of K_s were categorized by land use types and slope zones to bring out how variable the measurements were within and between land use types and slope zones. The land use types were numbered *1*, *2*, *3*, *4* and *5* for sparse/bare land, cropland land, grassland, shrubland and woodland respectively, while slope zones were designated as *l*, *m*, *s*, and *u* for lowlands, midlands, scarps, and uplands, respectively.

Owing to the influence of soil position (in terms of slope zone) and watershed management (in terms of land use type) on soil K_s, the statistical analysis in this study was designed to investigate the simultaneous effect of these two factors on soil K_s. Hence, a linear mixed effects model was used to explore the effect of these factors.

In the use of the linear mixed effects model, a priori knowledge of occurrence of certain land use types within given slope zones (statistically referred to as interaction) was utilized. Thus, in the model developed, allowance for interaction effects was made. Also, since land use type (which is amenable to watershed management) centres interest on K_s, land use type was treated as a fixed factor while slope zone was viewed as a random factor since inferences were to be made about the variability of K_s at landscape level.
The following model was adopted;

$$(\ln K_s)_{ijk} = \mu_o + \delta_i + \beta_j + (\alpha\beta)_{ij} + \varepsilon_{ijk} \qquad (3.22)$$

where

μ_o is a constant,

δ_i are constants subject to restriction $\sum\alpha_i = 0$ and is indicative of the land use main effects,

β_j are independent and distributed as N $(0, \sigma^2_\beta)$ and represents slope zone effects,

$(\alpha\beta)_{ij}$ are independent and distributed $N(0, \frac{u-1}{u}\sigma^2_{\delta\beta})$, subject to the restrictions

$\sum(\alpha\beta)_{ij} = 0$ for all j

$\sigma\{(\alpha\beta)_{ij}, (\alpha\beta)_{i'j}\} = -\frac{1}{a}\sigma^2_{\delta\beta} \quad i \neq i'$

ε_{ij} are also independent and distributed error terms as N $(0, \sigma^2)$

β_j, $(\delta\beta)_{ij}$ *and* ε_{ijk} are pair wise independent (Neter et al., 1990)

$i = 1,\ldots, u$; $j = 1,\ldots., o$ and $p = 1,\ldots, n$.

where u, o and p are the number of levels of land use type effect, number of levels of slope zone effect and total number of cases of measured K_s, respectively.

From the model, the covariance between measurements was given by;

$\varpi = \dfrac{\sigma_i^2}{\sigma_i^2 + \sigma^2}$, where values of ω > 50% represent good repeatability of measurement (Neter et al., 1990).

The construction of the analysis of variance (ANOVA) was carried on the data by fixing the land use type and randomizing the slope zone effect (Table 3.1). The process was achieved with S – Plus 2000 (Mathsoft Inc., 1999) based on the unequal number of the sample sizes of the factor effects.

Table 3.1: ANOVA for the mixed factor effect

Source of variation	df	Mixed factor levels
Effect of land use type	u -1	$\sigma^2 + nb(\sum\alpha^2_i/(a-1)) + n\sigma^2_\alpha$
Effect of slope zone	o - 1	$\sigma^2 + nu\sigma^2_\beta$
Effect of interaction	uo -1	$\sigma^2 + nu\sigma^2_{\beta\alpha}$
Error	(n – 1) - uo	σ^2

3.5.2 Calibration of spectral reflectance to hydraulic conductivity

Before calibrating the spectra to soil hydraulic conductivity, the spectral reflectance data were first pre-treated. This involved transforming the spectra with first derivative processing using Savitzky-Golay second order polynomial according to equation (3.23) (Savitzky and Golay, 1964):

$$\frac{dR}{d\lambda} = \frac{\frac{f_{i+1} - f_i}{(i+1) - i} + \frac{f_{i+2} - f_{i+1}}{(i+2) - (i+1)}}{2} \qquad i = 1, 216 \qquad (3.23)$$

where R is the relative reflectance, λ is the wavelength, and f_i is the functional relationship of the wave equation.

The transformation was done to minimize variation among samples caused by variation in grinding and optical setup (Martens and Naes, 1989). In this study, smoothing was done with The Unscrambler version 7.5 (CAMO Inc., 1998). The smoothed spectra were then screened for spectral regions with low signal-to-noise ratio. The regions that showed high spectral noise were then deleted from the spectra before calibration. The spectra were then matched to respective samples of K_s using query tables developed in Microsoft Access® (Leszyanski, 1997). Calibration of soil spectral reflectance to K_s was done using partial least squares (PLS) technique.

Since the number of X independent variables (spectral reflectance wavebands) were so many and that the possibility of association between the variables was possible PLS was adopted. The PLS technique attempts to solve the multicollinearity (association) among the independent variables by compressing the variables through a linear fit before relating them to the dependent Y variables. This procedure thus employs both X and Y variables in the estimation directly and involves a model structure given by the two equations;

$$\mathbf{t} = \mathbf{PX} + \varepsilon$$

$$\begin{bmatrix} T_i \\ T_2 \\ \cdot \\ T_n \end{bmatrix} = \begin{bmatrix} P_1 & 0 & \cdot & 0 \\ 0 & P_2 & \cdot & 0 \\ \cdot & \cdot & P_{n-1} & 0 \\ 0 & \cdot & 0 & p_n \end{bmatrix} \begin{bmatrix} X_1 \\ X_2 \\ \cdot \\ X_n \end{bmatrix} + \begin{bmatrix} \varepsilon_1 \\ \varepsilon_2 \\ \cdot \\ \varepsilon_n \end{bmatrix} \qquad (3.24)$$

and

$y_i = \mathbf{qt} + \xi$

$$Y_i = \begin{bmatrix} q_1 & q_2 & . & q_n \end{bmatrix} \begin{bmatrix} T_1 \\ T_2 \\ . \\ T_n \end{bmatrix} + \xi_i \tag{3.25}$$

where **P** is the matrix of loadings and **q** is the matrix of residuals estimated by regressing **X** and Y, while ε and ξ are the residuals which represents the noise or irrelevant variability in **X** and Y, respectively (Naes et al., 2002). Since the association between the independent variables is often directional (Naes et al., 2002), the PLS deals with each direction at a time in developing equations (3.24) and (3.25). Thus, the direction of the first PLS component (usually obtained by maximizing the covariance between Y and all possible linear functions of **X**), could be denoted as vector $\mathbf{w_1}$. This is a unit length vector and is often called the first loading weight vector (Naes et al., 2002). All the scores along this axis are then computed as $\mathbf{t} = \mathbf{X}\ \mathbf{w_1}$. From here, all **X** variables are regressed onto **t** to obtain the loading vector **P**. Similarly, the regression coefficient q, is obtained by regressing **Y** onto **t**. This procedure is then repeated for all the directions until the desired number of components has been extracted. To develop the regression model, the regression coefficient vector for each direction is computed using the equation;

$$\mathbf{b} = \mathbf{w}\ (\mathbf{pw})^{-1}\mathbf{q} \tag{3.26}$$

The estimated model parameters combined with independent **X** variables obtained from the spectral library can then be used on the model to predict the Y variables according to the equation (3.26).

$$\hat{y} = \hat{b}_o + \mathbf{X}\hat{\mathbf{b}} \tag{3.27}$$

In this study, The Unscrumbler version 7.5 (CAMO Inc., 1998) was used to develop a system of the above equations. The Y variables used in the regression model were those of log-transformed values of measured K_s.

However, in order to check on the consistency of the calibration model developed, the whole data set was first split into two groups based on Euclidean distances from the center sample in the principal composite space. Double cross-validatory procedure was used on the split dataset to test predictive consistency. In this procedure, regression models were developed on each half of split dataset and tested on the other half. This way, two measures of consistency and predictive ability of the models were obtained. The following statistics were used;

Coefficient of efficiency, $R^2 = 1 - \dfrac{\sum_{i=1}^{N}(P_i - O_i)^2}{\sum_{i=1}^{N}(O_i - \bar{O})^2}$, $-1 \le R^2 \le 1$

Index of agreement, $d = 1 - \dfrac{\sum_{i=1}^{N}(P_i - O_i)^2}{\sum_{i=1}^{N}(|P_i'| + |O_i'|)^2}$, $0 \le d \le 1$

Root mean square error, $RMSE = \sqrt{\dfrac{1}{N}\left(\sum_{i=1}^{N}(O_i - P_i)^2\right)}$

Bias $= \dfrac{1}{N}\left(\sum_{i=1}^{N}(O_i - P_i)\right)$

Where $|P_i| = P_i - \bar{O}$, $|O_i| = O_i - \bar{O}$, and O_i, P_i, $\bar{O}$ are the observed, predicted and median of the observed values, respectively.

Even though coefficient of determination r^2 and coefficient of correlation r have been used often to express the relationship between the predicted and observed values in a regression model, arguments have been rising against such use (Willmott, 1982). Willmott (1982) showed that statistically significant values of r^2 and r might be misleading, as they are often unrelated to the sizes of the differences between the observed and predicted values. He argued that the relationship between r^2 and r and model performance are not well defined and never consistent. Thus, statistics such as included above have been widely accepted as necessary statistics to depict consistency and accuracy of model prediction (San Jose et al., 2001; Bohler et al., 2002). These statistics take into consideration the magnitude and distribution of differences between the observed and predicted values.

3.5.3 Spatial structure of saturated hydraulic conductivity

In spatial estimation, the basic concern is to determine the relationship between two paired points $[Z(\mathbf{x}_i), Z(\mathbf{x}_i + s)]$ separated by a distance s in space. In this study, $Z(\mathbf{x}_i)$ was taken as a random variable which is a realization of a fixed measurement of hydraulic conductivity at a point $(\mathbf{x}_i)$ in the watershed, and $\mathbf{x}_i$ is a pair of co-ordinates (X_i, Y_i) obtained with GPS.

In geostatistical terms, the tools normally used for the determination of spatial characteristics of a property are the semivariogram and the spatial correlation coefficient. Thus, the spatial structure of hydraulic conductivity (taken as a random stochastic process) in the Awach watershed was described using the semivariogram and spatial correlation coefficient (or correlogram) (Journel and Huijbregts, 1978). However, before exploring the nature of the spatial structure, a three dimensional display of the scattergram was use to determine the directional trend of K_s in the study area. This directional was used as a priori knowledge in building semivariograms and spatial correlation coeffcicent.

In spatial statistics, for a random stochastic process, Z(**x**), the mean E [Z(**x**)] is the mean of all possible realizations of the process at points **x** ≡ (x, y). As the points are considered to act over a random field, the differenced random process Z (**x**) – E [Z(**x**)] is used to represent the departures of the original process from the mean at the points considered. The study of these processes is often based on the identification of appropriate characteristic of regularity in stochastic processes known as *stationarity*. The association of the values taken by the process Z(**x**) at two points $\mathbf{x}_1$ and $\mathbf{x}_2$ in a specified area is represented by the spatial covariance function given by,

$$Cov[x_1, x_2] = E\{(Z(x_1) - E[Z(x_1)])(Z(x_2) - E[Z(x_2)])\} \tag{3.28}$$

If $\mathbf{x}_1 = \mathbf{x}_2 = \mathbf{x}$, eq. (3.28) becomes the variance whose square root is the standard deviation of the process at the given point. The covariance function basically measures the association between two variables. However, where it is necessary to determine the '*disassociation*' between closely related variables in space, a term *semivariance* are used. The semivariance is given by,

$$\Gamma[\mathbf{x}_1, \mathbf{x}_2] = \frac{1}{2} Var[Z(\mathbf{x}_1) - Z(\mathbf{x}_2)] \tag{3.29}$$

and commonly written (Crassie, 1991) as,

$$\lambda(s) = \frac{1}{2N(s)} \sum_{i=1}^{N(h)} [Z(x_i) - Z(x_i + s)]^2 \tag{3.30}$$

where $N(s)$ is the number of pair of plots $[Z(\mathbf{x}_i), Z(\mathbf{x}_i+s)]$ separated by a distance s. With the semivariance model developed, the autocorrelation function of the stochastic process can be characterized using length scales known as the integral scale J (Lumley and Panofsky, 1964). Similarly, under the first and the second order of stationarities (Crassie, 1991), given by,

$E[Z(\mathbf{x}_1)] = E[Z(\mathbf{x}_2)] = \text{constant}$ .... (first order stationarity) (3.31)

$\mathrm{Var}[Z(\mathbf{x}_1)] = \mathrm{Var}[Z(\mathbf{x}_2)]$,

and

$\mathrm{Cov}[\mathbf{x}_1, \mathbf{x}_2] = \mathrm{Cov}[\mathbf{x}_1 - \mathbf{x}_2]$ (3.32)

$\Gamma[\mathbf{x}_1, \mathbf{x}_2] = \Gamma[\mathbf{x}_1 - \mathbf{x}_2]$ (3.33)

as second order stationarity condition, two characteristics of the empirical semivariogram can be considered. First, as the separation distance s increases, the semivariance approaches a constant value (according to eq. 3.30). This limiting state is known as the *sill* (Yevjevich, 1972). The sill is reached at a distance a (say) known as *range*. The range is the radius of influence beyond which the semivariance takes the variance around mean of individual values (Crassie, 1991). Second, from eq. (3.29) when $s = 0$, that is, at very close distances the disassociation between values of the variable approaches zero. However, in practice, due to local effects the semivariance at very close distances may be significantly different from zero, taking on residual values known as *nugget*. With these two characteristics and a fitted form of eq. (3.29), the spatial structure of saturated hydraulic conductivity was described. The fitting of a mathematical expression for eq. (3.29) was explored using the Minimum Squared Deviation (MSD) criterion. The calculated semivariances were fitted to a mathematical expression of the positive definite type (Panchev, 1971) for further linear interpolation in mapping.

The spatial covariance function of eq. (3.28), which is normally greater when there is a greater direct association between the variables close together, can be used to explain the spatial correlation between two measurements in space. When the spatial covariance function is divided by the spatial standard deviations (or semivariances, (Yevjevich, 1972)), a measure of the spatial correlation between the two points is estimated. In this study, the spatial correlation coefficient was estimated from (Yevjevich, 1972),

$$r(s) = \frac{\sum_{i=1}^{N}[Z_i(\mathbf{x}) - \hat{m}(x)][Z_i(x+s) - \hat{m}(x+s)]}{\sum_{i=1}^{N}[Z_i(x) - \hat{m}(x)]^2 \sum_{i=1}^{N}[Z_i(x+s) - \hat{m}(x+s)]^2} \tag{3.33}$$

where $\hat{m}(\mathbf{x})$ and $\hat{m}(\mathbf{x}+\mathbf{s})$ are the sample means of the observations at the two points.

Since the distances between measurements were not regular, the number *N(s)* became quite varied and so was determined differently. The procedure outlined in table 3.2 (Lawes Agricultural Trust, 2002) was used to determine values of *N(s)*.

Table 3.2: Determination of separation distances between irregularly spaced plots

Class of separation distance	**Class midpoints, (*s*)**	**Frequency**	***N(s)***
0 - 100	50	f_1	f_1
101 - 200	150	f_2	f_2
201 - 300	250	f_3	f_3
301 - 400	350	f_4	f_4
.	.	.	.
.	.	.	.

3.6 Mapping of hydraulic conductivity

Mapping of hydraulic conductivity was based on interpolation of estimated hydraulic conductivity values using the information provided by the semivariogram. The kriging was employed for this task (Journel and Huijbregts, 1978). Kriging is a weighted moving average with an estimator of the form

$$Z^*(\mathbf{x}_o) = \sum_{i=1}^{N} \lambda_i Z(\mathbf{x}_i) \tag{3.34}$$

where N is the number of values $Z(\mathbf{x}_i)$ involved in the estimation of the unrecorded point $(\mathbf{x}_o)$, λ_i are the weights. $Z(\mathbf{x}_i)$ was either the spectral based estimate of K_s or actual K_s at point x_i, and x_i is the geographical location defined by the co-ordinates (X_i, Y_i).

In kriging, the assumption of unbiased estimate is often made. The intrinsic assumption that the estimator is unbiased is on condition that the expectation of the difference between the estimator and the estimated values should be zero and that the variance between the two should be minimum (Snedecor, 1989). Thus,

$$E\{Z^*(\mathbf{x}_o) - Z\ (\mathbf{x}_o)\} = 0 \tag{3.35}$$

and

$$\sigma_k^2(\mathbf{x}_o) = E\{[Z^*(\mathbf{x}_o) - Z\ (\mathbf{x}_o)]^2\} = \text{minimum} \tag{3.36}$$

Substituting equation (3.35) into equation (3.36) and differentiating yields

$$\frac{\partial}{\partial z(\mathbf{x}_i)}\left[\sum_{i=1}^{N} \lambda_i z(\mathbf{x}_i) - z(\mathbf{x}_i)\right] = 0 \tag{3.37}$$

or

$$\sum_{i=1}^{N} \lambda_i = 1 \tag{3.38}$$

The condition for minimum variance expressed in equation (3.36) subject to equation (3.38) can be shown (Viera et al., 1982) to be

$$\sigma_k^2 = -\sum_i \sum_j \lambda_i \lambda_j C(\mathbf{x}_i, \mathbf{x}_j) + C(0) - 2\sum_i \lambda_i C(\mathbf{x}_i, \mathbf{x}_j) \tag{3.39}$$

which, in terms of semivariogram becomes

$$\sigma_k^2 = -\sum_i \sum_j \lambda_i \lambda_j \gamma(\mathbf{x}_i, \mathbf{x}_j) + 2\sum_i \lambda_i \gamma(\mathbf{x}_i, \mathbf{x}_j) \tag{3.40}$$

However, equation (3.40) can be minimized under constraint of equation (3.38). In this case Lagrangian multipliers were used with all the *N* partial derivatives were set to zero.

$$\frac{\partial}{\partial \lambda_i} \left[\sigma_k^2(\mathbf{x}_o) - 2\tau \sum \lambda_i \right] = 0 \tag{3.41}$$

where τ is a Lagrangian multiplier. Substituting equation (3.40) into equation (3.41) and differentiating yields

$$-2\sum_j \lambda_j \gamma(\mathbf{x}_i, \mathbf{x}_{jk}) + 2\gamma(\mathbf{x}_i, \mathbf{x}_j) - 2\tau = 0$$

or

$$\sum_{j=1}^{N} \lambda_j \gamma(\mathbf{x}_i, \mathbf{x}_j) + \tau = \gamma(\mathbf{x}_i, \mathbf{x}_j)$$

while

$$\sum_{j=1}^{N} \lambda_j = 1 \tag{3.42}$$

Expression (3.42) is popularly known as the kriging system (Vauclin et al., 1983).

In order to solve the kriging system, *N* needs to be known. *N* was determined by Mean Reducing Error (MRE) defined by

$$MRE = \frac{1}{n}\sum_{i=1}^{n}\left[Z(\mathbf{x}_i) - Z^*(\mathbf{x}_i)\right] / \sigma_k(\mathbf{x}_i) \tag{3.43}$$

where *n* is the total number of plots, which are close together. In this study *MRE* values were plotted as a function of neighbourhood size *N*. The value of *N* for which *MRE* was approximately zero was chosen. Solutions of equation (3.42) and (3.43) were established using IDRISI™ (Eastman, 1999). The original data and the kriged estimates were then plotted in a map of the study area using ArcInfo™ (Booth, 1999).

4. RESULTS AND DISCUSSIONS

4.1 Evaluation of point-measurement method

4.1.1 Time expenditure and costs involved

Time taken in the field to acquire a single data is one of the greatest limitations of point-measurement methods. The time taken includes time for setting up the experiment, execution and final derivation of saturated hydraulic conductivity, K_s. In addition to time, costs involved, amount of water used and complexity of the method all hinder the otherwise accurate methods for use in area-wide survey. For the methods that were tested in this study, Table 4.1 shows summary of the results.

Table 4.1: Summary of the test results on evaluating field methods

Method	**Time (hrs)**	**Cost**		**Complexity**		**Water**	**Surface modification**
		Materials	*Personnel*	*Weight*	*Fragility*	*(Litres)*	
Double ring	2	High	3	Heavy	No	30	Nil
Guelph	0.75	Low	1	Light	Yes	5	A little
Single ring	2.5	Low	1	Light	No	17	Nil
Rainfall Simulator	2.5	High	2	Heavy	Yes	10	A little
Negative head disc permeameter	1	High	1	Light	Yes	2.5	Yes
Positive head disc permeameter	1.5	Low	1	Light	Yes	3	A little

The values indicated in table 4.1 were the averages of the six replications. The numbers of personnel were looked at in terms of the number of persons collectively required to help in data recording, availing water needed for the test and moving the equipment to different sites. The need for soil surface modification was considered on such factors as leveling and hole auguring. The complexity criterion involved robustness of the equipment for large-area use in terms of how heavy the equipment was for rapid movement as well as the liability to breakage during the experimentation. On the other hand, the materials (under the cost criterion) implied number of accessories required to completely carry the experiment and included such things as infiltration sand, sledges, runoff receptors, etc.

The differences in time taken by the methods were observed to be in the order of 20 % to 60 % of each other, this is quite a lot in terms of runoff generation. The method, which requires surface modification and was expensive both in terms of time and materials, was not considered suitable for large area survey. Thus, at this level, Kamphorst rainfall simulator was highly not favoured.

4.1.2 Repeatability of measurements

Confidence and trust that scientists build in research depends on consistency of measurement by any method or equipment used. This confidence is quite affected by large variability in experimental measurements. In soil and water related studies, variability of measurements is not surprising. Variability in soils is so high that consistency is never talked of that much. However, the general understating attributes this variability to soil heterogeneity rather than to equipment used (Cornelis et al., 2001). An extra thinking is presented here to explain this point.

In case a 'near-homogeneous' field is used to test any equipment, the majority of variability encountered would be attributed to the equipment (Neter et al., 1990).

This kind of variability becomes vivid where a number of equipments are used in the test. In this study, the consistency was tested on different equipment in a presumably homogeneous field. Table 4.2 below shows the summary of the test results.

Table 4.2: Results of repeatability of measurement (values in cm/hr)

	Method					
Trial	Double rings	Guelph	Single ring	Rainfall simulator	Negative head permeameter	Positive Head permeameter
1	9.76	10.22	11.16	10.54	12.12	12.71
2	11.10	8.67	8.67	6.07	16.30	8.32
3	12.00	11.56	9.14	8.15	18.15	10.15
4	16.66	22.81	7.93	24.34	24.78	14.59
5	14.70	16.80	16.80	14.94	20.17	12.87
6	15.13	18.92	10.61	29.43	15.73	23.12
Mean	13.23	14.83	10.72	15.58	17.88	13.63
Median	13.35	14.18	9.88	12.73	17.23	12.79
Stdev	2.67	5.55	3.22	9.38	4.32	5.15
Range	6.90	14.14	8.88	23.36	12.67	14.80
% CV	20.00	39.15	32.56	73.65	25.08	40.27

Even though the methods do not statistically differ in their mean values (table 4.3) the variability (percent coefficient of variation, % CV) however, differ significantly. The significant differences in the variability shows how much the method can depict variability in measurements of field saturated hydraulic conductivity. The results in table 4.2 show that Kamphorst rainfall simulator was the most varied in this test. The double ring infiltrometers method appeared to be the most consistent in measuring surface K_s.

Table 4.3: Analysis of variation on different testing methods

Variate: lnksat					
Source of variation	**d.f.**	**s.s.**	**m.s.**	**v.r.**	**F pr.**
method	5	0.83	0.17	1.21	0.327
Percent C.variation	5	1.20	0.01	3.02	0.001
Residual	30	4.12	0.14		
Total	35	4.95			

4.1.3 Identification of rapid method

By considering all the factors that bedevil extensive use of point-measurement methods, table 4.3 below shows scores of each method based on a grading system adopted after Bouma (1983).

The scores in table 4.4, which range from 0 to 5 were awarded from considerations in tables 4.1 and 4.2 and indicated the relative favourability of the parameters at the top of each column. For example, double-ring infiltrometers which showed lower range of measured values than kamphorst rainfall simulator was more consistent than rainfall simulator. Hence, double-ring infiltrometer method scored higher while kamphorst rainfall simulator method.

Table 4.4: Grading of field methods for measuring K_s

Method	Surface modification	repeatability	Water (litres)	consistency	cost	Time (hrs)	Complexity	Total score
Double rings	5	5	0	5	0	0	1	16
Guelph	3	2	3	2	4	5	4	23
Single ring	5	3	1	4	5	2	5	25
Rainfall simulator	3	0	2	0	1	2	0	8
Negative head perm.	0	4	5	3	3	3	4	22
Positive head perm.	1	1	4	1	3	4	4	18

The scores suggested that the single rings method was the most suitable method for rapid field survey of saturated hydraulic conductivity while the Kamphorst rainfall simulator was the least suitable according to this procedure.

In this study, single-ring infiltrometer method was identified for rapid survey of surface saturated hydraulic conductivity. On the other hand, Guelph permeameter was identified as being most suitable for measurement of topsoil saturated hydraulic conductivity.

The use of single-rings for area-wide survey of surface saturated hydraulic conductivity has been gaining preference provided the analysis used would account for flow divergence. Currently, most studies monitoring flow in infiltration have used modification of single-rings (White and Perroux, 1988), as they are capable of accounting for the flow divergence emanating from the infiltration sources.

4.2 Field-measured saturated hydraulic conductivity

4.2.1 Variability of field-measured soil K_s

The measure field K_s was fitted according to eq. 3.21 and plotted against the normal quartiles as shown in figure 4.1. From figure 4.1, there was evidence of lack of normality for normal distribution on both surface and topsoil K_s. Further analysis using the Kolmogorov-Smirnov test at $p < 0.05$, however, revealed lognormal distribution of both surface and topsoil K_s (table 4.5 and figure 4.2).

Table 4.5: Normality test for the field-measured soil K_s (cm/hr)

Parameter	Cases	Mean	Range	Variance	p –value (of ln K_s)
Surface K_s	343	10.27cm/hr	0.12 – 40.62	69.55	0.001
Topsoil K_s	343	5.54cm/hr	0.01 – 28.50	34.63	0.002

These results conform to those reported in Sharma et al. (1983). Many literatures that have offered explanation on the lognormal distribution of soil K_s (Rawls et al., 1983; Sharma et al., 1983; and Russo and Bresler, 1981) attribute this distribution to the unsystematic variation and changes in continuity, size and extent of pores in soils.

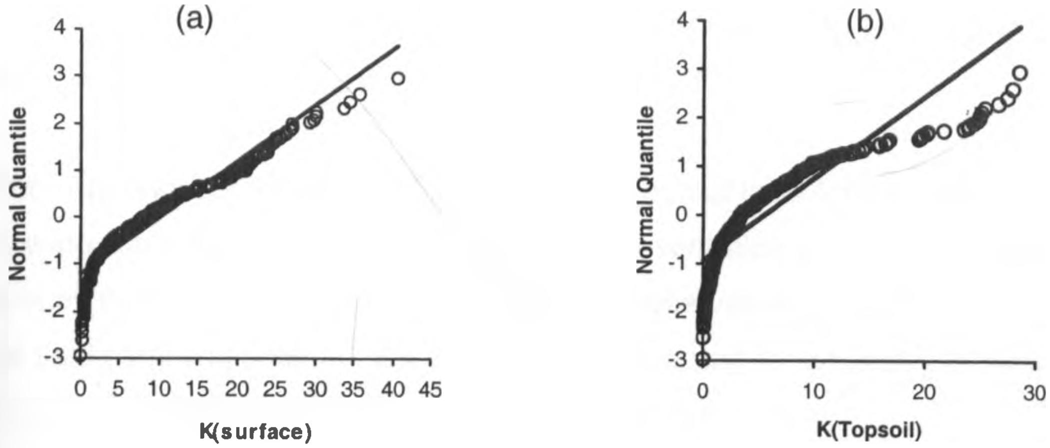

Figure 4.1: Normality test for surface and topsoil K_s measurements

In this study, since the field-measured soil K_s was carried over a wide area in a heterogeneous watershed these results quite echo the theories.

(a) (b)

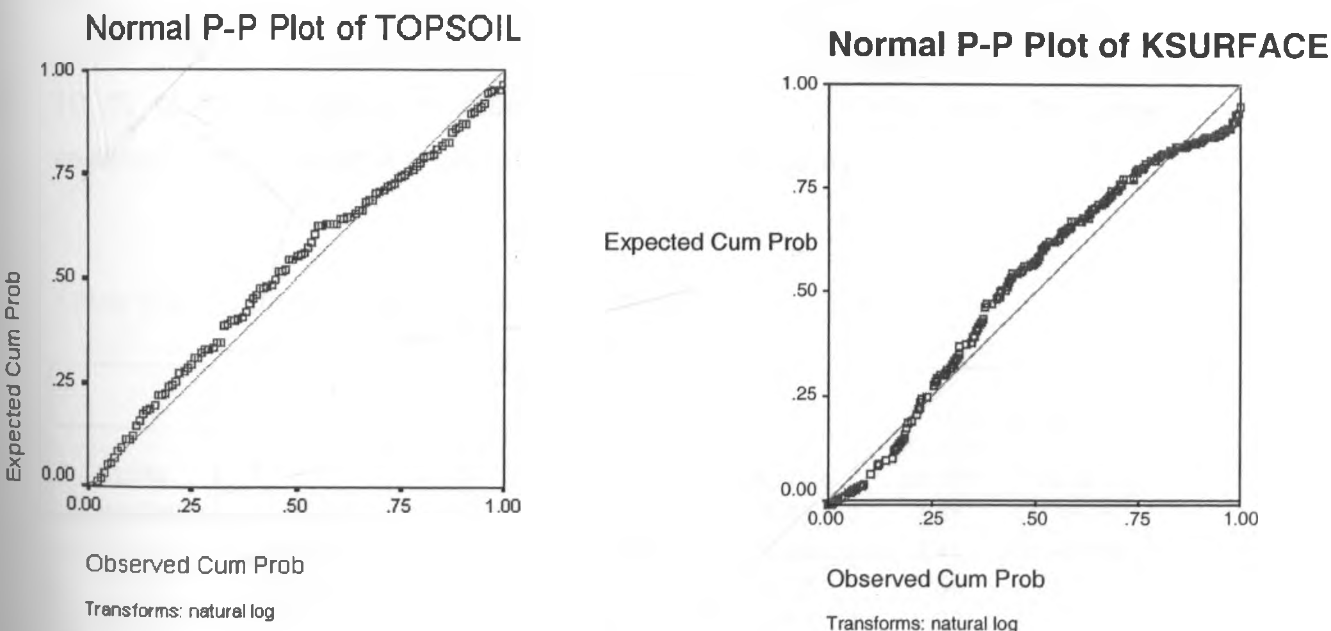

Figure 4.2: Probability distribution function of Soil K_s

Even though soil K_s was highly varied over a landscape, the sampling method adopted in this study depicted some extent of repeatability of measurements at plot level.

From Appendix E, the repeatability correlation at plot level for surface and topsoil K_s were each 63 %, showing fairly good representation of K_s values within plot level by three replications. The implication of these values is that by the design of the field-sampling scheme, it was possible to account for variability of over 60 % of K_s values in each plot using linear mixed effects modeling.

4.2.2 Effect of land use and slope zone on K_s

After accounting for variability of K_s at plot level, land use type and slope zone were further identified as the major factors responsible for explained variability in soil K_s. In the linear mixed effects model developed with S-Plus (Mathsoft Inc., 1999), land-use-type effect accounted for 12 % while slope zone accounted for 10 % of the variability in measurement of soil K_s. Other than the general variations above, table 4.6 below shows the individual K_s values.

Table 4.6: Summary of the results of field-measured soil K_s

		Number of cases	Surface Ks		Topsoil Ks	
Strata		N	Median (cm/hr)	variance	Median (cm/hr)	variance
Slope zone	Lowland	129	3.05	48.31	3.38	33.39
	Midland	148	9.06	48.92	3.41	27.58
	Scarps	24	22.48	94.33	5.58	87.28
	Upland	42	15.74	70.94	4.66	20.61
Land use	Sparse/bare	68	4.48	74.03	2.17	76.01
	Cropland	86	13.23	62.11	4.74	33.5
	Grazing	66	3.84	62.15	2.83	23.95
	Shrubland	75	7.8	63.84	3.04	21.32
	Woodland	48	14.25	22.06	4.67	18.28

From Table 4.6, Woodland and cultivation have high surface and topsoil K_S. Woodlands in general had a lot of litter on the surface which could have promoted the high K_s values due to animal activity and soil organic carbon. Similarly, high values of surface K_s on the tilled land could have resulted due to the nature in which the land use modifies the soil surface.

Table 4.7: ANOVA Table for measured K_s (ln K_s in cm/hr)

	Source	Ss	df	ms	F*	P-value
Surface Ks	Land use	42.2	4	10.55	5.28	0.004
	Slope zone	11.88	3	3.96	2.54	0.024
	Interaction	21.99	11	2	1.28	0.396
	Error	503.7	324	1.56		
Top soil Ks	Land use	57.11	4	14.28	3.99	0.001
	Slope zone	30.33	3	10.11	12.83	0.008
	Interaction	39.35	11	3.58	4.54	0.006
	Error	255.224	324	0.79		

In tables 4.7, land use was depicted as very significant in contributing to changes in soil K_s (at 5 % level of significance). Thus, by changing land use from one type to another, K_s is greatly affected. However, there were insignificant interaction effects between land use type and slope zone for the surface K_s, while for topsoil K_s, the interaction is quite important. The implications of these interactions are that wherever the soil position, surface K_s is still affected by land use type, while topsoil K_s is affected by land use depending mostly on where the soil is found on the landscape. This is actually true as the topsoil K_s is dependent on soil depth, which is varied across the landscape.

In this study, the scale of heterogeneity of the measured K_s was quantified in terms of variability in the measured values. As the values of variances is used to explain the disturbances (both anthropogenic and natural) imposed on soils in the watershed (Russo and Bresler, 1981), the high variation of measured surface K_s in upland slope zone could suggest the degree of surface soil disturbance. This disturbance is an indication of how less the upland hydrology (or upland watershed management) is conserved. The high values of variance registered in the scarps could, however, have been partly due to the high variation in soil depths on the scarps.

Corresponding to the apparent high disturbance meted on the upland soils are the higher values of soil K_s. These two factors generally results into bad hydrologic impacts in upland watershed. Nominally, during infiltration, once ponding has taken place on soil surface, control over the infiltration shifts from the rainfall intensity to characteristics of the soil. In such cases, surface-connected nonmatrix, interstructural pores and subsurface-initiated cracks become effective in transporting water down the soil profile. One of the prime soil characteristics governing the water transport down the soil profile is the soil K_s (Madramootoo and Elright, 1990). High surface K_s implies low surface runoff for deep soils and high surface runoff for shallow soils (Suresh, 1997). In this regard, the deep upland soils and shallow soils in the scarps associated with high K_s values (table 4.6) would suggest likelihood of increase in subsurface water flow from these areas. Subsequently, flooding of the lowlands can be eminent, as the subsurface flow would find outlet in form of springs at the footslopes of midland areas. This can explain the occurrence of gully erosion inception within this zone.

Still on the infiltration characteristics, Woodlands having the highest surface K_s pose high chances of increasing rainfall infiltration. They, therefore, in particular (and growing trees in general) have the capacity of increasing infiltration and reducing surface runoff. In addition, they have the potential of increasing subsurface recharge and increasing the length and magnitude of dry season flows of rivers in a watershed. This is a very important fact in rural water supply for domestic use and irrigation purposes.

In addition to acting as buffers for rainwater infiltration into the soil, Woodlands have also shown low variability in the measured K_s. This is an indication of restoration capacity the land use would have on impaired soil structure. This fact can be cross-checked against values of K_s in erosion-prone areas such as sparsely vegetated or bare lands. Hence, from table 4.6, erosion (with reference to sparse/bare land) can reduce Woodland soil K_s by over 50 %, while grazing effects can facilitate reduction of Woodland soil K_s by over 40 %. This last fact contributes to majority of reasoning behind flooding of lowland areas of the lake region during the rainy seasons as the lake region is known for its heavy livestock densities.

The variability of the measured K_s in the whole watershed can also be attributed to soil physio-chemical properties. Such factors as surface sealing (and contribution of sodicity) could play a role in this part, especially in the lower parts of the watershed where rain water temperature is high. The problem of sodicity (excess of sodium ions in the exchange complex), which is significant in these areas (Jaetzold and Schimdt, 1983) cause serious instability to soil structure. For example, in the lowland areas of the watershed there is substantial percent of ESP (in excess of 15 %, Jaetzold and Schimdt, 1983). Marshall and Holmes (1979) and Bresler et al. (1984) have shown that exchangeable sodium percent (ESP) greater than 15 percent greatly reduces hydraulic conductivity of soils. Thus, activities that lead to soil exposure such as burning or overgrazing would aggravate the negative effects on the hydrologic characteristics.

Another soil physio-chemical effect associated with infiltration and erosion characteristics is the soil hardsettingness on the surface. On the hardset surfaces of soil, the likelihood of the generated overland flow of runoff is high since hardsetting encourages surface ponding of rainwater. The effect increases the detention time for runoff on the soil surface, hence slowly dissolving the sodium in the soil. This effect will lead to entrainment of the soil in the runoff movement and eventual soil erosion. According to the theory of erosion generation (Morgan, 1986), this is the inception of weaknesses in a soil to runoff-water erosion. Sparse/bare lands, which were by majority in the upper lowland and lower midland areas, showed marked hardsetting. Gully erosion occurrence in these areas, thus would be explained by the low soil K_s. The knowledge of differential layering of soil profile in terms of saturated hydraulic conductivity classes would then be an important step in modeling soil erosion, in a watershed such as this, to solve the problem of gully erosion.

4.3 Soil spectral reflectance and calibration to K_s

4.3.1 Soil spectral signatures

The soils scanned in this study had relative spectral reflectance ranging from 0.04 to 0.49 with dominant absorption features occurring mainly in the 1400 nm – 1520 nm, 1880 nm – 1910 nm and 2160 nm – 2210 nm (figure 4.3). Most of the soils scanned had the principal absorption features around 1520 nm with spectral contrast of 0.3 (Montero et al., 2001).

The majority of the soils from the lowlands showed higher spectral variations and low symmetry of absorption (0.2) at NIR regions of the spectra. This was probably due to high silt content in these soils. Silt content has been shown to be the most significant parameter explaining the spectral variations in soils (Montgomery and Baumgardner, 1974).

The inverse relationship between particle size and soil reflectance (Atzberger, 2002) was also observed, as there was an increasing trend in relative reflectance with visually observed decreasing particle size. The soil spectral characteristics, which are affected mineralogy, clay content, organic matter content and particle size distribution share similar response as soil K_s. Thus, by extension one would suggest some degree of correlation of soil spectral reflectance with soil K_s.

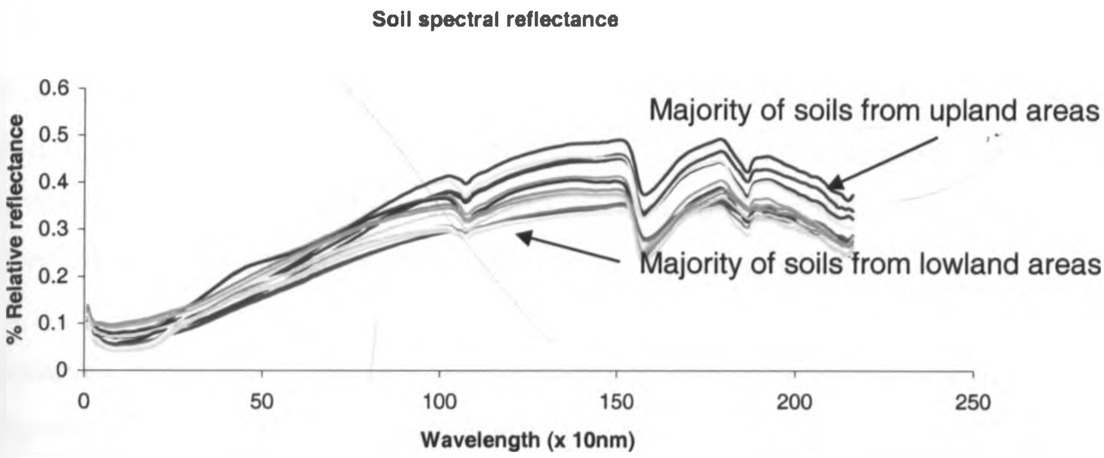

Figure 4.3: Spectral reflectance of soils from Awach watershed

4.3.2 Calibration of soil spectral reflectance to K_s

The calibration of spectral reflectance to soil K_s was achieved with partial linear least squares (PLS). The results of are shown in table 4.8.

Table 4.8: Results of spectral calibration

Statistic	**Surface K_s**	**Topsoil K_s**
Number of cases	343	343
Slope	0.54	0.03
Correlation coefficient	0.75	0.20
Offset	0.84	1.07
RMSEP	0.79	1.29
SEP	0.79	1.29
Bias	-0.002	-0.002

The data in table 4.8 shows that a good correlation exists between surface K_s and soil spectral reflectance. However, topsoil K_s is depicted not correlate well with soil spectral reflectance (Appendix D). Since one of the factors influencing K_s in soil as well as spectral reflectance is the amount of organic matter (Ben-Dor et al., 1999) and as it changes sharply with depth, it is suspected that this change would have caused the difference in relating spectral reflectance to surface and topsoil K_s. In addition, difference in the methods used in obtaining soil K_s could have also contributed to the wide difference in the correlation.

However, given that surface K_s correlated well with spectra, the accuracy of the regression model was further checked to ascertain its consistency. There was enough evidence that soil spectral reflectance calibrated consistently well and accurately to soil surface K_s (table 4.8).

Table 4.8: Results of consistency tests in a regression model

STATISTICS		**Data A**	**Data B**
Coefficient of efficiency	R^2	0.55	0.49
Root mean square	RMSE	5.21	6.30
Index of agreement	d	0.88	0.83
Coefficient of correlation	r	0.79	0.76
Coefficient of determination	r^2	0.60	0.53
Bias		0.12	1.86
Variance		75.59	60.75
Median		6.81	7.15

A model was therefore developed by the PLS to predict surface K_s from spectral signatures in the library containing samples from the same study area. Table 4.9 shows summary statistics of the predicted surface K_s (cm/hr). The overall predicted surface K_s had a maximum value of 28 cm/hr and a minimum of 0.054 cm/hr with a variance of 8.924 cm/hr. These values are in line with those reported by Vogel et al. (2001) for the soils similar to those found in this study area.

Table 4.9: Summary statistics of the predicted surface K_s (cm/hr)

Summary statistics for surface K_s	Lowlands	Midland	Uplands
Number of values	75	52	93
Median	1.2	6.1	17.04
Minimum	0.05	0.41	2.46
Maximum	26.6	24.5	37
Range	26.2	24	27.9
Standard deviation	3.7	6.4	5.1
Variance	13.9	40.6	26.5
Coefficient of variation	174.9	75	30
Skewness	4.9	0.59	0.82

4.4 Spatial structure of surface K_s

Figure 4.4 below shows approximate scattergram for the surface K_s in the watershed. As depicted in the scattergram, surface K_s take low values in the Northwest corner of the watershed and high values on the Southeast corner of the watershed. Thus, arising from the pattern along the NW-SE direction, spatial structure model was developed to describe the watershed heterogeneity.

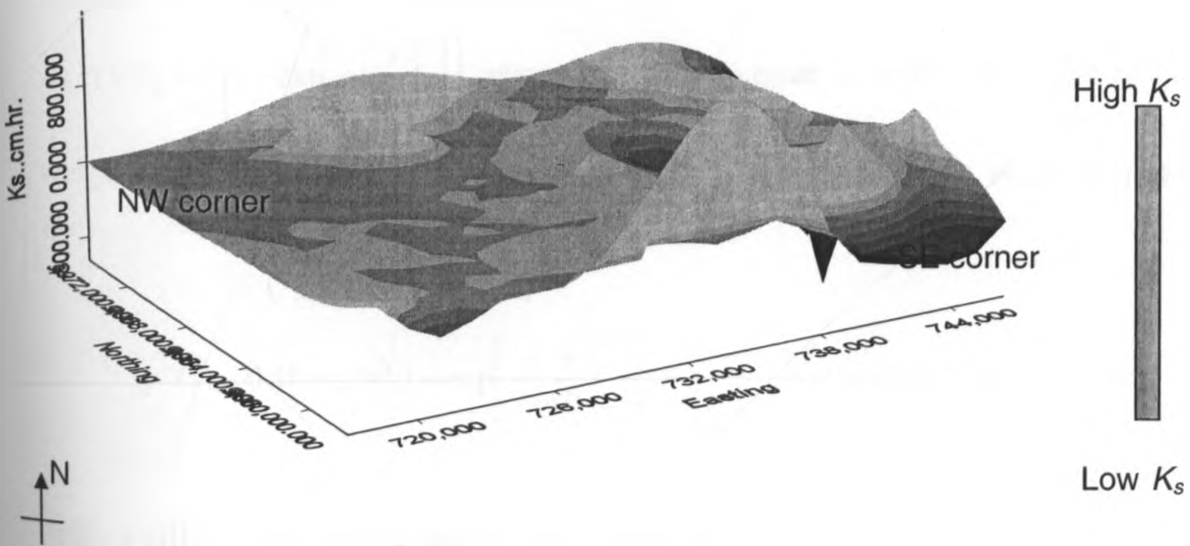

Figure 4.4: Approximate stratification of surface K_s

A number of positive-definite-type mathematical expressions were fitted to the surface K_s. Table 4.10 below shows results of 9 expressions fitted.

Table 4.10: Results of fitted semivariogram models for surface K_s

Type of model	% Variance accounted for	MSD	Variance ratio	Standard error of observation
Linear	55.5	0.394	57.15	4.94
Bounded linear	94.0	0.161	30.91	4.64
Exponential	82.7	0.182	33.54	4.87
Circular	90.7	0.168	31.80	4.72
Spherical	89.4	0.175	36.86	4.77
Double spherical	95.3	0.164	25.17	4.64
Pentaspherical	95.6	0.159	22.80	4.45
Bessel K	87.9	0.174	31.98	4.80
Gaussian	96.7	0.154	22.74	4.36

From table 4.9 and based on the minimum squared deviations (MSD), Gaussian model was chosen (figure 4.5).

The general Gaussian model is given by

$\gamma(x) = C_0 + C\left(1 - \exp\left(-\left(\frac{x}{A}\right)^2\right)\right)$ where C_o is the nugget, C is the sill and A is the range (Yevjevich, 1972). The Gaussian model developed in this study is given by;

$$\gamma^*(x) = 0.88 + 2.08\left(1 - \exp\left(-\left(\frac{x}{80}\right)^2\right)\right)$$

with a sill = 2.08, nugget = 0.88 and range = 80 m

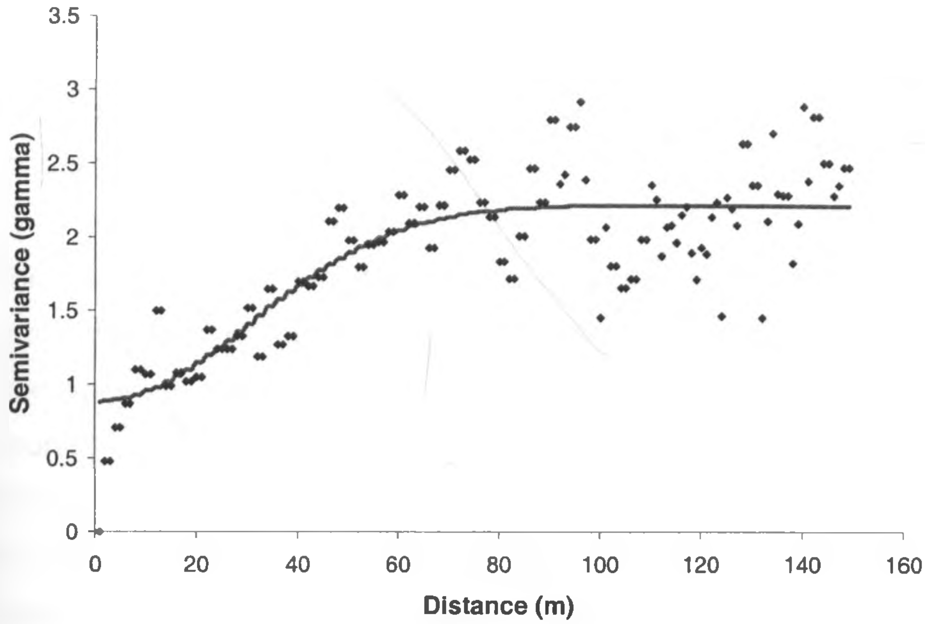

Figure 4.5: Semivariogram model for surface K_s

The model developed depicted a radius of influence of 80 m within which measurements of surface K_s reveal spatial correlation. The spatial correlation coefficient is shown in figure 4.6 below.

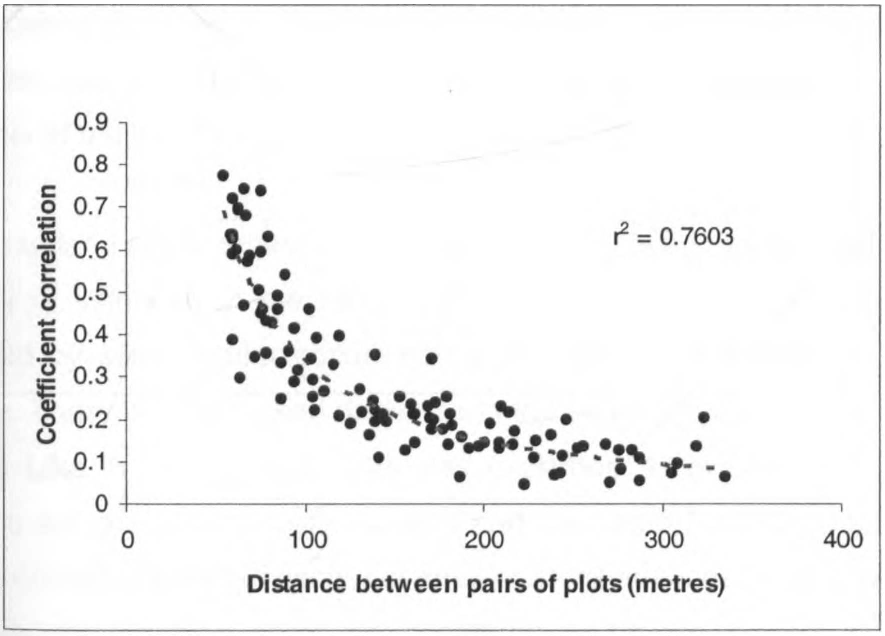

Figure 4.6: Spatial coefficient of correlation for surface K_s in Awach watershed.

The spatial coefficient of correlation in figure 4.6 above showed an exponential decay with distance depicting higher correlation between measurements which are close together. Based on the radius of influence of 80 m the coefficient of spatial correlation is about 0.6.

The general spatial structure was also devolved into different slope zones to verify the assumption of isotropy for the watershed. Thus, in the lowlands calculation of semivariogram in the NW –SE direction involved crossing of boundaries within the strata (Figure 4.7a). Here there appeared to be a 'hole effect' between lags 70 and 90. These hole effects could have been attributed to the occurrence of local strata in the spatial structure. The physical meaning of these 'hole' effects may be explained due to soil disturbances or management effects or depositional erosion which have the potential of causing local variations in the surface K_s.

In the midland slope zones, the calculation of semivariogram in the W-E direction involved very little crossing of boundaries between strata (Figure 4.7b). Consequently, the semivariogram for this direction had a smooth sill of 1.49 (approximately equal to the global variance) at lag 60. This implies that the soils in these areas are either virgin or effect of land use change had not been that serious at the time of experimentation.

In the upland slope zones, the semivariogram showed pronounced effect of short zones of influence in the NW – SE direction. These zones could have been caused by semi regular occurrence of low values of surface K_s from different strata. There was a marked decrease in the semivariances at larger lags (Figure 4.7c). Like in the lowlands, this was explained as hole effects (that is higher values are paired with higher values and the same for lower values, leading to large covariance and consequent smaller semivariances). The physical meaning of this phenomenon could be construed to be the presence of pockets of cropland lands (say) in the bush thickets; an indication of advancing land use change in the area.

Ks in the lowlands (NW – SE direction)

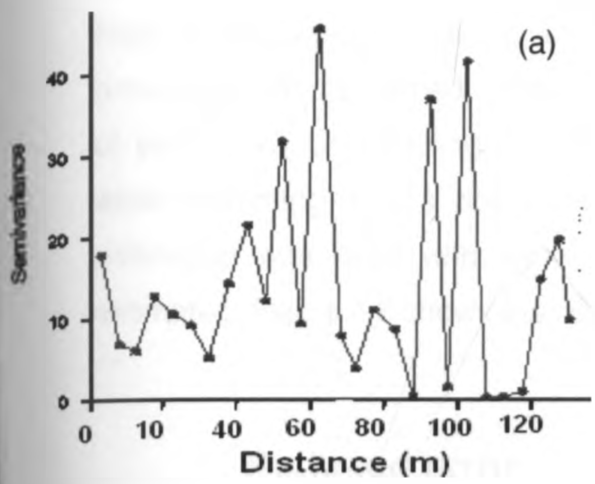

Ks in the midlands (W –E direction)

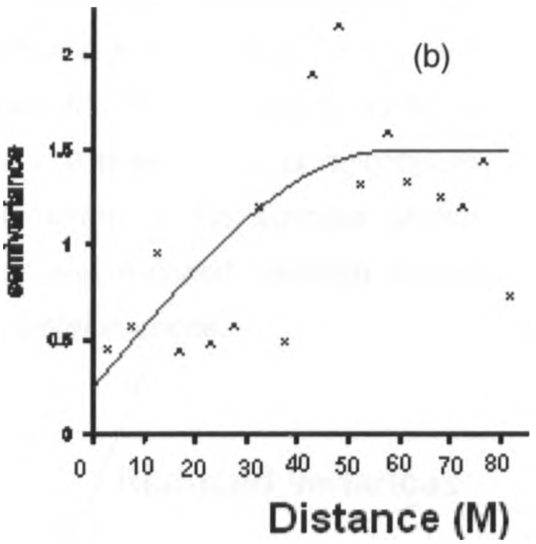

Ks in the uplands (NW – SE direction)

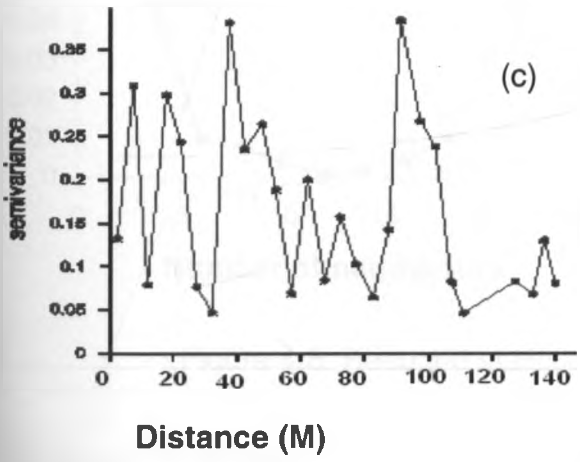

Figure 4.7: Semivariogram for surface K_s in Awach watershed

4.5 Mapping of surface K_s

Mapping of surface K_s was achieved by the Kriging technique on the actual and spectral based estimates of surface K_s. A set of 1375 observations was used in the 400 km^2 area of Awach watershed. As in any other estimation method, there were errors involved whose magnitudes were a measure of the validity of the kriging estimation. In order to improve on the Kriging estimation, a Jack-knifing procedure was performed on both the original and the spectral based estimates of surface K_s. Jack-knifing involved estimation of a point using its neighbours while assuming it was not known. The confirmation of the success of the estimation was done with mean reduced error and reduced variance of the estimates. Figure 4.8 shows the results of the estimation check.

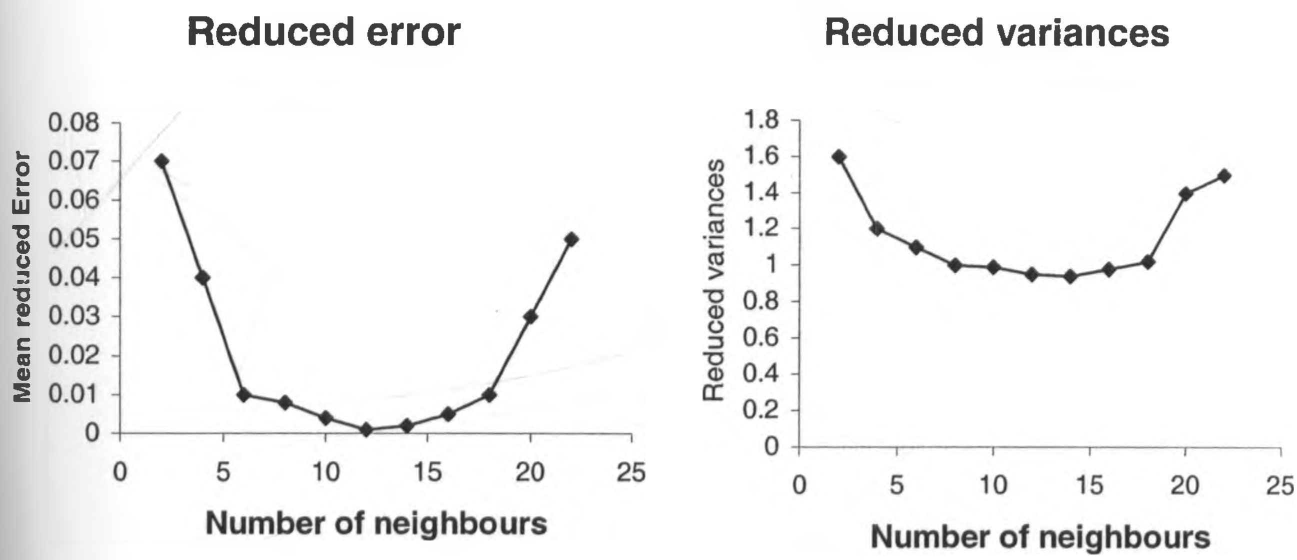

Figure 4.8: Reduced statistics for the kriging estimation

According to equation 3.43 and from Figure 4.8, 12 neighbours seemed an acceptable compromise between mean reduced error and reduced variance. Thus, for each point (x_o) the distances between that point and twelve nearest neighbours were kept smaller than the range (80 m) in the semivariogram model. For the 1375 observations of surface K_s, which were taken as Z_i, there were a set of estimation errors $\epsilon_i = Z^* - Z_i$ The mean for the estimation errors for these observations was -6.22 x 10^{-4} cm/hr, showing the unbiasedness condition of the Kriging estimation.

A surface interpolation of the actual, spectral based estimates and the kriged estimates is shown in figure 4.9 (and Appendix F). The map depicts very low infiltration rates in the lowlands (the lake plain) and moderately high values in the upland areas of the watershed. The very high values in the junction between the uplands and the midlands were possible due to the variable soil depth on the scarps. Scarps were observed between the uplands and the midlands. Appendix (F) also substantiates this outcome by illustrating a trend of surface K_s with altitude.

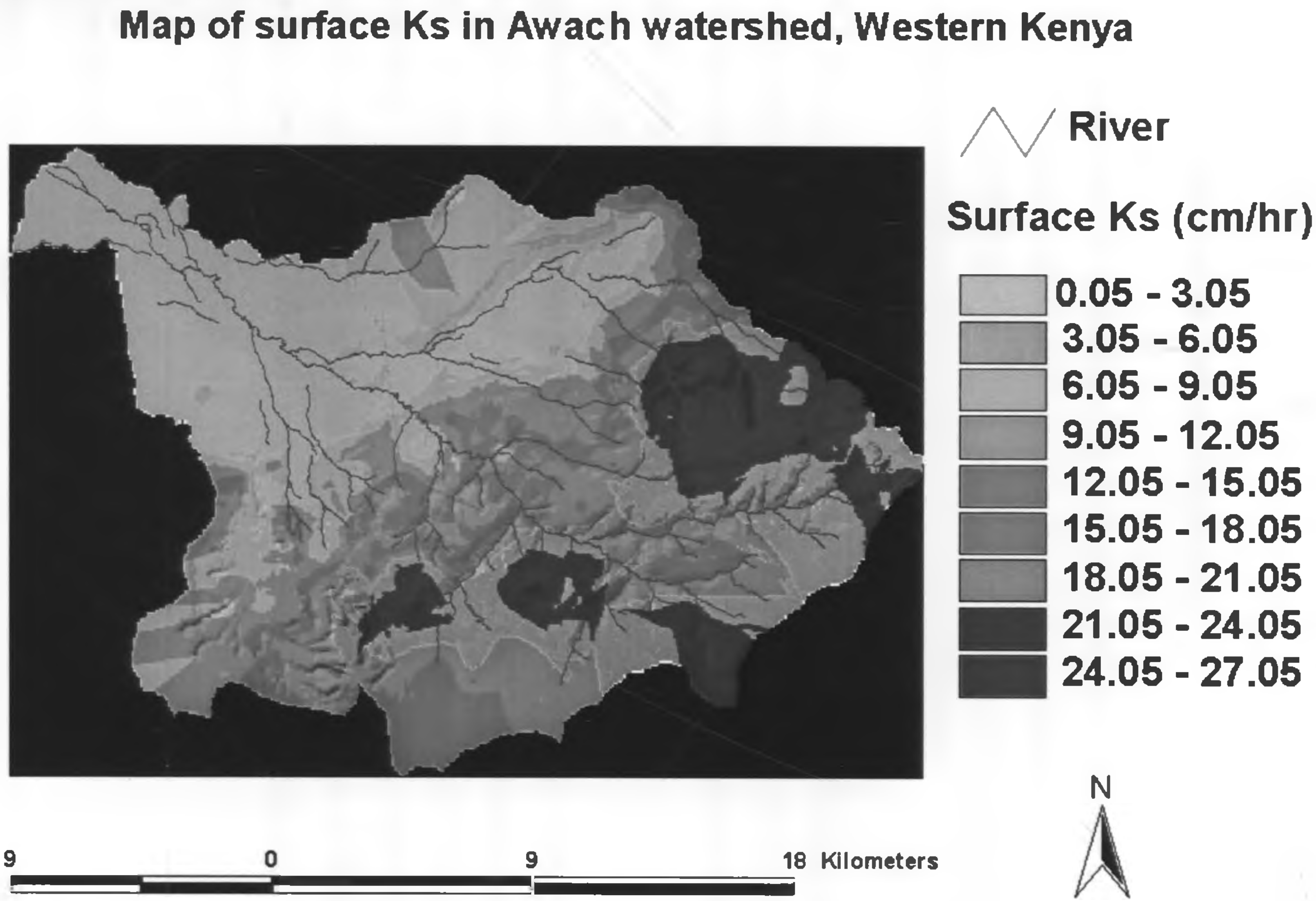

Figure 4.9: Surface interpolation map of surface K_s in Awach watershed

CHAPTER V

5. CONCLUSIONS AND RECOMMENDATIONS

5.1 Conclusions

5.1.1 Suitable method for sampling field K_s

For logical selection of a suitable method for rapid field survey of saturated hydraulic conductivity, the criteria need to be clearly defined. In this study, the criteria chosen were based on time required to execute the experiment, costs involved, and complexity and accuracy of the measurement.

Using the above criteria, the single-ring infiltrometers were identified as a suitable method for measurement of surface saturated hydraulic conductivity. Apart from their simple construction and use, single-rings were shown to offer opportunity for rapid large-area survey.

Not only did the infiltrometers show most promise for large-area measurement of soil surface K_s but also allowed inclusion of soil pore-size distribution index in the analysis. In addition, the old notion that double rings are needed in K_s measurements is no longer valid because robust single ring methods include analysis of critical factors such as soil texture and structure index (alpha parameter), diameter of cylinder ring used, depth of ring insertion, and the ponding depth.

5.1.2 Area-wide survey of field K_s

A potentially important requirement for capturing variability of K_s is the ability to include a large number of replications. By sampling soil K_s in plots that are stratified within land use types and nested in slope zones, this study showed that K_s can be described across a watershed. The use of 30 m by 30 m plots with at least three replications of K_s measurements was shown to ensure coefficient of concordance of more than 60 % at the plot level. It was also shown in this study that soil K_s was lognormally distributed over the watershed. Thus, in representing saturated hydraulic conductivity classes in a watershed, median values should be generally used rather than average values.

5.1.3 Effects of land use change on soil K_s

In this study, land use type and slope zone were found to explain a high level of variability in K_s measurement. These factors, therefore, should be considered in predictive models for K_s and especially in hydrological models.

The knowledge of variation of soil K_s with landscape slope helped to explain the hydrologic phenomenon observed in this watershed. High K_s values in upland slope zones and very low K_s values in the lowlands are likely to be the cause of 'hydrologic pressure' in the midland. This near-surface hydrologic suppression compounded with heavy tropical storms could be a primary cause of the adverse environmental consequences seen on the lake plains, including gully development and flooding.

5.1.4 Extent of correlation of surface K_s with spectral reflectance

The soil spectral reflectance determined from the laboratory was found to correlate well with field-measured surface soil K_s but not with field-measured topsoil K_s. With minimum soil disturbance, field-measured soil surface K_s related well with laboratory–measured soil spectral reflectance. The correlation is stronger in the short wave infrared wavebands than the visible range of the soil spectral reflectance signatures.

The soil spectral approach was also found to provide a valid and promising opportunity for spatially characterizing soil saturated hydraulic conductivity in a watershed. The approach is fast and cheap and provides a robust prediction model between soil spectral reflectance and soil saturated hydraulic conductivity.

5.1.5 Spatial distribution of surface K_s

The results of this study demonstrated that semivariograms are useful tools for designing sampling schemes for K_s measurements. The semivariograms predicted the minimum distances needed between sampling points. Thus, if the semivariogram model developed in this study can be assumed to be a sound semivariogram model for the area, the optimal sampling separation distance between field measurements of hydraulic conductivity is 80 m.

The low estimation error, ϵ = -6.22 x 10^{-4} cm/hr, which is not significantly different from zero, and the low variance σ_{ε}^{2}= 2.371x 10^{-1} cm/hr show that the kriging estimation in this study was good. The surface interpolation map illustrated a smooth geographical pattern of surface saturated hydraulic conductivity values over the Awach watershed.

The surface interpolation map of surface K_s shows low to moderately low values of surface K_s in the lake plains and moderately high to high values of surface K_s in the midland and upland zones of the watershed. These classes of surface K_s coincide with values reported in USDA (1993).

5.2 Recommendations

1. In the determination of a suitable method for measuring K_s, emphasis was placed on surface K_s. Further study is recommended to come up with a suitable method for profile K_s. In addition, such criteria as automation could be considered alongside the criteria used in this study.

2. It is also recommended that for finding a suitable method for determining soil K_s, a study should test the relative performance of the methods in different homogeneous soils including on steep slopes, stony soils, hardsetting soils etc.
3. There is need to repeat the procedures presented here for area-wide survey at the same location at different times to capture the much needed tempo-spatial variability of K_s in a watershed.
4. Since it has been shown that land use type strongly influences soil K_s, this study should be extended to other land use types such as improved fallow systems, roads and paths, homesteads, etc, to evaluate the effects of these land use types more precisely on watershed hydrology.
5. In order to benefit hydrologic modeling, the spectral library procedure outlined in this study should be extended to other soil hydraulic properties such as water retention characteristics, sorptivity, wetting front suction, diffusivity, etc.
6. The use of data mining techniques that allow for non-linearity between K_s and soil reflectance factors that may improve K_s–spectral reflectance calibrations should be tested.
7. Some of the prime factors which were apparent during field measurements and that were though to affecting reliability and success of field measurement of surface K_s were the quality of infiltration water used and the amount of sun heat to which the experimentation is subjected. A study is recommended to quantify this fact.
8. Slope and land use type were identified in this study as major factors influencing K_s and should therefore be included in regression models that relate K_s to soil reflectance spectra.
9. A relationship between K_s and integrated spectral indices of fertility and erosion should be explored, as they have been shown to map out well from Landsat imagery (http://www.icraf.cgiar.org). In addition, the spatial interpolation of soil K_s using Landsat imagery should be compared with the kriging approach used in this study.

10. The mapped K_s values should be used in conjunction with simple hydrologic models to investigate management effects on watershed hydrology.

REFERENCES

Ahuja L.R., Naney J.W., Green R.E., and Nielsen D.R. (1984): *Macroporosity to Characterize spatial variability of Hydraulic Conductivity and Effects of Land Management.* Soil Sci. Soc. Am. J. 48: 699 – 702.

Ahuja L.R., Naney J.W. and Williams R.D (1985): *Estimating Soil Water Characteristics from Sample Properties or Limited Data*, Soil Sci. Soc. Am. J., 49:1100 – 1105.

Amoozeger A and Warrick A, W (1986): *Field Measurements of Saturated Hydraulic Conductivity: Methods of Soil Analysis, Part I*, Agronomy Monograph Series no. 9, ASA and SSSA, Madison.

Analytical Spectral Devices Inc. (1997): *FieldSpec™ User's Guide.* Analytical Spectral Devices Inc., Boulder, Company.

Ankeny D.M., Ahmed, M., Kaspar T.C. and Horton R. (1991): *Simple Field Method for Determining Unsaturated Hydraulic Conductivity*, Soil Sci. Soc. Am. J. 55:467-470.

Ankeny M.D. (1992): *Methods and Theory for Unconfined Infiltration Measurements.* In Advances in Measurement of Soil Physical Properties: Bringing Theory into Practice, SSSA Special Publication no. 30. Madison, WI 53711.

Arya L.M., Leij F.J., Shouse P.J. and van Genuchten T.M. (1999): *Relationship Between the Hydraulic Conductivity Function and the Particle-Size distribution*, Soil Sci. Soc. Am. J., 63:1063 – 1070.

Asol R.N. (1984): *Salinity/Alkalinity Studies at Kimorigo/Kamleza Scheme*, Unpublished Postgraduate Diploma Thesis, University of Nairobi.

Atzberger C (2002): *Soil Optical Properties – A Review*, Remote Sensing Report, D-54286 Tier, Germany.

Becker F., Ramanantsizehena P. and Stoll M.P. (1985): *Angular Variation of the Bidirectional Reflectance of Bare Soils in the Thermal Infrared Band*, In Remote Sensing for Earth Sciences: Manual of Remote Sensing, John Wiley and Sons, London.

Ben-Dor E. and Benin A. (1990): *Diffuse Reflectance Spectra of Smectite Minerals in the Near Infrared and their Relation to Chemical Composition,* Sci. Geol. Bull., 43(2-4):117-128.

Ben-Dor E., Irons J.R. and Epema G.F. (1999): *Soil Reflectance*, In Remote Sensing for Earth Sciences: Manual of Remote Sensing, John Wiley and Sons, London.

Bohler T., Karatzas K., Pienel G., Rose T. and Jose R.S (2002): *Providing Multi-Modal Access to Environmental Data-Customisable Information Services for Disseminating Urban Air Quality Information in APNEE*, Computers, Environment and Urban Systems, 26(1): 39 - 61

Booth B. (1999): *Getting Started with ArcInfo™,: Spatial* Analysis, Environment Research Institute Inc., USA.

Bouma J., Hillel D., Hole F.D. and Amerman C.R. (1971): *Field Measurement of Unsaturated Hydraulic Conductivity by Infiltration Through Artificial Crusts*, Soil Sci. Soc. Am. Proc., 35:362-364.

Bouma J. (1983): *Use of Soil Survey Data to Select Measurement Techniques for Hydraulic Conductivities*, Agric. Water Management, 9: 107 - 111.

Bouma J. (1989): *Using Soil Survey Data for Quantitative Land Evaluation*, Adv. Soil Sci., 9: 177-213.

Bouwer H. (1961): *A double Tube Method for Measuring Hydraulic conductivity of Soil In Situ Above the Water Table*, Soil Sci. Am. Proc., 25:334-339.

Bouwer H. (1966): *Rapid Field Measurement of Air Entry Value and Hydraulic conductivity as Significant Parameters in Flow Systems Analysis*, Water Resour. Res., 2:729 – 738.

Bouwer H. (1978): *Groundwater Hydrology*, McGraw-Hill, New York.

Bressler E., Dagan G., Wagnet R.S. and Laufer A. (1984): *Statistical Analysis of Salinity and Texture Effects on Spatial Variability of Soil Hydraulic Conductivity*, Soil Sci. Soc. Am. J., 48: 16 – 25.

Brooks R.H. and Corey T.A. (1964): *Hydraulic Properties of Porous Media*, Hydrol. Pap. 3. Colorado State University, Collins.

CAMO Inc. (1998): The Unscrambler: User's manual. Corvallis, OR.

Campbell G.S. (1974): *A simple Method for Determining Unsaturated Conductivity from Moisture Retention Data*, Sci. Paper no. 4005, College of Agric. Resech. Center, Washington SU. Pullman. Project no. 0079.

Cassel D. K. and Bauer A. (1975): *Spatial Variability in Soils Below Depth of Tillage: Bulk Density and Fifteen Atmospheres percent*, Soil Sci. Soc. Am. J., 39:247 – 250.

Childs E.C. and Collis-George N. (1950): *The Permeability of Porous Materials*, Proc. Roy. Soc., A. 201:392-405, London. In Trans. 7Th Int. Congr. Soil Sci. Madison, Wis.

Chapman T.G. and Dunin F.X. (1975): *Prediction in Catchment Hydrology*, Aust. Acad. Sci., Canberra.

Cheruiyot S.K. (1984): *Infiltration Rates and Sediment Production of a Kenyan Woodland as Influenced by Vegetation and Prescribed Burning*, MSc. Thesis, A and M University, Texas.

Chow V.T., Maidment D.R. and Mays L.W. (1988): *Applied Hydrology*, McGraww-hill, NewYork.

Clark R.N. and Roush L.T. (1984): *Reflectance Spectroscopy: Quantitative Analysis Techniques for Remote Sensing Applications*, J. Geophy. Res., 89:6329-6340.

Clothier B.E. and Smetten K.R.J. (1990): *Combining Laboratory and Field Measurements to Define the Hydraulic Properties of Soil*, Soil Sci. Soc.Am. J. 54:299-304.

Comegna V., Damiani P. and Somella A. (1989): *Use of Fractal Model for Determining Soil Water Retention Curves*, Geoderma, 85: 307 – 323.

Cooper K. and Smith J.A. (1985): *A Monte Carlo Reflection Model for Soil Surfaces with 3D Structure,* IEEE Trans. Geosci. Remote Sensing, 23:668-673.

Constantz J. (1983): Adequacy of a Compact Double-Cap Infiltrometer Compared to ASTM Double-Ring Infiltrometer, *In Advances in Infilt. Proc. of the Nat. Cont. on Adv. In Infiltr.* ASAE, 11: 226 – 230.

Condit H.R. (1970): *The Spectral Reflectance of American Soils*, Photogramm. Eng., 36:955-966.

Cornelis W.M., Rousyn J., van Meirvenne M. and Hartmann R. (2001): *Evaluation of Pedo-Transfer Functions for Predicting the Soil Moisture Retention Curve*, Soil Sci. Soc Am. J. 65:638 – 648.

Crassie N.A.C (1991): *Statistics for Spatial Data*, John Willey and Sons, New York.

Cresswell H.P., Smiles D.E. and Williams J. (1992): *Soil Structure, Soil Hydraulic Properties and the Soil Water Balance*, Aust. J. Soil Res. 30:265-283.

Cowe I.A and McNicol J.W (1985): *Spectral Applications*, Appl. Spectrsc., 39, 257-263.

Cudahy T. J. and Ramanaidou E.R. (1997): *Measurement of the Hematite:Geothite Ratio Using Visible and Near Infrared Reflectance Spectrometry in Channel Iron Deposits*, Western Australia J. of Earth Sciences 44:411 – 420.

Da Costa, L.M (1979): *Surface Soil Colour and Reflectance as Related to Physiochemical and Mineralogical Soil Properties*, In Remote Sensing for Earth Sciences: Manual of Remote Sensing, John Wiley and Sons, London.

Davies T.M.C. and Fern T. (2002): *Sorting the Wheat from the Chaff*, Spectroscopy Europe, 14 (2): 16 – 17.

Decagon Devices Inc. (2000): *Mini-disk Infiltrometer,* Pullman, Washington.

Eastman J.R (1999): *IDRISI™ Version 32: Tutorial*, Clark University, USA

Eijkelkamp Agrisearch Equipment Inc., (1983): *Cylinder Infiltrometers: Operations Manual*, The Netherlands.

Elsenbeer H. and Vertessy R.A. (2000): *Hydrologic Flow Paths in Tropical Rainforest Soils Capes – A Review*, Hydrological Processes 14:2367-2381.

Elrick D. E. and Reynolds W.D. (1992): *Infiltration from Constant-Head Well Permeameters and Infiltrometers,* In Adv. In Measurements of Soil Physical Properties: Bringing Theory into Practice, Soil Sci. Soc. Am. Spec. Publ. 30 p 1 – 22, Madison, WI.

Fern T (2000): *Near Infra-Red News*, JNIR, 11(6): 14 - 15

Freeze R.A and Cherry J.A. (1979): *Groundwater*, Prentice-Hall, NJ

Gachene C.K.K. (1995): *Effects of Soil Erosion on Soil Properties and Crop Response in Central Kenya*, PhD Thesis, Swedish University of Agricultural Sciences.

Gallichand J., Marcotte D., Prasher S.O. and Broughton R.S. (1992): *Optimal Sampling Density of Hydraulic Conductivity for Subsurface Drainage in the Nile Delta*, Agriculture Water Management, 20: 299-312.

Gardner W.R. (1959): *Solutions of the Flow Equation for Drying of Soils and Other Porous Media*, Soil Sci. Soc. Am. Pro., 23: 183 – 187.

Gerberman D. and Neher J. (1979): *Reflectance of Varying Mixtures of Clay Soil and Sand*, PERS, 45: 1145 – 1151.

Gonclaves C.M. (1999): *Pedotransfer Functions for Portuguese Soils*, European Soil Bureau, Research Report 4:489-491.

Gupta S.C. and Larson W.E. (1979): *Estimating Soil Water Characteristics from Particle Size Distribution, Organic Matter Percent and Bulk Density*, Water Resour. Res., 15: 1633 – 1635.

Hecky R. (1993): *The Eutrophication of Lake Victoria*, Proc. Int. Ass. Theor. Appl. Limnol., 25: 39 – 48.

Hecky R. (2000): *Eutrophication and Biodiversity Decline in Lake Victoria*, In Proc. Internl. Decade of E. African Lakes (IDEAL) 2nd Int. Symp. 10th – 13th 2000, Club Makokola, Malawi.

Hoekstra D. and Corbett J. (1995): *Sustainable Agricultural Growth for Highlands of East and Central Africa: Prospects to 2020.* Paper

Presented at the Ecoregions of the Developing World: A lens for Assessing Food, Agriculture and Environment to the Year 2020, held at Washington DC, USA, Organized by the Int. Food Policy Research Institute (IFPRI).

Holland D.F., Yitayew M., Asce M. and Warrick A.W. (2000): *Measurement of Subsurface Unsaturated Hydraulic Conductivity*, Journ. Irrg. and Drnge. Engin. Vol. 126, no. 1.

Horton R.E. (1933): *The Role of Infiltration in the Hydrologic Cycle*, Trans. Am. Geophys. Union, 14: 446-460.

Hunt G. R. and Salisbury J.W. (1970): *Visible and Near-Infrared Spectra of Minerals and Rocks: I Silicate Minerals*, Modern Geology, 1: 283 – 300.

Jackson R.D. (1972): *On the Calculation of Hydraulic Conductivity*, Soil Sci. Soc.Am Proc., Vol. 36; 5 - 19.

Jaetzold R. and Schmidt H. (1983): *Farm Management Handbook of Kenya*, Vol IIB, Ministry of Agriculture, Nairobi, Kenya.

Journel A. G. and Huijbregts C.J. (1978): *Mining Geostatistics,* Academic Press Inc., NewYork.

Kachanosky R. G., Rolston D.E. and De Jong E. (1985): *Spatial Variability of a Cultivated Soil as Affected by Past and Present Microtopography*, Soil Sci. Soc. Am. J., 49: 1082-1087.

Kanake J.K. (1982): *Semi-Detailed Soil Survey Report no. 56*, Kenya Soil Survey, Nairobi.

Kariuki P. C., Woldai T. and van Der Meer F.D. (2001): *Determination of Soil Activity in Kenyan Soils from Spectroscopy*, The Intnl. Archives for Photogrammetry, Remote Sensing and Spatial Inf. Sci. Vol. 24 part 6/W6.

Kessler J. and Oosterbaan R. J. (1962): *Drainage Principles and Applications: Surveys and Investigations*, Publc. 16. Vol. III, pg 292-294, Inst. For Land. Recl. And Imprvt. The Netherlands.

Klute A. and Dirksen C. (1986): *Hydraulic Conductivity and Diffusivity: Laboratory Methods*, In Methods of Soil Analysis, Part 1. Physical and

Mineralogical Methods – Agronomy Monograph no.9, p687-734, Madison, WI.

Kutilek M. and Nielsen R.D. (1994): *Soil Hydrology*, Catena Verlag, Germany.

Lagerwerff J. V., Nakayama F.S. and Frere M.H. (1969): *Hydraulic Conductivity Related to Porosity and Swelling of Soil*, Soil Sci. Soc. Am. J., 33: 3-11.

Lawes Agricultural Trust (2002): *Genstat for Windows, Release 6.1*, Experimental Station.

Leger R.G., Millere G.J.F. and Chomchan S. (1979): *The Effects of Organic Matter, Iron Oxides and Moisture on the Colour of Two Agricultural Soils Of the Quebec*, Can. J. Soil Sci., 59:191-202

Leszynski S. (1997): *Access 97®: Expert Solutions*, Que® Corporation, USA.

Linsen L.P.M. (1969): *Double Tube Method of Measuring Hydraulic Conductivity*, Univ. of Agric., Wageningen.

Madramootoo C. A. and Enright P. (1990): *Prediction of Runoff Using the Green – Ampt Infiltration Model and Estimated Soils Parameters*, Canadian Agric. Eng. 32: 39 – 45.

Marshall T.J. (1958): *A relation Between Permeability and Size Distribution of Pores*. J. Soil Sci. 9:1-8.

Marshall T.J and Holmes S. (1979): *Soil Physics*, Princeton, London.

Martens H. and Naes T. (1989): *Multivariate calibration* in Shepherd and Walsh (2002): Development of Reflectance Spectral Libraries for Characterization of Soil Properties, Soil Sci. Soc. Am. J. 66:988 – 998.

Messing I. (1989): *Estimation of the Saturated Hydraulic Conductivity in Clay Soils from Soil Moisture Data*, Soil Sci. Soc. Am. J., 53: 665 – 668.

McBratney A. B. and Webster R. (1983): *How Many Observations are Needed for Regional Estimation of Soil Properties*, Soil Sci. 135: 177 –183.

Miller I. and Freud J.E. (1985): *Probability and Statistics for Engineers,* Prentice Hall, London.

Millington R.J. and Quirk J.P. (1961): *Transport in Porous Medium*, Int. Congr. Soil Sci. Trans. Vol. 1.3, 97-106.

Montero S., Irene C. and Brimhall G.H. (2001): *Semi-Automated Mineral Identification Algorithm for Ultraviolet, Visible and Near-Infrared Reflectance Spectroscopy*, Paper presented in Annual Conference of the intnl. Assoc. for Math. Geology. Pg 14.

Montgomery S. and Baumgardner K. (1974): *Reflectance Properties of Soils*, Adv. in Agronomy, 38: 1 – 44.

Mood A. M. and Graybill F.A. (1963): *Introduction to Theory of Statistics*, McGraw – Hill, NY.

Morgan R. P. C. (1986): *Soil Erosion and Conservation*, Longman, London.

Mualem Y. (1986): *Hydraulic Conductivity of Unsaturated Soils: Prediction and Formulas*, In Methods of Soil Analysis, Part 1. Physical and Mineralogical Methods – Agronomy Monograph no. 9, p799-823, Madison, WI.

Mugidde R. (1993): *The Increase in Phytoplankton Productivity and Biomass in lake Victoria (Uganda)*, Intnl. Ass. Theor. Appl. Limnol. Proc. 25: 39 – 48.

Neter J., Wassermann W. and Kutner M.H. (1990): *Applied Linear Statistical Models*, IRWIN, Illinois.

Naes T., Isaksson T., Fern T. and Davies M.H. (2002): *Multivariate Calibration and Classification*, NIR Publication, West Sussex.

Nielsen D.R, Giggar J.W and Erth K.T. (1973): *Spatial Variability of Field Measured Soil-water Properties*, Hilgardia, 42: 215 – 259.

Obiero J.P (1994): *Evaluation of Infiltration Using Green-Ampt Model and Hydrologic Data for Kenyan Catchments.* M.Sc. Thesis, Univ. Of Nairobi, Nairobi.

Okwach G.E (1994): *Evaluation of Management Effects on Surface Hydrology on the Luvisols of Semi-Arid Eastern Kenya*, PhD Thesis, Griffith University, Australia.

Onyando J.O and Sharma T.C (1995): *Simulation of Direct Runoff Volumes and Peak Rates from Rural Catchments in Kenya, East Africa*, Hydrol. Sci. J., 40(3): 367-380.

Omulabi E.A.J (1996): *The Effects of Secondary Stalinization on Soil Physical Properties of Salt Affected Soils in Makindu, Kenya*, MSc. Thesis, University of Nairobi.

Omulabi E.A.J., Kinyali S.M. and Tirop S.K. (2000a): *The Influence of the Soil Physical Properties on the Infiltration Rates in the Salt Affected Soils in Makindu, Makueni District, Kenya*, Proc. Soil Sci. Soc. East Africa, 3:209-219.

Omulabi E.J., Kinyali S.M., Ndari I. and Gichobu A. (2000b): *Saturated Hydraulic Conductivity – Physical Properties Relationships of Salt Affected Soils in Makindu, Makueni District, Kenya*, Proc. Soil Sci. Soc. East Africa, 3:220-224.

O'Neill B., Kachanoski R.G. and Elrick D.E. (1990): *Effects of Management on Soil Hydraulic Properties*, SWEEP Report no. 18, Ont.

Ophori D. U. and Maharjan B. (2000): *First Approximations of Soil Moisture Retention Curves*, 14: 1131 – 1138.

Oswal M. (1983): *A Textbook of Soil Physics,* Vickas Publishing House, PVT.

Otieno J.N. (1990): *Drainage for Salinity Control in Kimorigo/Kamleza Irrigation Scheme*, MSc. Thesis, University of Nairobi.

Panchev S. (1971): *Random Functions and Turbulence*, Pergaman Press, Oxford.

Parlange J.Y. (1972): *Theory of Water Movement in Soils: 4. Two and Three Dimensional Steady Infiltration Rate*, Soil Sci., 113:96-101.

Perroux K.M. and White I. (1988): *Design for Disc Permeameters*, Soil Sci. Soc. Am. J, 52:1205-1215.

Philip J.R. (1985): *Approximate Analysis of the Borehole Permeameter in Unsaturated Soil*, Water Resour. Res., 21(7): 1025-1033.

Philip J.R. (1957): *The Theory of Infiltration: Sorptivity and Algebraic Infiltration Equations*, Soil Sci. 84:257-264.

Rawls W.J. and Brakensiek D.L. (1983): *A Procedure to Predict Green and Ampt Infiltration Parameters*, In Advances in Infiltration, Proc. Nat. Conf. Adv. Infil. ASAE, 11:102-112.

Rawls W.J. and Brakensiek D.L. (1982): *Estimating Soil Water Retention from Soil Properties.* J. Irrg. Drainage Div. ASCE, 108: 166 – 171.

Rawls W.L. and Brakensiek D.L. (1985): *Prediction of Soil Water Properties for Hydrologic Modeling,* p 293 299, in Jones E and Ward T.J (ed) Watershed management, Eighties, Proc. Symp. ASCE. Denver, CO, 30 Apr – 2 May. 1985, ASCE, NewYork.

Rawls W.J., Brakensiek D.I. and Logsdon S.D. (1993): *Predicting Saturated Hydraulic Conductivity Using Fractal Principles,* Soil Sci. Soc. Am. J., 57: 1193 – 1197.

Reginato R.J. and van Bevel C.H.H. (1962): *Pressure Cell for Soil Cores,* Soil Sci. Soc. Am. Proc,. 26: 1 – 3.

Remy J.P. (1973): *The Measurement of Small Permeabilities in the Laboratory,* In Methods of soil Analysis, Part I. Physical and Mineralogical Methods – Agronomy Monograph no. 9, Madison, WI

Reynolds W.D., Elrick D.E. and Topp G.C. (1983): *A Re-Examination of the Constant Head Well Permeameter Method for Measuring Saturated Hydraulic Conductivity Above the Water Table,* Soil Sci., 136:250-258.

Reynolds W.D., Elrick D.E. and Clothier B.E. (1985): *The Constant Head Well Permeameter: Effect of Unsaturated Flow,* Soil Sci., 139:172-180.

Reynolds W.D. and Elrick D.E. (1990): *Ponded Infiltration from a Single Ring: I. Analysis of Steady Flow,* Soil Sci. Soc. Am. J., 54:1233-1241.

Reynolds W.D. and Elrick D.E. (1991): *Determination of Hydraulic Conductivity Using a Tension Infiltrometer,* Soil Sci. Soc. Am. J., 55:633-639.

Rogers W.F. (1970): *A Portable Infiltrometer,* Agric. Engin. 51:469-471.

Russo D. and Bresler E. (1981): *Soil Hydraulic Properties as a Stochastic Process: I. An Analysis of Field Spatial Variability,* Soil Sci. Soc. Am. J., 45: 682 – 687.

Salford Systems Inc. (2001): *MARS^{TM} Version 2,* Salford systems Inc. USA.

San Jose R., Stohl A., Karatzas K., Bohler T., James P. and Salas I. (2001): *An Extraordinary Ozone Episode in Madrid (April 2000) During Night Time: A Modeling Study,* Proc. 7th Intnl. Conf. Harmonization within

Atmospheric Dispersion Modeling for Regulatory Purposes, Beilgerate (Lake Maggorie), Italy, May 28 – 31, 2001, pp. 390 – 394.

Savitzky A. and Golay J.E.M. (1964): *Smoothing and Differentiation of Data by Simplified Least Squares Procedure*, Analytical Chemistry 36(8): 1627 – 1639.

Schaap M.G., Leij F.J and van Genuchten T.M. (1998): *Neural Network Analysis for Hierarchical Prediction of Soil Hydraulic Properties*, Soil Sci. Soc. Am. J. 62: 847 – 855.

Scheidegger A. E. (1960): *Physics of Flow Through Porous Media*, Macmillan, New York.

Scotter D.R., Clothier B.E. and Harper E.R. (1982): *Measuring Saturated Hydraulic Conductivity Using Twin Rings*, Aust. J. soil Res., 20:295-304.

Sharma M.L., Gander G.A. and Hunt C.G. (1980): *Soil Spatial Variability in a Watershed*, J. Hydrol., 45: 101 – 122.

Sharma M.L., Barron R.J.W. and de Beer E.S (1983): *Spatial Structure and Variability of Infiltration Parameters*, Adv. In Infiltration in Proc. of the Nat. Conf. on Adv. In Infiltration ASAE 11: 113 – 121.

Shepherd K.D. and Walsh M.G (2002): *Development of Reflectance Spectral Libraries for Characterization of Soil Properties*, Soil Sci. Soc. Am. J., 66: 988 – 998.

Simunek J. and van Genuchten T. M. (1997): *Estimating Unsaturated Hydraulic Properties from Multiple Disc Infiltration Data*, USDA, CA.

Sirya K.S.J. (1994): *A Hydrologic Study of Water Harvesting Micro Catchments in a Semi Arid Area*, Unpublished MSc. Thesis, Moi University, Eldoret, KeNew Yorka.

Smetten K.R.J. and Clothier B.E. (1989): *Measuring Unsaturated Sorptivity and Hydraulic Conductivity Using Multiple Disc Permeameters*, Soil Sci. J., 40: 563-568.

Snedecor G. (1989): *Statistical Methods*, Prentice-Hall, London.

Soilmoisture Equipment Inc. (1991): *Instructors Manual for Guelph Permeameter*, Santa Barbara.

Stephens D.B. (1992): *Application of the Borehole Permeameter*, Soil Sci. Soc. Am. J., 53: 711- 805.

Stone M. (1974): *Cross–Validatory Choice and Assessment of Statistical Prediction*, J. of the Ry. Stat. Soc. B 36: 111 – 147.

Suits G.H. (1983) : *The Nature of Electromagnetic Radiation*, In Simmonet D.S. and Ulaby F.t. edition :Manual of Remote Sensing. Vol. I. Am. Soc. Photogrammetry, falls Church, Va. Pp 37 – 60.

Suleiman A.A. and Ritchie J.T. (2001): *Estimating Saturated Hydraulic Conductivity from Soil Porosity*, Trans. ASAE 44(2):1-15.

Suresh R. (1997): *Watershed Hydrology*, Nem Chand Jain, New Delhi.

Swartzendruber D. and Olson T.C. (1961): *Sand-Model Study of Buffer Effects in the Double-Ring Infiltrometer*, Soil Sci. Soc. Am. Proc., 25:5-8.

Talsma T. and Hallam P.M. (1980): *Hydraulic Conductivity Measurement of Forest Catchments. Aust.* J. Soil Res. 30:139-148.

Tietje O. and Tepkenhinrichs M. (1993): *Evaluation of Pedo-Transfer Functions*, Soil Sci. Soc. Am. J. 57: 1088 – 1095.

Tuli A., Kosugi K. and Hopmans J.W. (2001): *Simultaneous Scaling of Soil Water Retention and Unsaturated Hydraulic Conductivity Functions Assuming Lognormal Pore-size Distribution*, Adv. Water Res., 24:677-688.

Tsai F. and Philpot W. (1998): *Derivative Analysis of Hyperspectral Data*, Remote Sensing of Environment, 66:41 – 51.

Thomas D.B. (1997): *Soil and Water Conservation Manual for Kenya*, Ministry of Agriculture, Livestock Development and Marketing, Govn. of Kenya, Nairobi.

Tyler S.W and Wheatcraft S.W (1989): *Application of Fractal Mathematics to Soil Water Retention Estimation*, Soil Sci. Soc. Am. J., 53: 987 – 996.

USBR (1978): *Land Drainage Techniques and Standards: Reclamation Instructions*, USBR, Colorado.

USDA (1993): *Soil Survey Manual*, United States Department of Agriculture, Handbook No. 18, Washington D.C

Vandervaere J.P., Peugeot C., Vauclin M., Jaramillo R.A. and Lebel T. (1997): *Estimating Hydraulic Conductivity of Crusted Soils Using Disc Infiltrometers and Minitensiometers*, J. Hydrology, 11:171 -128.

Van Genuchten T.M. (1980): *A Closed-Form Equation for Predicting the Hydraulic Conductivity of Unsaturated Soils*, Soil Sci. Soc. Am. J.,, 44:892-898.

Vauclin M., Viera S.R. and Nielsen D.R. (1983): *The Use of Cokriging with Limited Field Soil Observations*, Soil Sci. Soc. Am. J.,, 47: 175 – 184.

Vereecken H. (1988): *Pedotransfer Functions for the Generations of Hydraulic Properties for Belgian Soils,* European Report no. 18 p 489-499.

Vereecken H., Darius J. and Feyen J. (1989): *Estimating Soil Moisture Retention Characteristic from Texture, Bulk Density and Carbon Content*, Soil Sci. 148:389 – 403.

Viera S.R., Nielsen D.R. and Biggar J.W. (1982): *Spatial Variability of Field Measured Infiltration Rate*, Soil Sci. Soc. Am. J.,, 45: 1040 –1048.

Vijay P.S (1992): *Elementary Hydrology*, Prentice Hall, New Jersey.

Vogel T., van Genuchten T.M. and Cislerova M. (2001): *Effect of the Shape of the Soil Hydraulic Functions Near-Saturation on Variably-Saturated Flow Predictions*, Adv. Water Res., 24:133-144.

Ward R.C. (1989): *Principles of Hydrology*, McGraw-Hill, London.

Warrick A.W. and Nielsen D.R. (1980): *Spatial Variability of Soil Physical Properties in the Field p 319 – 344*, in Hillel D. (ed) Spatial Variability of Soil Physical Properties in the Field, Academic Press New York.

White I. and Sully M. J., (1987): *Macroscopic and Microscopic Capillary Length and Time Scales from Field Infiltration*, Water Resour. Res., 23:1514-1522.

White I. and Perroux K.M. (1987): *Use of Sorptivity to Determine Field Soil Hydraulic Properties*, Soil Sci. Soc. Am. J., 51: 1093 – 1101.

White I., Sully M.J., and Perroux K.M. (1992): *Measurements of Surface-Soil Hydraulic Properties: Disc Permeability, Tension Infiltrometers and Other Techniques*, Soil. Sci. Soc.Am. J., 44: 1201-1222.

Webster R. and Burgress T.M. (1980): *Optimal Interpolation and Isarthmic Mapping of Soil Properties III: Changing Drift and Universal Kriging*, J., Soil Sci. 31: 505 – 524.

Willmott C.J., (1982): *Some Comments on the Evaluation of Model Performance*, Bull. Am. Met. Soc. 63(11); 1307 – 1313.

Wooding R.A. (1968): *Steady Infiltration from a Shallow Circular Pond,* Water Resour. Res., 4:1259-1273.

Yevjevich V. (1972): *Stochastic Process in Hydrology*, Water Resour. Res. Pub., Fort Collins. Colo.

Zangar C.N. (1953): *Theory and Problems of Water Percolation*, In Hydraulic Conductivity Measurement of Forest Catchments, Aust. J., Soil Res., 30:139-148.

Zhang R. (1997): *Determination of Soil Sorptivity and Hydraulic Conductivity from Disk Infiltrometer*, Soil Sci. Soc. Am. J. 61: 1024 – 1030.

APPENDICES

Appendix A

Determination and use of soil alpha parameter

(i) *Determination of alpha*

This portion shows a sample calculation of determination and use of soil alpha parameter in calculating soil surface K_s using single rings cylinder.

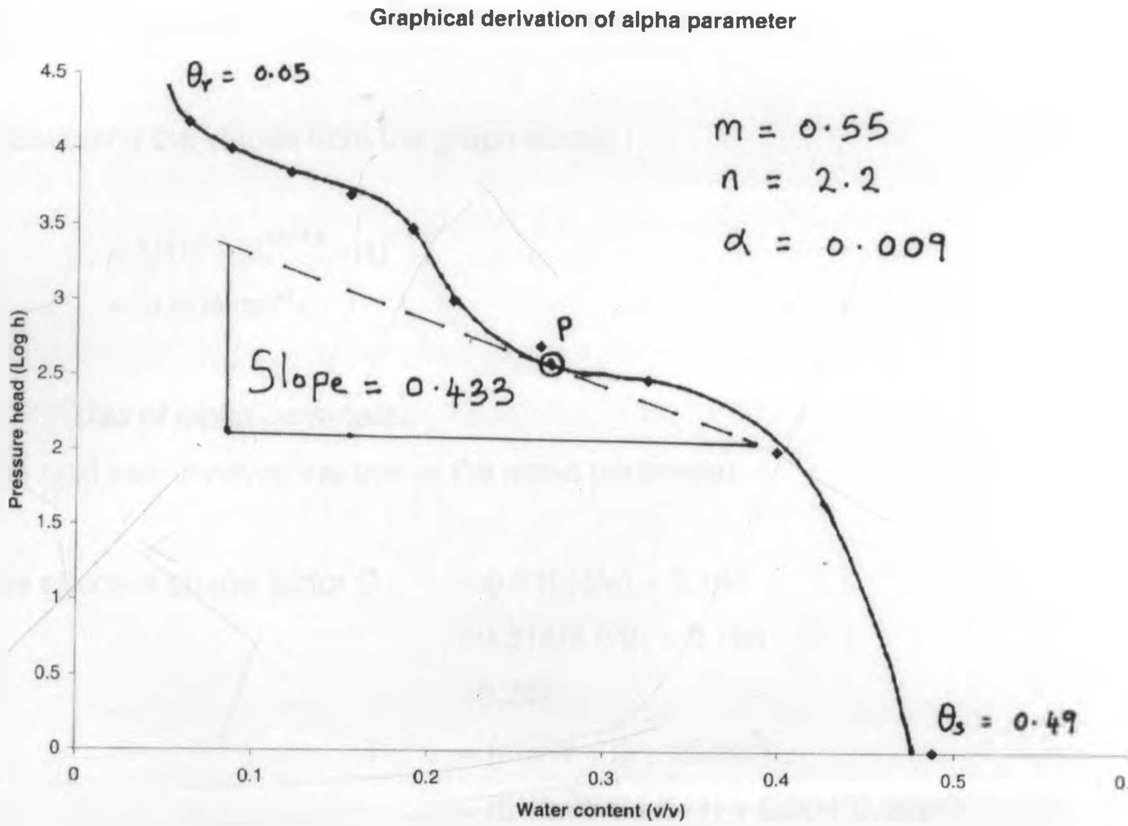

From the pF curve, $(\theta_s-\theta_r)$ is obtained so that the midpoint P can be located from the water content axis; P{$(\theta_s-\theta_r)/2$, log(h)}. Once P has been located, a tangent is drawn at the point and its gradient estimated.

Abs slope = abs $[d\theta/d(\log(h))] = (0.39 - 0)/(3.2 - 2.3) = 0.433$

The dimensionless slope S_p = abs slope $/(\theta_s-\theta_r) = 0.433/0.44 = 0.985$

From the dimensionless slope, the scaling parameter m is obtained from the absolute value theorem. In this case

$$m = 1 - \exp((-0.8*0.985) = 0.55$$

and from eq. (3.9), at the midpoint of the curve, saturation = 0.5, thus,

$$\alpha = 1/h_p \{2^{1/m} - 1\}^{1-m}$$

Substituting the values from the graph above,

$$= 1/10^{2.6} \{2^{1/0.55} - 1\}^{0.45}$$
$$= 0.004 \text{ cm}^{-1}$$

(ii) *Use of alpha parameter.*

The next part involves the use of the alpha parameter.

The effective shape factor G $= 0.316(d/a) + 0.184$

$=0.316(4.5/8) + 0.184$

$=0.362$

T $= \{a(\alpha W + 1) + \alpha G\pi a^2\}$

$= \{8*(0.004*4.5+1) + 0.004*0.362*3.14*64\}$

$= 8.370937$

K_s $= \alpha * G * Q_s/T$

$=0.004*0.362*1930.19/8.371$

$= 0.33$ cm/hr

Q_s = steady rate * cylindrical area = 0.16 cm/min* pi*8*8 = 1930.19 cm^3/hr

If the steady rate was multiplied by 60, the K_s would have been 0.16*60 = 9.6cm/hr (really overestimated, approximately 30 times).

Appendix B

Climatic data around Awach watershed

(a) *At the lower end of the Lowlands*

Station No. : 9034086
Station Name : Ahero Irrig. Res. Station
Location : latitude 0 8 S
: longitude 34 56 E
Period of Record : 1962 - 1980
Altitude : 1219 m

Month	Temperature				Relative Humidity		Daily sunshine hours (hrs)	Daily wind run (km)	Daily Evapo-ration (mm)	Monthly mean rainfall (mm)	Nos. of Raindays (days)
	Daily maximum (degree)	Daily minimum (degree)	Extreme high (degree)	Extreme low (degree)	Daily maximum (%)	Daily minimum (%)					
Jan	31.3	14.2	36.6	8.0	63	41	8.4	87.2	210	84	7
Feb	31.4	14.6	36.7	7.6	66	42	8.1	91.0	203	97	9
Mar	31.3	15.5	36.7	9.0	68	47	8.1	87.6	221	140	10
Apr	29.4	15.9	36.5	10.5	72	52	7.2	76.4	182	192	16
May	29.0	15.9	32.8	8.0	74	55	7.1	65.5	163	126	14
Jun	28.7	14.8	32.2	7.0	73	51	6.7	65.9	154	77	9
Jul	28.7	14.5	32.2	8.0	73	48	6.8	65.3	160	77	8
Aug	29.2	14.3	34.6	6.0	70	46	6.8	73.6	170	75	9
Sep	30.4	14.1	35.4	7.5	64	45	7.1	79.0	181	72	10
Oct	31.0	14.7	35.6	8.4	62	43	7.4	78.8	189	76	10
Nov	30.3	14.8	35.6	9.5	64	49	7.1	76.2	172	101	12
Dec	30.3	14.4	36.7	6.7	65	43	8.2	81.1	189	87	9
Total	361.0	177.7	421.6	96.2	814	562	89.0	927.6	2194	1204	123
Max.	31.4	15.9	36.7	10.5	74	55	8.4	91.0	221	192	16
Min.	28.7	14.1	32.2	6.0	62	41	6.7	65.3	154	72	7
Ave.	30.1	14.8	35.1	8.0	67	46	7.4	77.3	182	100	10

(b) *At the upper end of the Uplands*

Station No. : 9035244
Station Name : Kericho Timbilil T.R.I.
Location : latitude 0 21 S
: longitude 35 21 E
Period of Record : 1963 - 1980
Altitude : 2134 m

Month	Temperature				Relative Humidity		Daily sunshine hours (hrs)	Daily wind run (km)	Daily Evapo-ration (mm)	Monthly mean rainfall (mm)	Nos. of Raindays (days)
	Daily maximum (degree)	Daily minimum (degree)	Extreme high (degree)	Extreme low (degree)	Daily maximum (%)	Daily minimum (%)					
Jan	24.2	8.5	29.0	2.5	60	46	8.1	92.4	148	94	8
Feb	24.4	8.9	29.3	2.8	63	47	7.6	89.3	134	112	11
Mar	24.4	9.2	28.6	1.5	64	50	7.5	86.5	149	167	15
Apr	22.9	9.9	28.7	6.1	73	68	5.8	68.4	108	251	21
May	22.2	9.6	28.5	5.8	75	75	5.9	69.9	101	291	22
Jun	21.4	8.9	27.8	4.0	76	69	6.2	77.6	102	228	20
Jul	20.8	8.9	24.1	4.8	78	69	5.6	80.2	98	206	20
Aug	21.1	8.8	25.0	5.0	74	69	5.6	83.0	104	226	21
Sep	22.3	8.2	26.6	2.0	66	66	6.3	85.6	111	181	19
Oct	22.7	8.7	26.5	3.5	63	64	6.3	84.1	113	161	20
Nov	22.5	9.2	26.7	5.6	66	63	5.9	81.7	103	136	15
Dec	23.3	9.0	27.4	5.0	62	52	7.3	85.7	124	81	11
Total	272.2	107.8	328.2	48.6	820	738	78.1	984.4	1395	2134	203
Max.	24.4	9.9	29.3	6.1	78	75	8.1	92.4	149	291	22
Min.	20.8	8.2	24.1	1.5	60	46	5.6	68.4	98	81	8
Ave.	22.7	9.0	27.4	4.0	68	61	6.5	82.0	116	177	16

(a) *Stratification of watershed into slope zones*

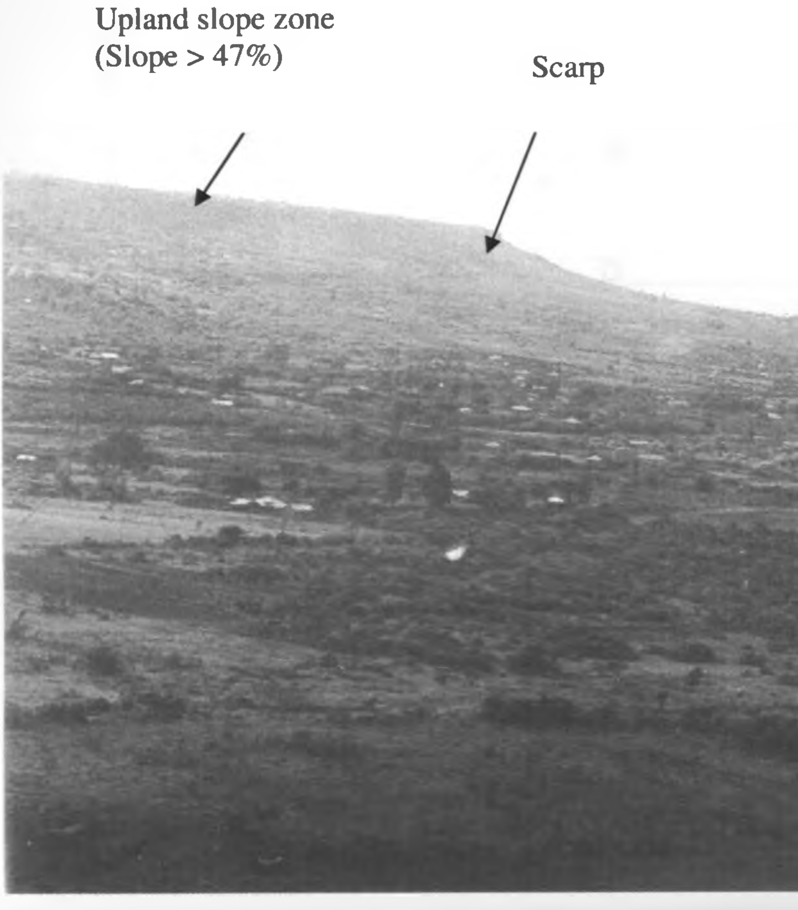

Appendix C

Field protocols

Midland slope zone (12% < Slope < 47%)

Lowland slope zone (Slope > 12%)

(b) *Field sampling plan at plot level*

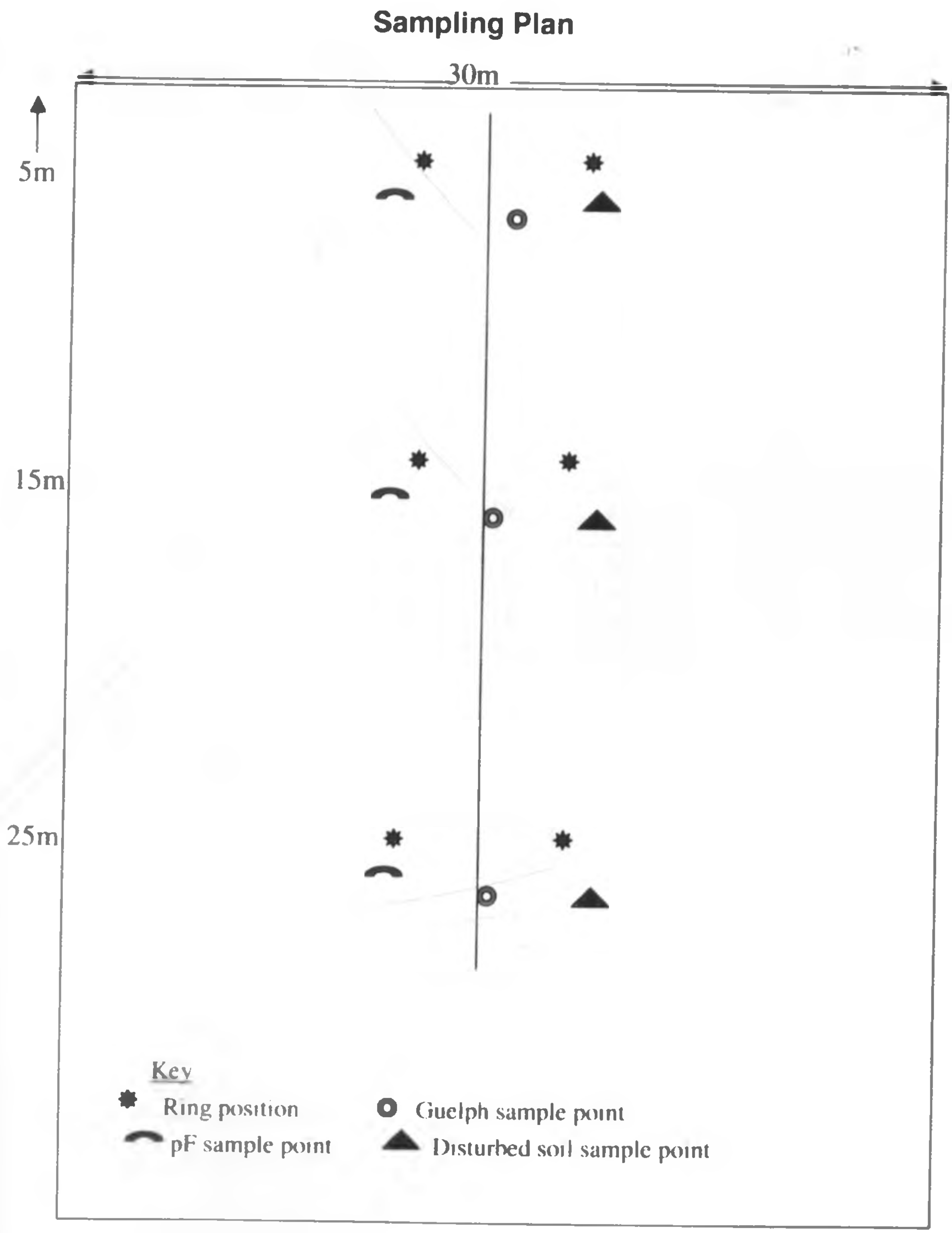

(c) *Measurement of field saturated hydraulic conductivity with single rings*

INFILTRATION EXPERIMENTS USING RING CYLINDERS			Project: MS		Site No. MS 20	
Ring position: 3	Source of water: tap water	No. of filling before reading starts: 1	Date 27/1/02	Sheet No.	Time in: 9:30 am	Time out: 12:10 p.m
Height of zero above soil surface (cm) 18.0 cm		Depth of insertion of ring (cm) 4.5 cm			Land class: Midland	
Surface features: Ploughed					Soil type: clay loam	

Ring number: A

Local Time (min)	Time Interval (min)	Cumulative infiltration. (cm)	Infiltration Intake (cm)	Infiltratio. Rate (cm/min)
11:30	~	11.2	~	
11:35	5	10.1	1.1	0.22
11:40	5	9.1	1.0	0.2
11:45	5	8.2	0.9	0.18
11:50	5	7.2	1.0	0.2
11:55	5	6.4	0.8	0.16
12:00	5	5.6	0.8	0.16
12:05	5	4.8	0.8	0.16
12:10	5	3.8	1.0	0.2

Steady infiltration rate = 0.16 cm/min

Ring number: B

Local Time (min)	Time Interval (min)	Cumulative infiltration (cm)	Infiltration. Intake (cm)	Infiltratio. Rate (cm/min)
11:30	~	12.7	~	
11:35	5	11.7	1.0	0.2
11:40	5	10.8	0.9	0.18
11:45	5	10.0	0.8	0.16
11:50	5	9.2	0.8	0.16
11:55	5	8.4	0.8	0.16
12:00	5	7.6	0.8	0.16
12:05	5	6.8	0.8	0.16
12:10	5	6.0	0.8	0.16

Steady infiltration rate = 0.16 cm/min

Comments:

The plot was ploughed, ready for planting

(d) *Measurement of field saturated hydraulic conductivity with guelph permeameter*

Standardized procedure for the Guelph permeameter readings and calculations

Reservoir constants: **Check reservoir used**

Combined Reservoirs	X	35.45	cm^2	
Inner Reservoir	Y	2.18	cm^2	✓

Auger Depth	12.09m

1st set of readings with height of water in well (H_1) set at 5 cm ✓

Reading number	Time (min)	Time interval (min)	Water level in reservoir (cm)	Water level change (cm)	Rate of water level change R_1 (cm/min)
1	9:37	~	0	~	~
2	9:39	2	3	3	1.5
3	9:41	2	6	3	1.5
4	9:43	2	9	3	1.5
5	9:45	2	11.7	2.7	1.35
6	9:47	2	14.3	2.6	1.3
7	9:49	2	16.8	2.5	1.25
8	9:51	2	19.3	2.5	1.25
9	9:53	2	21.8	2.5	1.25
10	9:55	2	24.3	2.5	1.25
11	9:57	2	26.8	2.5	1.25
		$\bar{R}_1$	= 1.25		

2nd set of readings with height of water in well (H_2) set at 10 cm ✓

Reading number	Time (min)	Time interval (min)	Water level in reservoir (cm)	Water level change (cm)	Rate of water level change R_2 (cm/min)
1	10:00	~	0	~	
2	10:02	2	4.6	4.6	2.3
3	10:04	2	9.6	5.0	2.5
4	10:06	2	14.4	4.8	2.4
5	10:08	2	19.2	4.7	2.35
6	10:10	2	23.9	4.6	2.3
7	10:12	2	28.5	4.5	2.25
8	10:14	2	33.0	4.5	2.25
9	10:16	2	37.5	4.5	2.25
10	10:18	2	42.0	4.5	2.25
11	10:20	2	47.5	4.5	2.25
		$\bar{R}_2$	=	2.25	

$\bar{R}$, **the steady rate of flow, is achieved when R is the same in three consecutive time intervals.**

For the 1st set of readings $\bar{R}_1 = (R_1 : 1.25)/60 = 0.0208 \; cm/sec$

For the 2nd set of readings $\bar{R}_2 = (R_2 : 2.25)/60 = 0.0375 \; cm/sec$

Field Saturated conductivity:

$K_{fs} = [(0.0041)*(XorY : 2.18)*(\bar{R}_2 : 0.0375)] - [(0.0054)*(XorY : 2.18)*(\bar{R}_1 : 0.0208)] =$
$K_{fs} = 3.3 \times 10^{-1} \; cm/sec$

Matrix flux potential:

$\phi_m = [(0.0572)*(XorY : 2.18)*(\bar{R}_1 : 0.0208)] - [(0.0237)*(XorY : 2.18)*(\bar{R}_2 : 0.0375)] =$
$\phi_m = 6.6 \times 10^{-4} \; cm^2/sec$

Alpha parameter:

$\alpha = (K_{fs} : 3.3 \times 10^{-1}) / (\phi_m : 6.6 \times 10^{-4}) = 500 \; cm^{-1}$

Delta theta:

$\Delta\theta = (\theta_{fs} : \ldots\ldots) - (\theta_i : \ldots\ldots) = \ldots\ldots \; cm^3/cm^3$ **Estimated / Checked**

Sorptivity:

$S = \sqrt{2(\Delta\theta : \ldots\ldots)*(\phi_m : \ldots\ldots)} = \ldots\ldots \; cm * sec^{-1/2}$

Appendix D

Results of spectral calibration

(a) *Calibration of surface K_s with soil spectral reflectance*

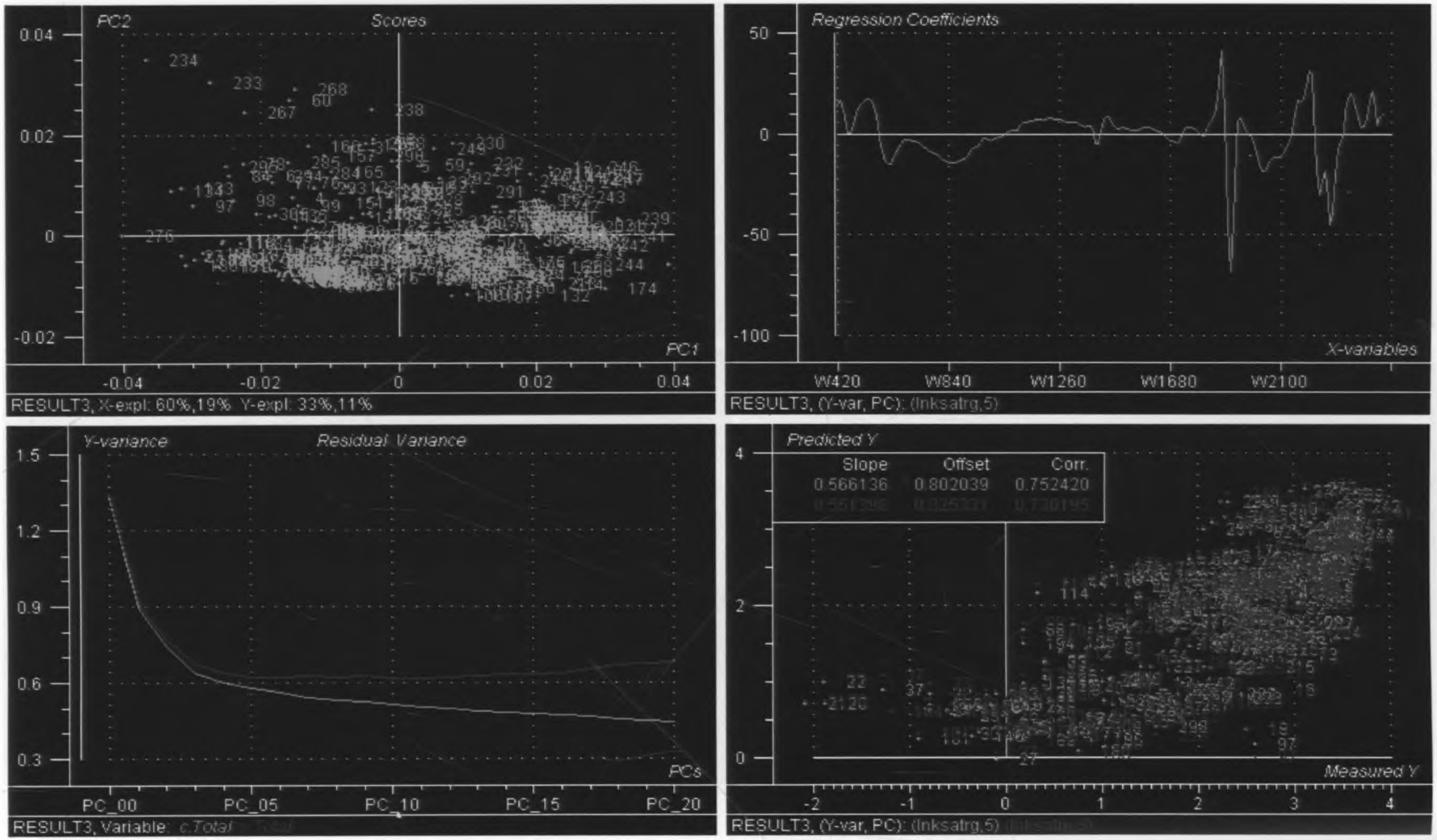

(b) *Calibration of Topsoil K_s with spectral reflectance*

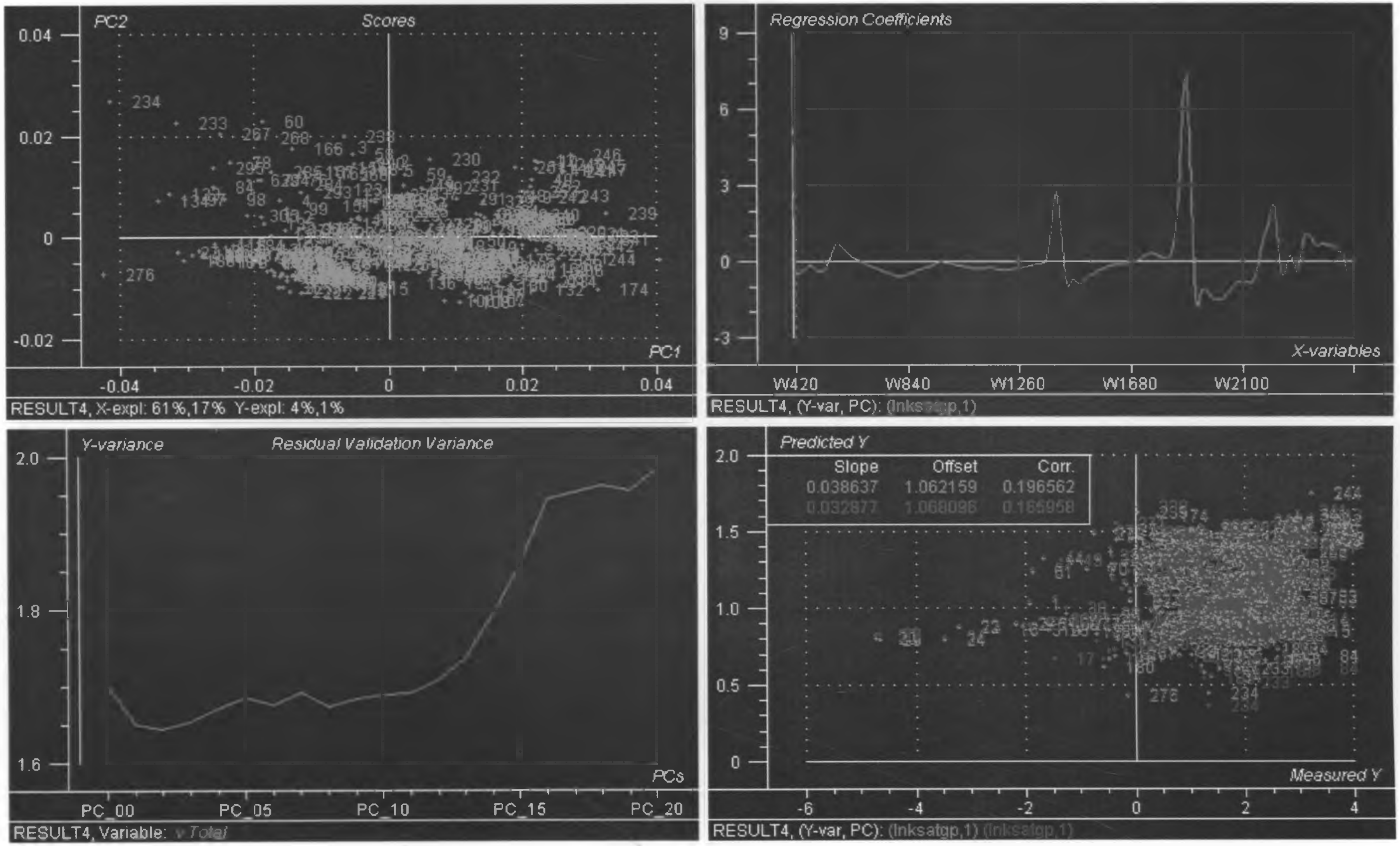

Appendix E

Linear Mixed Effects Model
Assessment of variability at plot level

Variable: Surface K_s
Linear mixed-effects model fit by REML
Log-restricted-likelihood: -352.1016
Fixed: lnksatrg ~ lctpye

(Intercept)	lctpye1	lctpye2	lctpye3	lctpye4
1.871803	0.4996878	-0.151518	0.2455756	-0.03220298

Random effects:
Formula: ~ 1 | Plot
(Intercept)
StdDev: 0.9790133
Formula: ~ 1 | Position %in% Plot

	(Intercept)	Residual
StdDev:	0.3533925	0.2065712

Number of Observations: 343
Number of Groups:

Plot	Position %in% Plot
115	343

Repeatability within plot = 63%

Variable: Topsoil K_s
Linear mixed-effects model fit by REML
Log-restricted-likelihood: -416.2717
Fixed: lnksatgp ~ lctpye

(Intercept)	lctpye1	lctpye2	lctpye3	lctpye4
1.137888	0.34143	0.02732	0.1802089	-0.05708

Random effects:
Formula: ~ 1 | Plot
(Intercept)
StdDev: 1.180696
Formula: ~ 1 | Position %in% Plot

	(Intercept)	Residual
StdDev:	0.4278757	0.2498391

Number of Observations: 343
Number of Groups:

Plot	Position %in% Plot
115	343

Repeatability within plot =63%

Variable: Surface K_s

Linear mixed-effects model fit by REML

AIC	BIC	logLik
100.5116	131.0959	-342.2558

Random effects:

Formula: ~ 1 | Slpzone

	(Intercept)
StdDev:	0.5566842

Formula: ~ 1 | Plot %in% Slpzone

	(Intercept)	Residual
StdDev:	0.8623952	0.4093322

Fixed effects: lnksatrg ~ lctpye

	Value	Std.Error	DF	t-value	p-value
(Intercept)	2.021	0.2981	228	6.7781	<.0001
lctpye1	0.401	0.1264	107	3.17520	0.0020
lctpye2	-0.214	0.077	107	-2.7833	0.0064
lctpye3	0.1457	0.0649	107	2.2431	0.0269
lctpye4	-0.030	0.0406	107	-0.7393	0.4614

Repeatability = 68%

Variable: Topsoil K_s

Linear mixed-effects model fit by REML

AIC	BIC	logLik
148.5434	179.1278	-416.2717

Random effects:

Formula: ~ 1 | Slpzone

	(Intercept)
StdDev:	0.0002199256

Formula: ~ 1 | Plot %in% Slpzone

	(Intercept)	Residual
StdDev:	1.180696	0.4954767

Fixed effects: lnksatgp ~ lctpye

	Value	Std.Error	DF	t-value	p-value
(Intercept)	1.1379	0.11550	228	9.8510	<.0001
lctpye1	0.3414	0.16970	107	2.0120	0.0467
lctpye2	0.0273	0.10320	107	0.2647	0.7917
lctpye3	0.1802	0.0838	107	2.1491	0.0339
lctpye4	-0.0570	0.05520	107	-1.0340	0.3035

Repeatability = 70%

Appendix F

Maps

Surface Saturated Hydraulic Conductivity patterns with respect to elevation in the Awach watershed

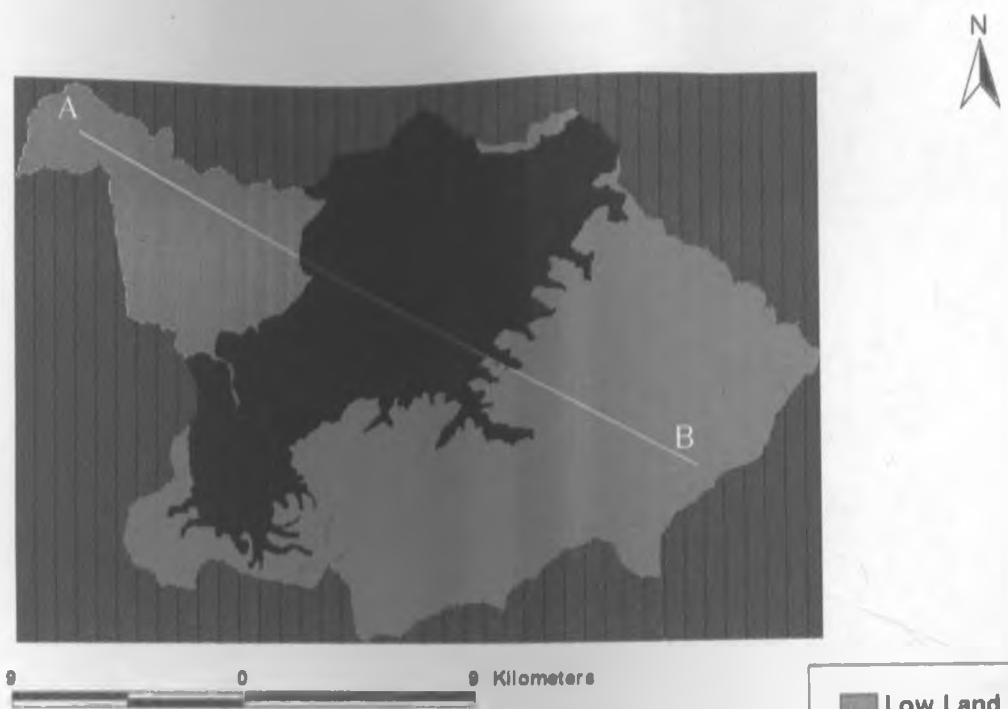

Elevation Classes in the Awach River Watershed

Elevation profile

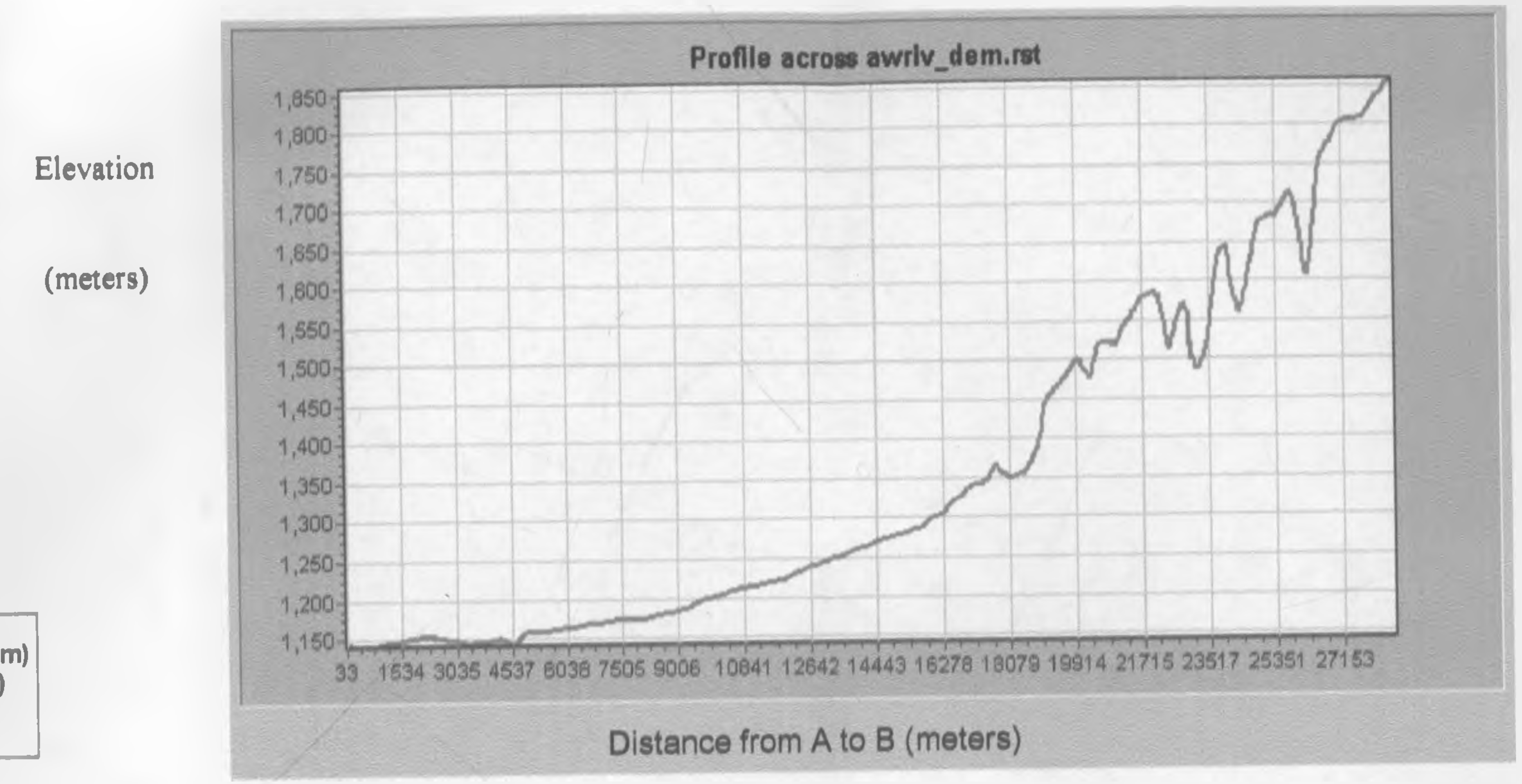

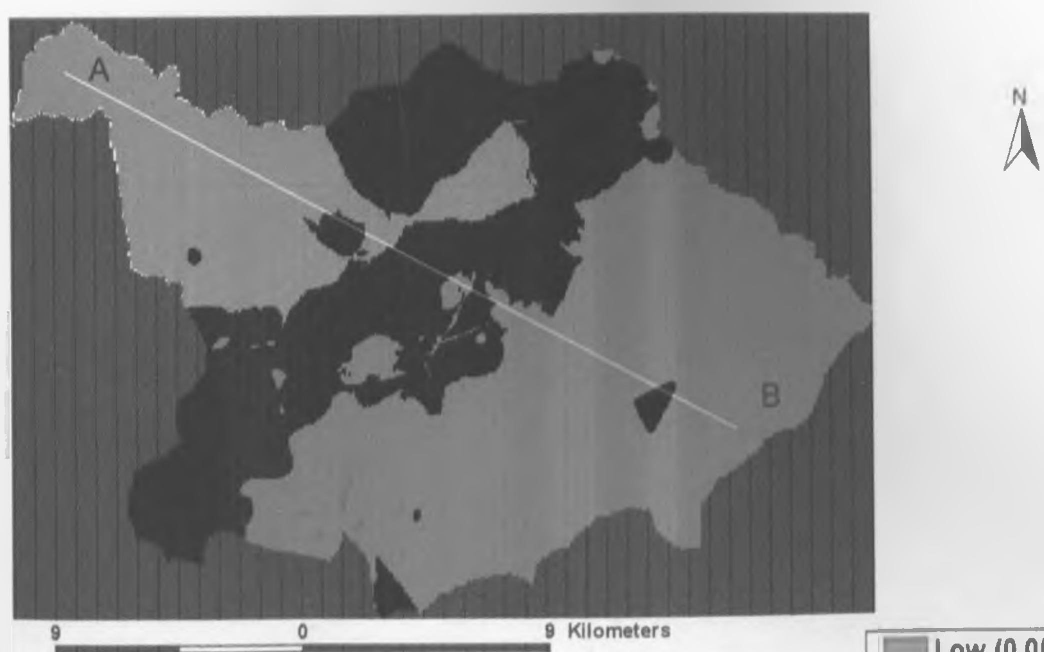

Surface Ks Classes in the Awach River Watershed

Surface hydraulic conductivity profile